ISSN 1173-5996

A Comparison Between Predicted and Actual Behaviour of Domestic Smoke Detectors in a Realistic House Fire

by

D R Brammer

Supervised by:

M J Spearpoint

Fire Engineering Research Report 02/2

May 2002

This report was presented as a project report as part of the ME (Fire) Degree at the University of Canterbury

School of Engineering
University of Canterbury
Private Bag 4800
Christchurch, New Zealand

Phone 643 364-2250
Fax 643 364-2758
www.civil.canterbury.ac.nz

Abstract

This report describes an investigation into various methods for predicting the activation times for domestic ionisation and optical smoke detectors when detecting flaming fires. The prediction methods studied were the temperature correlation method where the detector is assumed to activate when the gas that surrounds it rises a certain temperature above ambient, the pseudo-heat detector method in which an RTI is assumed for the smoke detector, and Heskestad's method which is based on optical density. The activation times predicted by these methods were then compared with those that were recorded during actual fire tests within a full size two-storey test house. The house was modelled on the field modelling software FDS.

Two test fires were considered in this study. Both were lounge chair fires in a room on the ground floor of the house, and were flaming fires under vitiated conditions. The energy output reached by the two fires was between 600 and 1000 kW. Data collected during these tests included gas temperatures, optical density and the mass loss history of the chairs. There were also a number of radiators throughout the house that were left on for some time to heat the house before the fires were ignited.

It was found that there was little difference between the temperature correlation and the pseudo-heat detector methods when a value for RTI of 1 $m^{½} s^{½}$ was considered. It was also found that the use of an activation temperature of 20 °C above ambient within the temperature correlation method was the most appropriate method for predicting the activation times for the detectors. This value for activation temperature is high compared with other researchers, but it is likely that the radiators within the house created airflow currents that had an effect on the behaviour of the detectors.

Acknowledgements

A special thanks to my supervisor Mike Spearpoint for his support and guidance during the course of this study.

Gratitude is expressed to Peter Coursey and Joost Stenfert-Kroese for providing ample computing facilities as well as much technical advice. I found this advice to be particularly useful during some of the more disheartening moments of my research.

I am also indebted to my classmates for their assistance during this study, especially during similar disheartening moments.

I acknowledge the assistance of the staff of the Engineering School Library in finding reference papers.

Finally, I would like to express my gratitude to the NZ Fire Service for not only supporting the Fire Engineering programme at the University of Canterbury, but also for funding my own scholarship.

Table of Contents **Page**

List of Figures **Page**

Chapter 1 INTRODUCTION

1.1 Background To Study

Most fire related deaths occur in residential dwellings, and as most fire deaths occur as a result of smoke inhalation, it is typically accepted that the majority of these deaths could be avoided if the installation of smoke detectors in houses was mandatory. As part of the ongoing research into smoke detectors, it will be useful to model the behaviour of detectors in realistic fires.

In the study into the effects of fire in the past, most tests that have involved realistic fires have been conducted in single, well ventilated rooms which will not necessarily replicate the behaviour or life hazards that would occur in a typical under ventilated, multi-enclosure building or recreate the effects of interconnected spaces, corridors, or consider the influence that any heating systems within the building will have on a smoke detection system. While some fire studies have been performed in actual houses, the fuel for such fires have not necessarily been representative and the data collected has not always been extensive.

As part of ongoing research into the hazard assessment of domestic fires, the Building Research Establishment (BRE) conducted a number of test fires within an actual house within its test facility at Cardington, England. These tests considered the effects of fires in upholstered furniture in a two-storey residence under vitiated conditions. The results of these tests formed the basis for this study.

There are numerous advantages in comparing the outcomes of actual fires with predicted results. These include providing some level of validation to the many different computational methods that are available for predicting the effects of such events. While there are a variety of published theories for modelling the behaviour of smoke detectors, ranging from the extremely crude to the computationally complex, different methods of prediction can produce very different outcomes. The more complicated methods do not necessarily provide more accurate predictions.

1.2 Objectives of Study

The objectives of this study are as follows:

1. Create an effective analysis model for the test house. Emphasis will be placed on temperature and optical density, which is necessary for modelling the behaviour of smoke detectors.
2. Investigate the effects of the physical features of the house. This will include the consequences of modelling only a portion of the house, and the significance of various obstructions to the flow of smoke.
3. Compare the predicted with the actual test behaviour.
4. Give recommendations as to parameters and methods of prediction for the behaviour of smoke detectors for use within current analysis software.

1.3 Behaviour of Smoke Detectors

The performance of smoke detectors is dependent on the behaviour of smoke, and smoke is difficult to model. Fires can either be smouldering or flaming depending on the fuels and ventilation involved. The velocity and temperature of smoke both tend to reduce with distance as the smoke migrates from the fire source. Smoke particles will coagulate with travel which will effect the size distribution and some particles will be deposited on surfaces en route, which will also alter the properties of the smoke. Some studies into the behaviour of smoke have assumed that the particles are spherical in shape whereas they are typically angular, which will alter optical properties of the smoke, as does the smoke's colour. Furthermore, at some stage during a compartment fire a window can break which will increase the level of ventilation into the compartment, which will immediately affect the properties of the smoke. Every aspect of this erratic behaviour will have an influence on the performance of smoke detectors.

There are commonly two different types of smoke detectors in domestic use. The chamber inside an ionisation type of detector consists of two electrodes in which an electric field is maintained by applying a voltage between the electrodes. A radioactive source produces ionisation radiation. The ions produced are driven by the applied electric field to the electrodes. This results in a small current flow between the

electrodes, which can be measured by an electrometer. If aerosol particles enter the chamber, ions attach to the particles. Because the electrical mobility of the particles will be less than ions, the resulting reduction in current flow will be detected by the electrometer and thus the alarm will be activated.

The functions of optical types of detectors are dependent on the properties of light scatter from the smoke particles that migrate within the detector's chamber. Light scatter is dependant on the particle's size, surface conditions and colour, and the light source is a typically a light emitting diode (LED).

Numerous models exist for predicting the behaviour of smoke detectors, and more complex models are under development. For the simplest method, referred to as the temperature correlation method, the detector is assumed to activate when the gas temperature that surrounds the detector achieves a certain activation temperature T_{act} above ambient conditions. In another slightly more complex method, referred as the pseudo-heat detector method, the response time index (RTI) is used as a measure of sensitivity of the detection component

An important aspect of the behaviour of smoke detectors is the relative ease or otherwise that smoke will have in entering the detector's chamber in order to be detected. The characteristic length L, which has to be derived for a particular design of detector as described by Bukowski et al., quantifies this transport delay.

1.4 Cardington Tests

The test house was a fairly standard two storey, three bedroom detached house of typical 1970's design and construction as described by Spearpoint and Purser et al. All of the test fires occurred in single lounge chairs within the fire room, which was a lounge on the ground floor. In some cases additional furnishings were provided within the fire room to further create realistic domestic fire scenarios.

The motivation for the tests was to examine the relationship between fuel load, ventilation, detector activation and tenability. To monitor the progress of these tests,

the house was fitted out with instruments to measure temperatures, gas concentrations, heat flux, optical density, and for some tests video cameras were also installed. A weighbridge was installed within the fire room to quantify the mass loss history for the fire event. A number of domestic and commercial smoke detectors were also placed at various locations around the house, and their activation times were logged. A total of ten fire tests were performed within the house during this particular series of tests.

Steps were taken to create different types of fires in the house assuming winter occupancy. External doors and widows were closed to create vitiated conditions, and several radiators were in operation before the test commenced so as to generate airflow currents throughout the house. The internal door between the fire room and the rest of the house varied between fully open to closed for different tests to alter the level of ventilation available into the fire room.

There were significant variations in the smoke detector activation times for the different types of fires. For flaming fires, in general the ionisation detectors activated before the optical detectors. For smouldering fires the reverse was true, although the ionisation detectors did not activate at all. The results of these tests are available on a CD-ROM database.

1.5 Fire Modelling Software

A fairly recent development in computer analysis is field modelling, which divides the physical analysis space into a large number of prismatic cells. This is similar in concept to the better-known zone modelling which divides a compartment into a small number of distinct layers, and mass and energy balance are enforced within each layer, while other models replicate other physical processes of gas flow. The gas velocity, temperature and other properties are assumed to be uniform within each cell but are all functions of time. Likewise for field modelling, equations of conservation of mass, momentum, energy and species are solved for each time step. The accuracy of field models is dependant on the number of cells that the computational space has been divided into, and so is the computational time for each fire scenario.

The National Institute of Standards and Technology (NIST) has developed the software package Fire Dynamics Simulator (FDS) that will simulate the mixing and transport of the products of combustion by modelling fire driven fluid flow. The ongoing development of Computational Fluid Dynamics (CFD) allows the modelling of fires in complex geometries incorporating a variety of physical phenomena. One such phenomenon is Large Eddy Simulation (LES), which is a simulation of the turbulent mixing of the gaseous fuels and combustion products within the local environment immediately surrounding the fire. The significance of LES is that it determines the burning rate in most fires and controls the spread of smoke and hot gases. However, it is extremely difficult to model, and the equation solving algorithms of field models can suppress the effects of LES.

In these analyses, FDS was set to perform LES rather than the alternative Direct Numerical Simulation (DNS), the latter being more suited to small scale combustion experiments, not to multi-room enclosures because of the computational resources this type of analysis requires.

Another useful feature of the FDS software package is SMOKEVIEW, which is a software application that will provide a visual representation of the house being modelled. The user can upload the house's geometry using SMOKEVIEW to check it for correctness, and also upload various items of output such as temperature and velocity to view this data.

1.6 Scope of Study

In this study of the behaviour of smoke detectors, two fire tests from the Cardington house are chosen, and with the help of the analysis package FDS version 2 (which is still under development), the temperatures, air velocity and optical density are predicted. With this information the activation times for the domestic smoke detectors within the house are predicted by three different methods, and are then compared with the actual activation times that resulted during the fire tests.

This study does not consider the commercial detectors, or the gas concentrations and tenability limits within the house.

1.7 Outline of Report

Chapter 2 justifies the analysis methods that were used in this study by referring to previous research that covered similar ground. It also gives descriptions of the various parameters that form the conclusions for this study, and gives ranges for typical values for these parameters. Likely future developments in the modelling of fire and smoke detector behaviour are also discussed.

Chapter 3 gives descriptions of the type of occupancy and the uses of the various rooms within the test house. The two domestic type test fires (referred to as CDT17 and CDT20) that this study is based on are defined, and the relevant test data that was gathered from these tests is described, as well as the instrumentation that was installed inside the house to collect this data.

Chapter 4 discusses the process of modelling the features within the house, including some of the difficulties that had to be overcome. The methods for both deriving and correcting the heat release rate (HRR) curves for the test fires are given. The modelling that was necessary to establish the air currents that were in place inside the house because of the heating system before the tests commenced is also discussed, as are some of the more interesting outcomes that were found while developing the house domain geometry

Chapter 5 presents graphs of some of the more significant comparisons for temperature, optical density, and makes some comparisons between different grid sizes that were used during the analyses. Also presented are bar graphs that compare the actual and predicted smoke detector activation times within each room for both types of detector, for both fires, and for all three prediction methods. It also makes some observations about the trends of the three prediction methods.

The significant conclusions from the previous chapter are emphasized in Chapter 6, and recommendations for further research are also presented.

Plans of the test house, including dimensions, locations of measuring devices and ratings for radiators are given in Appendix A. Diagrams and temperature curves for the varying types of balustrades that were investigated are given in Appendix B. Appendix C presents the family of curves for HRR, temperature and optical density for the 100mm grid analysis for test CDT17. Appendix D presents the same for test CDT20, and Appendix E presents curves that compare the predictions for HRR and temperatures between the 75mm and 100mm grid size simulations for test CDT17.

Chapter 2 PREVIOUS RESEARCH

2.1 Introduction

There are numerous methods to emulate both the fire conditions within the house and the behaviour of the smoke detectors. This chapter describes the modelling parameters and methods of analysis that were utilized in this study.

This chapter justifies the methods of analysis by describing previous work involving multi-compartment modelling, and the use of the fire simulation application FDS. It also defines the various methods that were used to model the behaviour of the smoke detectors, gives descriptions for the various parameters that this study was based on, and gives a range of magnitudes of these parameters which were derived from previous research. There is also a general description of probable future developments in fire and smoke detector modelling.

In later chapters, the results of the above mentioned methods are given with recommendations as to the magnitudes of the parameters that most reasonably replicate the results of the actual test fires that were considered in this study.

2.2 Validation of FDS

Friday et al discusses simulations of a series of seven full-scale fire tests that were performed in an enclosure that was approximately 18m x 12m x 6m high that had little leakage. Instrumentation included in the test apparatus included thermocouples, gas analysers, flow probes, optical density meters and heat flux meters. The fires that were simulated were either propylene or heptane, were either a steady state or t^2 growth, and ranged in size from 500 kW to 2 MW. Maximum temperatures ranged from 115 °C to 370 °C. As an investigation into the effect of varying the grid sizes, for various tests these ranged from 75mm to 600mm, and it was concluded that reducing the grid sizes does not necessarily improve predictions of temperature. It was also concluded that FDS is capable of providing accurate results for the scenarios that were tested.

2.3 Multi-Compartment Modelling

Continuing on from the previous section on FDS, Cleary et al (2001) describes the modelling of actual tests using FDS in a three-room suite and comparing predicted and actual results. The enclosure that was tested had a total size of approximately 26m x 15.5m x 2.9m high, had a HVAC system in operation, and the internal doors between the rooms were fully open throughout the test. To model the suite for the FDS analysis the entire enclosure was divided into grids which had a size of 150mm x 75mm x 27mm high, and the resulting smoke concentrations were converted into extinction (related to optical density). The source of the fire was a flaming polyurethane mat, which represented a medium t^2 growth fire that peaked at approximately 200 seconds. In the examination of the results there is some discussion about some apparent errors in the predicted temperatures, and it is postulated that these errors are due to the coarse grid that was chosen. It was concluded that FDS was capable of emulating the environmental conditions that a detector may experience during an actual fire. More particularly that FDS was able to predict the transportation of smoke, heat and gas species as is necessary to predict detector performance.

Collier reported on a series test fires within a typical New Zealand house. He describes a number of fire tests in a typical three bedroom single storey dwelling with a floor area of $69m^2$ to determine the smoke and gas movement, and temperatures within the house. Some of these tests involved burning items of furniture causing both flashover and non-flashover fires.

Instrumentation was installed within the house to measure air temperatures, smoke spread, gas species' concentrations, heat radiation, and a weigh bridge was installed to assess the mass loss history, although the results were compared with predictions made with a zone model rather than FDS. The house was also fitted with domestic smoke detectors. In one test, the source of the fire was a waste paper bin, the fire then spread to a nearby curtain, and then involved a polyurethane foam rubber filled chair, generating a fast t^2 growth fire (as shown in a later chapter in Figure 5-19). All of the house's internal doors were open, as were the external windows to the fire room. There is no mention of a heating system within the house. It was concluded that the activation times for smoke detectors could be predicted by determining when the gas

temperatures in the smoke layer around the detector raises to approximately 2-4°C above ambient, as long as smoke is present.

2.4 Modelling of Smoke Detector Behaviour

A common problem for designers is the uncertainty as to the fire's type and location, as different types of detectors are more suited to different types of fires. Qualey et al. reports the generally accepted view that ionisation detectors are more responsive to invisible particles typically produced by flaming fires, whereas optical detectors are more responsive to larger particles typically produced by smouldering fires. He also states that the position of the detector in terms of ease of smoke entry into the sensor chamber will have an impact on its behaviour.

Most domestic detectors operate under a principle where smoke has to flow into its sensor chamber by some natural means, but there is often a delay in achieving this. The sensing regions are enclosed for reasons of reducing the velocity normal to the ion flow in ionisation detectors, to prevent the ingress of insects and to prevent damage to the sensors. The temperature correlation method discussed below does not take into consideration the difficulties that could exist with this time delay. The pseudo-heat detector and Heskestad' s methods are an improvement in that they have a level of dependence on velocity, but the time lag is not exclusively a function of velocity as Cleary et al (2000) reports. His comments will be discussed later.

These difficulties aside, the prediction models considered in this study are discussed below. Each model will be applied to the prediction of both ionisation and optical detectors.

2.4.1 Temperature Correlations

The simplest method for predicting the behaviour of smoke detectors is to assume that the detector will activate when the gas temperature around the detector rises to a temperature of T_{act} above ambient. This method is more suited to higher energy fires, and is not considered valid for all types of fuel.

Typical values for T_{act} range from 2 - 4°C as reported by Collier (as discussed in section 2.3 of this report) up to 13°C and even 20°C as discussed by Bukowski et al. Notably, Peacock et al state that the zone modelling software application FAST has a default value of 13°C.

2.4.2 Pseudo-Heat Detector Method

While it is not a common prediction method for smoke detectors, it is feasible to use a variation on the temperature correlation method to model smoke detectors as if they are heat detectors. Schifihiti et al (1995) reports the method concerned:

$$\frac{\delta T_d}{\delta t} = \frac{U^{1/2}\left(T_g - T_d\right)}{RTI} \qquad (2\text{-}1)$$

where T_d = temperature of detector

t = time

U = gas velocity

T_g = temperature of gas

RTI = response time index

The response time index (RTI) is a measure of the sensitivity of the detector, and is typically assumed to be negligible for smoke detectors.

The detector is assumed to activate when the temperature of the detector T_d increases from ambient by an amount T_{act}. Various values were given in the previous section for the activation temperature T_{act}, although the use of these values is not necessarily consistent with this particular prediction method.

2.4.3 Heskestad's Method

The activation time lag due to entry resistance has already been discussed above. A well-reported method for allowing for these delays was proposed by Heskestad. In general, the response time of a detector can be expressed as:

$$\frac{\delta D_{ui}}{\delta t} = \frac{1}{\tau}\left(D_{uo} - D_{ui}\right)$$

where D_{ui} = optical density inside detector

t = time

τ = time constant

D_{uo} = optical density outside detector

Substituting in $\tau = \frac{L}{U}$, and assuming $\frac{\delta D_{ui}}{\delta t} \equiv \frac{\delta D_{uo}}{\delta t}$

$$\frac{\delta D_{uo}}{\delta t} = \frac{U}{L}\left(D_{uo} - D_{ui}\right)$$

where U = gas velocity around detector

L = detector characteristic length

Rearranging:

$$D_{ui} = D_{uo} - \frac{L\left(\delta D_{uo} / \delta t\right)}{U} \qquad (2\text{-}2)$$

Published values for L differ markedly as shown in Table 2-1:

Researcher	Ionisation (m)	Optical (m)
Bukowski et al	1 - 2	1 - 2
Schifihiti (2001)	1.8 - 9.5	5.3 - 13.0
Bjorkman et al	3.7	6.8

Table 2-1. Table of Values for Effective Length

Values for L are not widely published, and are a function of the design of the detector. The aerodynamic properties of early detectors were extremely poor with relatively high entry resistance. In an addendum to Bjorkman et al's paper, a description is given

as to tests conducted in wind tunnels with the objective of deriving values for L in the late 1970's. Difficulties were faced because as smoke ages its properties would change, and values found from the tests were never published.

Because of the historical modelling difficulties in estimating an optical density, a proposal was made to replace the optical density terms in Equation 2-2 with temperature rise and a detector material number (DMR). DMR was a function of the fuel, combustion conditions and sensor design. However, as modern zone and CFD model easily deal with soot, Bukowski et al makes the recommendation that Heskestad's model should be revisited.

Cleary et al. (2000) reports that the effective length is acceptable for high velocities, but a single parameter is not sufficient to model the behaviour over a full range of operating conditions, especially with weak plumes at the beginning of a fire, which is the time when a smoke detector would be expected to activate. A further alternative method is proposed which is based around two parameters; a dwell time and a characteristic mixing time, which are both based on the physical description of a generic detector head.

Research into these issues continues, and no doubt there are several other variations on Heskestad's model. But as this method is widely referred to, it is this method that is considered in this study.

To predict the optical density for use in Equation 2-2, some input is required into the fire model as to smoke yield Y_s. Tewarson gives values for flexible polyurethane foams between 0.13 to 0.23 kg/kg, although these values do not necessarily relate to combustion modified foam, which was the padding to the chairs in the Cardington tests. For the computer modelling in this study a nominal value of 0.10 kg/kg was used, although it was later concluded that this value was too high.

2.4.4 Future Developments

As smoke ages, its properties can change markedly. Its temperature and velocity will both drop, and it has been demonstrated that both of these behaviours can be

adequately modelled. But with age, particles can also coagulate, change colour and shape, particles can deposit on enclosure surfaces, and the level of ventilation into a space can change very quickly which can alter the smoke's properties once again. These latter behaviours will affect the response of smoke detectors, but no attempt has been made to model any of them in any of the models described thus far.

The activation of ionisation detectors is caused by a decrease in the electric current in its sensing chamber due to the blending of smoke and ions. An ionisation detector's response is approximately proportional to the smoke particle's diameter, and as Snegirev et al describes, if coagulation is not modelled then the response of ionisation detectors will tend to be overestimated. An optical detector's activation is based on the intensity of light scattered by the smoke particles. As the light scattering coefficient decreases with coagulation, if its coagulation is not modelled then the response of optical detectors will tend to be underestimated. Snegirev et al presents models that allow for coagulation.

However, combining coagulation into the models described in the previous sections in some way will not adequately imitate the behaviour of smoke particles. Schifihiti (2001) comments that while researchers often report optical density as obscuration (although obscuration would more accurately be called attenuation since light may be absorbed, reflected or refracted by the smoke), while such values are useful for assessing visibility, neither ionisation or optical detectors operate under a principle of light attenuation. Furthermore, detectors may use complex response algorithms, which are generally not made known.

The combination of coagulation into smoke detector models is definitely a progression, and such developments into detector modelling need to continue. Models should also be developed for other behaviours such as the change of smoke particle size and shape. Furthermore, Newman describes a model for ionisation detectors, which is based on the sensitivity to an electrical charge carried by some aerosols. Schifiliti (2001) also commented that developers of fire and smoke detector models should work together so that models will evolve together.

2.5 Modelling of Fire Behaviour

The development of the HRR history curve is dependant on the effective heat of combustion ΔH_{eff}, which is a measure of how much energy is released when a unit mass of material is combusted. The distinction must be made between the complete heat of combustion when all of the fuel is consumed, and ΔH_{eff} when some residue remains. It is generally assumed that ΔH_{eff} will be constant throughout the fire, which is typically not the case.

Previous research performed at the University of Canterbury by Girgis involved the combustion of lounge chairs in an ISO room that measured 3.6m x 2.4m x 2.4m high with the only ventilation being a standard width doorway. From his results it can be derived that the average for ΔH_{eff} varied between approximately 30-38 MJ/kg.

Chapter 3 FULL SCALE FIRE TESTS

3.1 Introduction

Although a series of ten similar tests emulating domestic fires were performed within the Cardington house, this study is based on the results of only two. This chapter provides descriptions of these two tests as well as the configuration of the test house.

Initially a description of the house's occupancy is given as well as the locations and uses of the various rooms. Distinguishing features about the house are discussed, and descriptions are given of the test fires, the relevant data collected from these tests, and the instrumentation that was installed within the house to measure this data.

The test fires that were conducted within the house were modelled according to the methods that were described in the previous chapter, and the results of these analyses will be given in later chapters.

3.2 Description of House

The same house was used for all of the fire tests considered in this study. This test house was one of a number of test structures inside the BRE test facility at Cardington. It was a two storey, three-bedroom detached house of typical 1970's U.K. design and construction. There was a lounge, entry hall, kitchen and dining room on the ground floor, a bathroom and three bedrooms on the top floor as shown in Figure 3-1. Dimensional plans are given in Appendix A. The kitchen, dining room, bathroom and two bedrooms were sealed off from the rest of the house, and therefore from the flow of smoke in the particular tests considered. These areas are shown shaded in Figure 3-1. Most of the sealed off rooms were used to house measuring and recording equipment for the tests. The internal doors to the lounge and bedroom 2 are fully open 750mm, while the external doors and windows were closed to create vitiated fire conditions, and the windows to the fire room were of wired glass to stop them from breaking out. Lighting throughout the house was provided by standard incandescent domestic light bulbs.

Because a heating system within the house can affect the behaviour of smoke detectors, a number of radiators were located around the house to replicate winter occupancy. Three were located upstairs; one in each bedroom. On the ground floor there was one in the entry hall and one in the lounge (fire room) as shown in Figure 3-1, and identified in more detail in Appendix A. These radiators were started before ignition of the test fire and left for some time to create airflow currents throughout the house. The radiator in the lounge was removed from the space shortly before ignition to avoid it from being damaged by the chair-fire, but all of the other radiators remained on for the duration of the test. The ambient temperatures that were created varied around the house and tended to be higher within the upper floor, as shown in Figure 4-5 in a later chapter. The ratings for the radiators varied between 1 - 2 kW, and are specifically given in Appendix A.

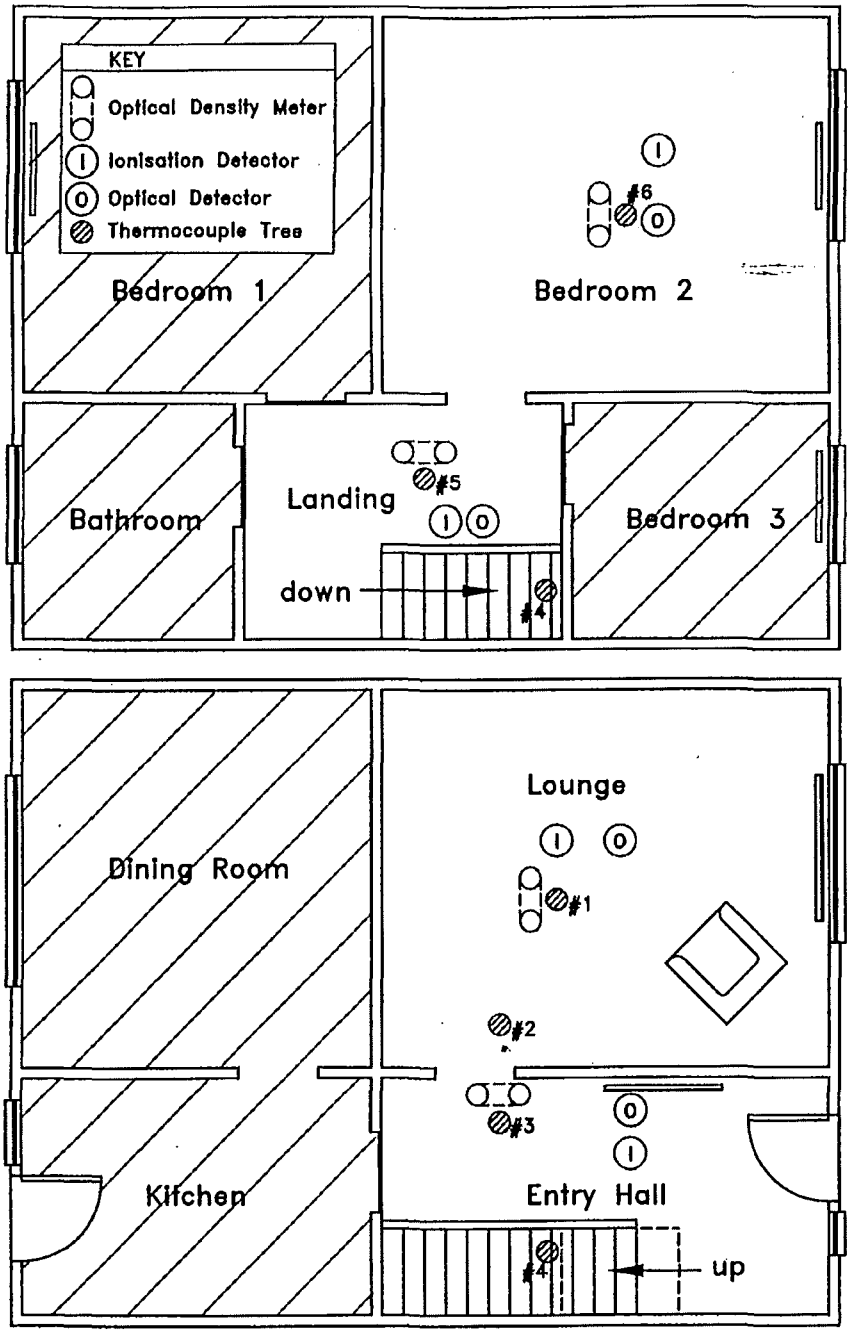

Figure 3-1. Floor Plans for Test House

3.3 Instrumentation/Data Collection

While the house had numerous items of measuring equipment to monitor the progress of the fire, only a portion of this instrumentation is pertinent to the tests that are studied. Four pairs of ionisation and optical smoke detectors were located within the house, one pair in the lounge, entry hall, landing and bedroom 2 as shown in

Figure 3-1. Optical density meters were located in the lounge, in the entry hall by the lounge door on the landing, and within bedroom 2, all at 1.5m above the floor. There were several thermocouple trees within the house, which located thermocouples at varying heights. Tree #1 was near the middle of the lounge and is designated as #1 in Figure 3-1, tree #2 was also in the lounge but nearer to the door to the hall, tree #3 was near the same door but within the entry hall, tree #4 was on the stairs, tree #5 was on the landing and #6 was located near the middle of bedroom 2. There was also a weighbridge in the lounge, which allowed the mass of the chair to be measured continuously throughout the fire tests. From this instrumentation the temperatures at various heights could be measured, as well as optical density, mass loss history, and the activation times for the various detectors. This information is available on a CD-ROM database available from BRE.

3.4 Description of Tests

Two fires were considered in this study, referred to by the BRE researchers as CDT17 and CDT20. Both tests were performed on single chairs with timber frames, upholstered with combustion modified high-resilient foam (CMHR) with a fire retardant (FR) cotton cover. Both chairs weighed 23.8 kg including 4.7 kg of foam. The fires took place on a weighbridge in the lounge on the ground floor.

The test fires were started by an electrical igniter and match head, which lit a small wooden crib on the seat of the chairs. Both chairs developed flaming fires, and after approximately 720 seconds both fires had self-extinguished without completely consuming the chair that had been ignited.

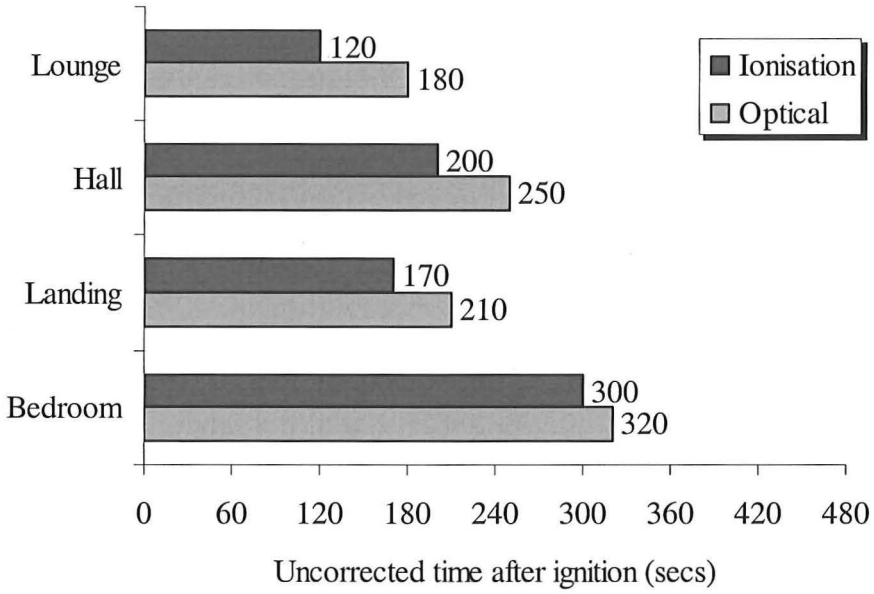

Figure 3-2. Uncorrected Detector Activation Times, Test CDT17

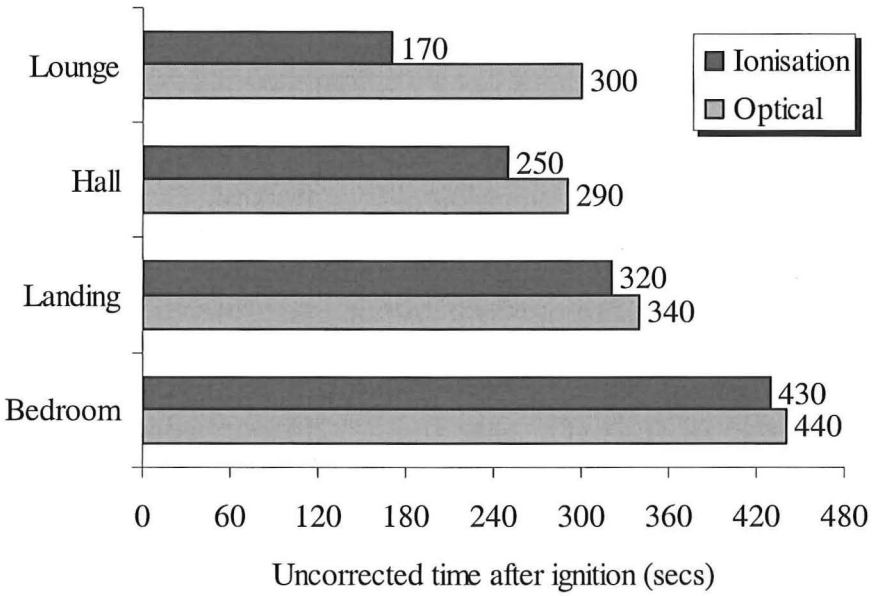

Figure 3-3. Uncorrected Detector Activation Times, Test CDT20

The activation times for both types of smoke detectors for tests CDT17 and CDT20 are presented in Figures 3-2 and 3-3 respectively. The activation times are described as uncorrected as described late in Section 4.7. While as expected the detectors in the lounge activated first, and within bedroom 2 last. But for CDT 17 the detectors on top

of the landing activated before the ones in the entry hall, while for CDT20 the reverse was true. In each room the ionisation detector responded before the optical.

Chapter 4 COMPUTER MODELLING

4.1 Introduction

Having defined the test house and the methods for modelling and analyzing the data that was collected, this chapter goes on to describe the process of modelling the house and the two test fires that were studied.

This chapter begins with a discussion on emulating the features within the house, and goes on to describe the derivation of the heat release curves for the test fires. Some of the difficulties that were faced are also discussed, and schematic diagrams of the house are given. It also discusses some corrections that were necessary to the test data that was collected. The method for establishing the airflows that were present before the tests began is described, as is the method for calculating the amount of soot that was generated from the fire. Finally, some of the more interesting findings while developing the house model are given.

The results of this modelling process are analysed by the methods that were defined in an earlier chapter, and the results of these analyses are given in the next chapter.

4.2 Configuration of House

To analyse the house in FDS, an accurate representative model must be constructed. While this house has been described in several documents, there are a number of discrepancies in the information given as to the sizes of the rooms and locations of instrumentation. The dimensions and locations that were adopted in this study are given in Appendix A. From the schematic drawings of the house model shown in Figure 4-1 and 4-2 it can be seen that only a part of the house was modelled.

Figure 4-1 shows the entry hall on the ground floor and landing on the top floor, and the open doorway that leads to bedroom 2. The kitchen/dining room on the left hand side was sealed off from the path of the smoke, as was bedroom 3 on the right hand side of the top floor. Figure 4-2 shows most of the smoke path from the lounge on the right hand side of the ground floor, through the open door into the entry hall, up the stairs to the landing above, and through a doorway again and into bedroom 2.

Some concessions were necessary to accommodate a working model. As FDS requires some form of ventilation into the analysis space to prevent pressure build-up, a vent was positioned at the location of the front door, and is one grid in width as shown in Figure 4-2. In addition to this the chair was assumed to remain at a constant height throughout the fire.

FDS allows thermal boundary conditions to be set for surfaces. For the simulations the internal walls were assumed to be Gib board, and the external walls and top floor ceiling are adiabatic (i.e. they will not permit heat loss).

To analyse the simulation, measuring points were located at various locations around the house model to collect the following data:

- Temperature at the locations which represent thermocouple trees #1 (lounge), #3 (entry hall), #4 (stairs), #5 (landing) and #6 (bedroom 2).
- Visibility at 1.5m above the floor in the lounge, entry hall, landing and bedroom 2 to compare the results of the simulation with the actual test data.
- Temperature, visibility and two perpendicular velocities in the global u and v directions at the locations of all eight smoke detectors (four ionisation and four optical).

4.3 Grid Generation

FDS calculates within a rectilinear grid within a rectangular domain defined by the user. The obstructions and ventilation must conform to the defined grid. In developing the model for this study a 100mm grid size was adopted initially. While this size suited the house in many respects, it created difficulties in the following areas:

- Internal doors are 750mm wide, which cannot be modelled with a 100mm grid.
- Ventilation as mentioned in the previous section had to be 100mm wide.
- Balustrades also had to be the same width.

- There were difficulties with modelling the sloping ceiling over the stairs as will be discussed later.

As the chair was positioned at an angle to the grid layout, it had to be positioned over an array of cells as can be seen in the lounge of Figure 4-2. The chair was assumed to have a size of 800mm x 800mm, and the collection of grids that make up the chair have a combined area equal to this.

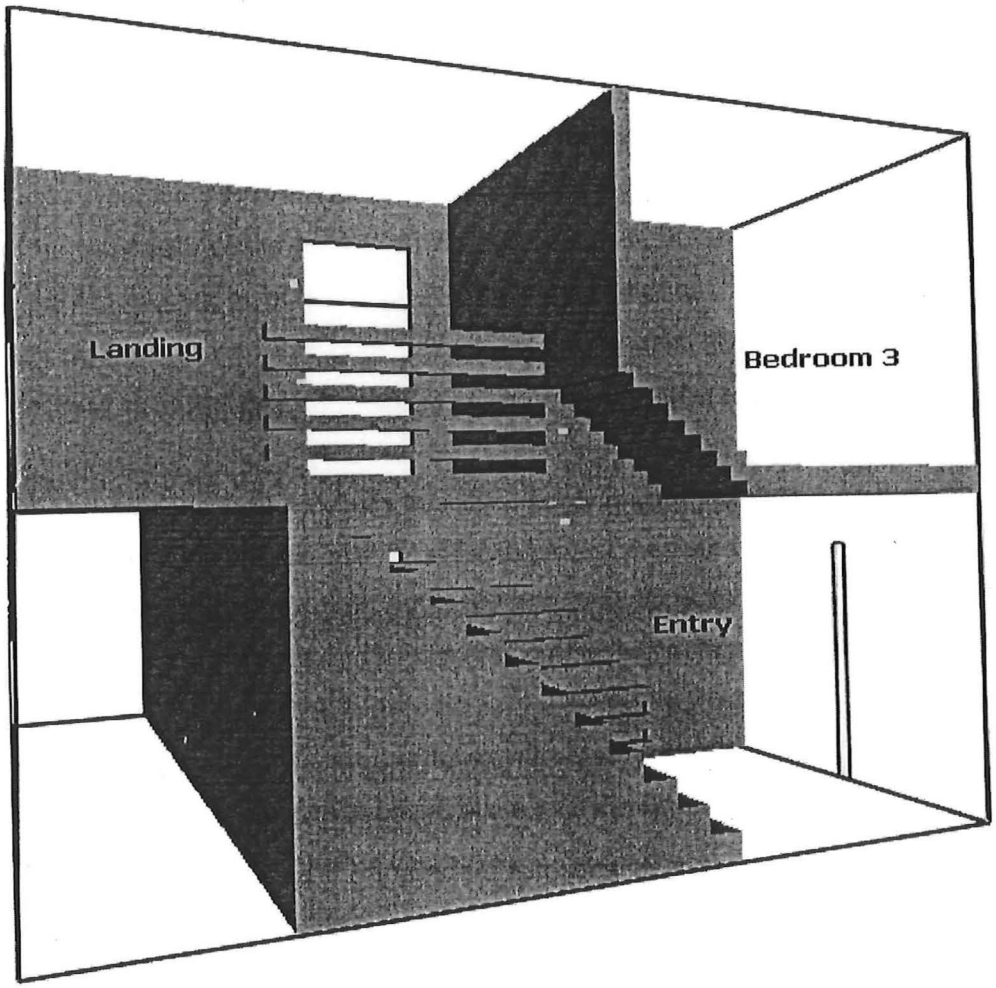

Figure 4-1. SMOKEVIEW Image of House, View From South Wall

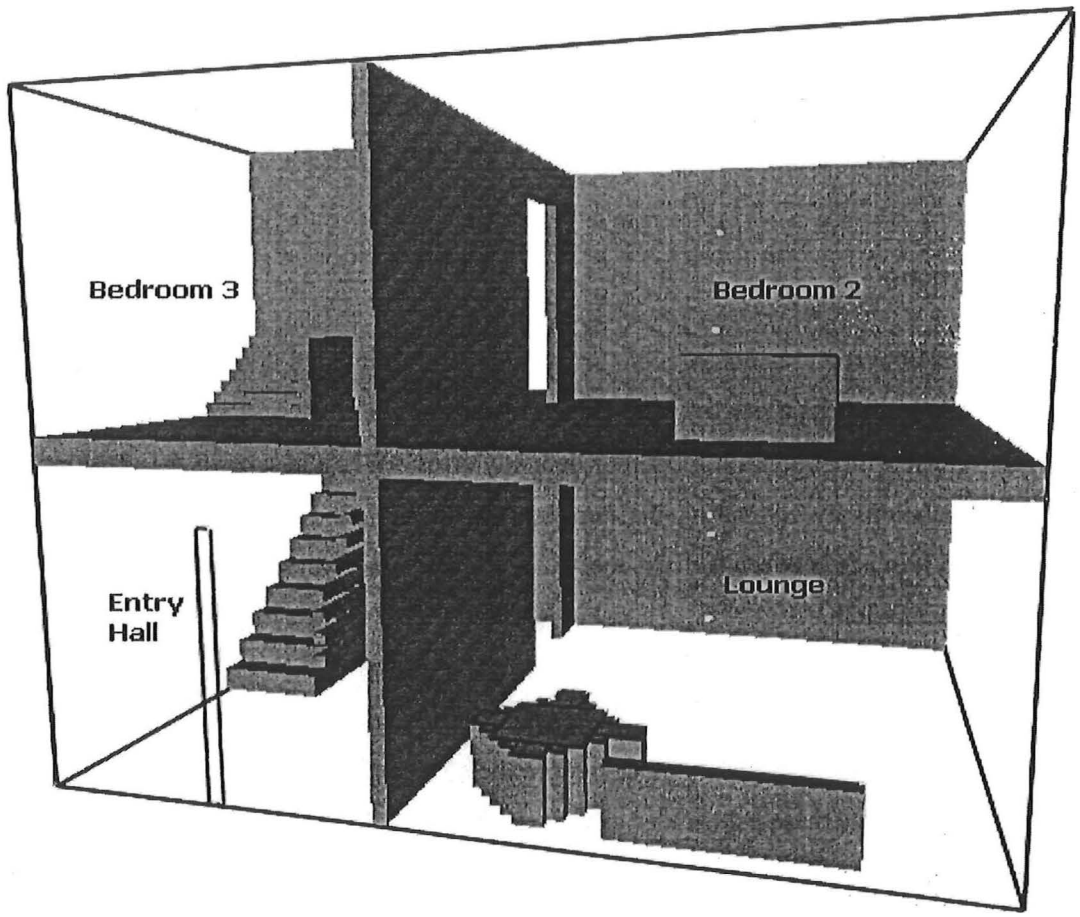

Figure 4-2. SMOKEVIEW Image of House, View From East Wall

Later in the study, in order to check the sensitivity of the choice of grid size, another simulation was developed which had a grid size of 75mm. While this grid size allowed narrower ventilation and balustrades, and allowed the 750mm doorways to be modelled at their actual width, it created the following difficulties:

- Wall thickness was 75mm instead of the actual 100mm.
- Floor thickness was 225mm instead of the actual 200mm.

The difficulties with the sloping ceiling and balustrades remained, as will be discussed in the next section.

4.4 Obstructions

As mentioned above, it was not possible to model a 750mm internal doorway with a 100mm grid. To assess the sensitivity over the choice of doorway size, two successive simulations were performed with 700mm and 800mm doorway sizes. When analyzing the results from the two simulations by comparing the temperatures in all four rooms, there was barely a discernable difference between the two door sizes. Subsequent to this, the study was based on the 800mm door width.

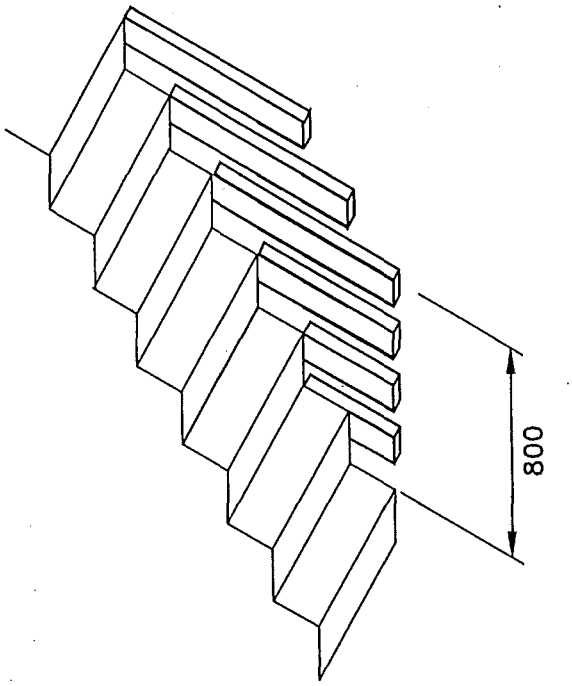

Figure 4-3. Details of Balustrade to Stairs

In the test house the balustrades to the stairs were on an angle that matched the slope of the stairs. As this was also difficult to model within the allocated grid structure, several attempts were made to emulate these balustrades as are presented in Appendix B. The option chosen is shown in Figure 4-3. This was chosen because it most closely emulates the temperatures in the stair thermocouple tree (tree #4).

A further difficulty arose because there was a sloped ceiling above a portion of the stairs. Because of the grid structure this slope had to be modelled as a series of steps, which can be seen in Figure 4-1. This creates difficulties for the airflow in that as the

hot gases from the fire move up the stairwell, eddies will be created in these steps in the ceiling which will change the flow pattern near this feature.

The effects of gas flow around light bulbs, smoke detectors (both domestic and commercial) or the instrumentation within the house have not been considered in this study.

4.5 Ambient Temperatures

The varying ambient temperatures at various locations around the house can have an effect on the activation times of the detectors, and so can the heating system within the house. There were five radiators in the house, three upstairs and two downstairs. However, two radiators were located in bedrooms 1 and 3 which had their doors closed for the duration of the tests. In light of all of this, two extra investigations took place:

- How long do the radiators have to be left on to create steady ambient temperatures within the house?
- Do the radiators in bedrooms 1 and 3 have to be considered in the simulations given that they were behind closed doors?

A simulation with three radiators was run for some time to answer the first question, and the results are shown in Figure 4-4. This graph presents the temperature plots for a number of thermocouple trees as indicated in the key. It also shows that the simulations have to be run for at least 600 seconds for steady conditions to be achieved.

To investigate whether the extra radiators in bedrooms 1 and 3 had any significant impact on ambient temperatures, two consecutive simulations were performed, one with three radiators and the other with five. For the five-radiator simulation there were wall openings near the door locations to bedrooms 1 and 3 similar to those at the front door on the ground floor. Figure 4-5 presents the temperatures at various heights for different thermocouple trees located in various rooms, and compares the ambient

temperatures for both simulations at 600 seconds, with little difference between the two.

With this information it was decided that with future simulations the radiators would be left for an incipient phase of 600 seconds before the chair fire began, and that only three radiators would be modelled in the house. The radiator in the lounge would stop at the same time that the chair fire started, and all of the other radiators would remain in operation for the duration of the simulation.

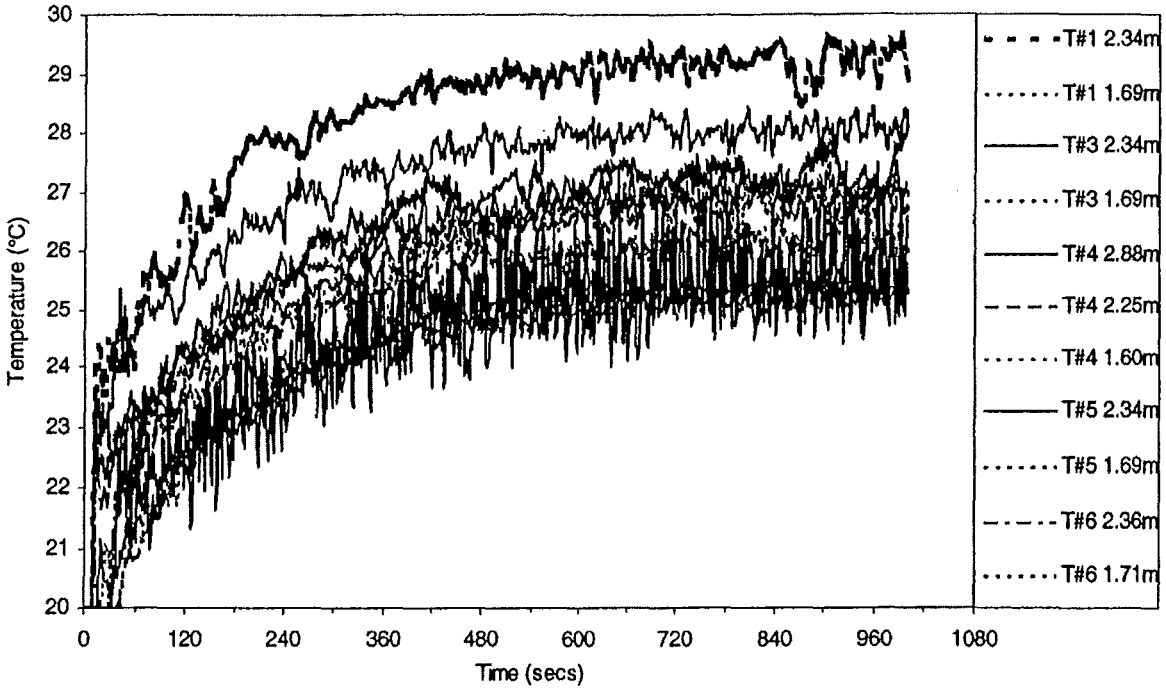

Figure 4-4. Generation of Ambient Temperatures

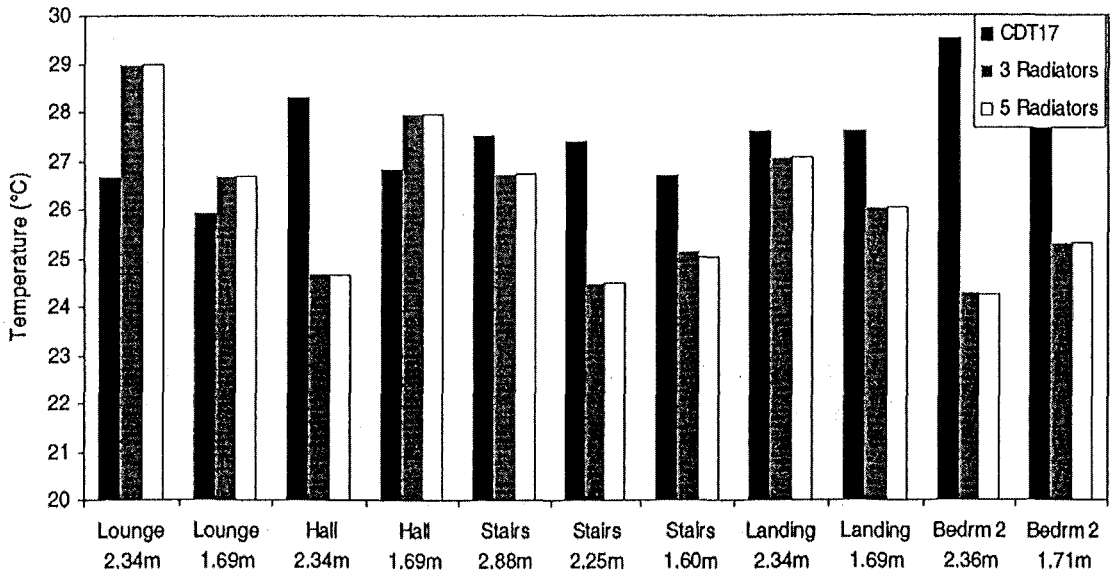

Figure 4-5. Comparisons of Ambient Temperatures

Figure 4-5 also compares the predicted ambient temperatures with those for test CDT17. This shows that the predicted temperatures are overestimated in the lounge, and tend to switch from overestimated to underestimated in the direction that gases would migrate in a fire, i.e. from the lounge up to bedroom 2. The predicted temperatures varied from approximately 24°C to 29°C.

During later stages of the study it was decided to model soot production, which is related to HRR. While FDS is able to model soot, it seemed unable to discern between the various sources of the total HRR. In other words, the radiators produced soot. To circumvent this problem it was decided that, for simulations when soot behaviour was required, there would be no radiators in the house, and the ambient temperatures throughout the house would be set at 27°C.

4.6 Derivation of HRR Curves

FDS is able to model non-steady fire behaviour by allowing the inclusion of time-dependant boundary conditions. The user can input fractions of heat release rate at specific times, which FDS then combines with the input value for heat release rate per unit area (HRRPUA) to emulate the required fire behaviour.

The actual HRR curve was not measured during the actual tests because of the difficulties in doing so. As this information is fundamental to the modelling of the fire, the HRR was derived from the mass loss history. This history from test CDT17 is shown in Figure 4-6. The values for the mass burning rate $\dot{m}$ were then derived, as shown on Figure 4-7 after being multiplied by the effective heat of combustion ΔH_{eff}. Figure 4-7 also shows the idealized trend of the HRR curve that was input into FDS. Simulations were then run based on this data, and the resulting temperatures were compared with those, which were measured during the actual fire test. The HRRPUA was adjusted and the simulations rerun until a good match existed between the magnitudes of the predicted and actual temperatures in the lounge as shown in Figure 4-10. Having derived a good match for temperatures, the corresponding HRR for the actual test was deemed to have been found. Figure 4-7 compares the HRR curve from the temperature matching simulation output with that derived from the mass loss history (CDT 17) which both demonstrate a similar trend.

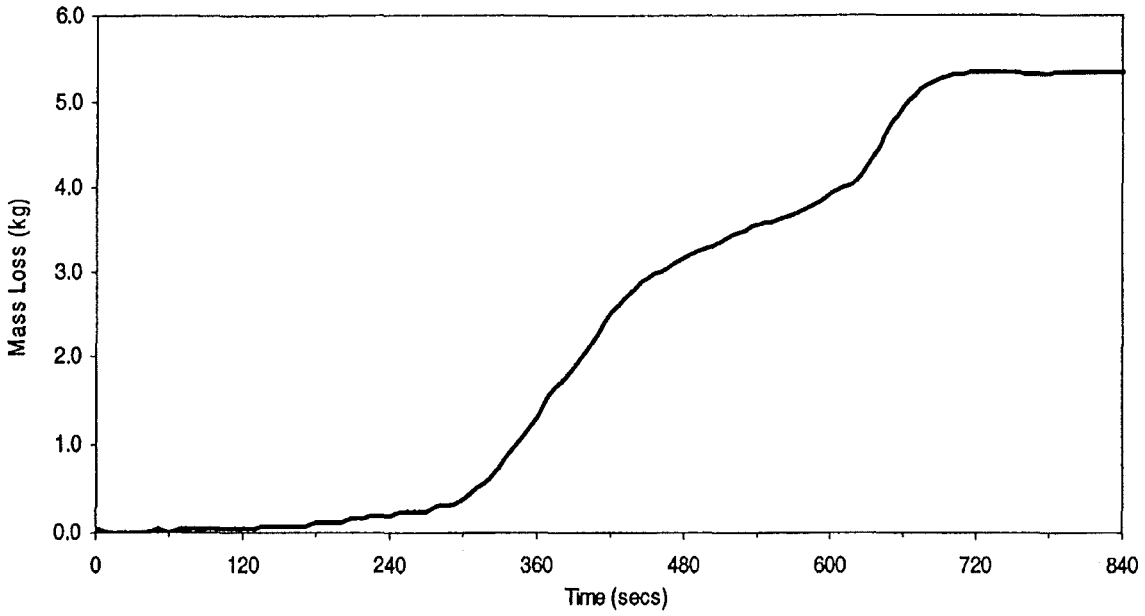

Figure 4-6. Mass Loss History – Test CDT17

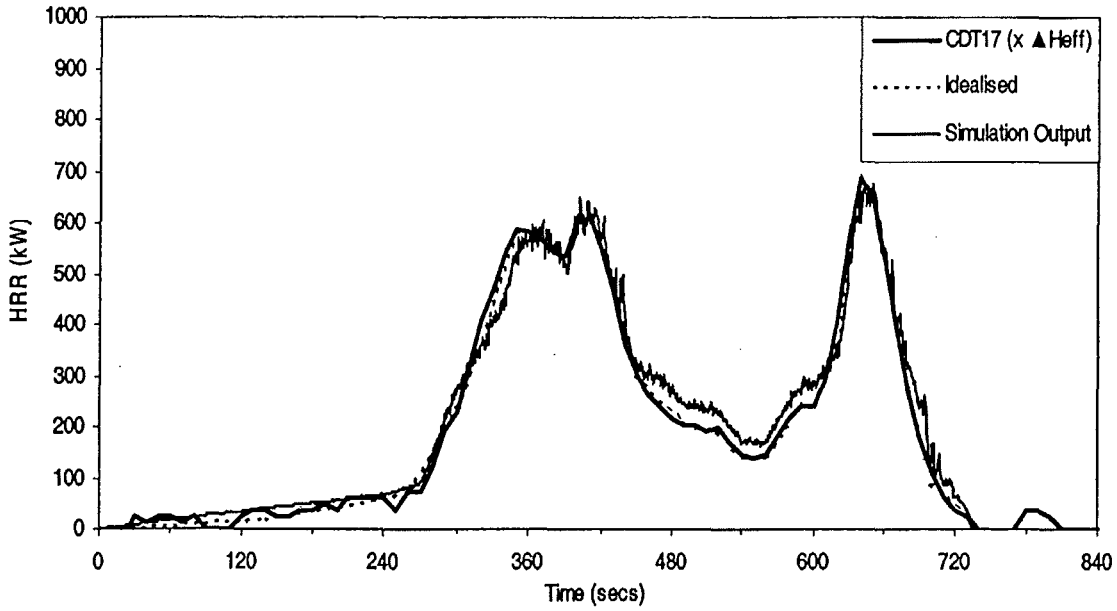

Figure 4-7. Derivation of HRR Curves – Test CDT17

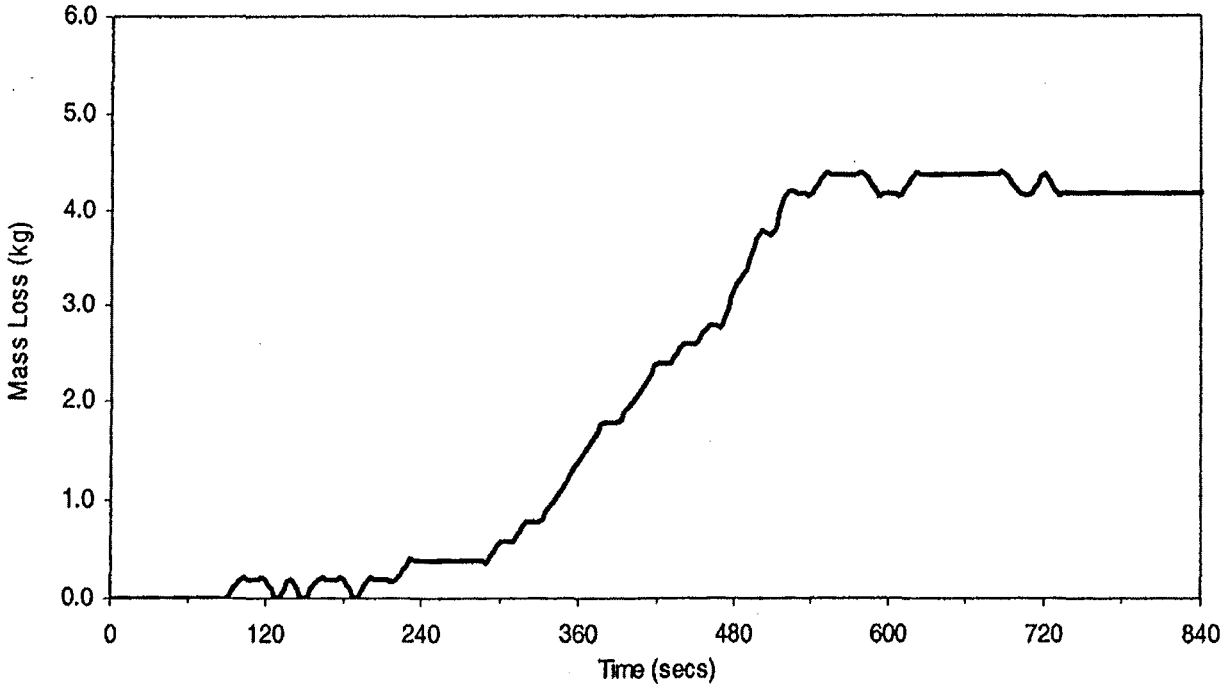

Figure 4-8. Mass Loss History – Test CDT20

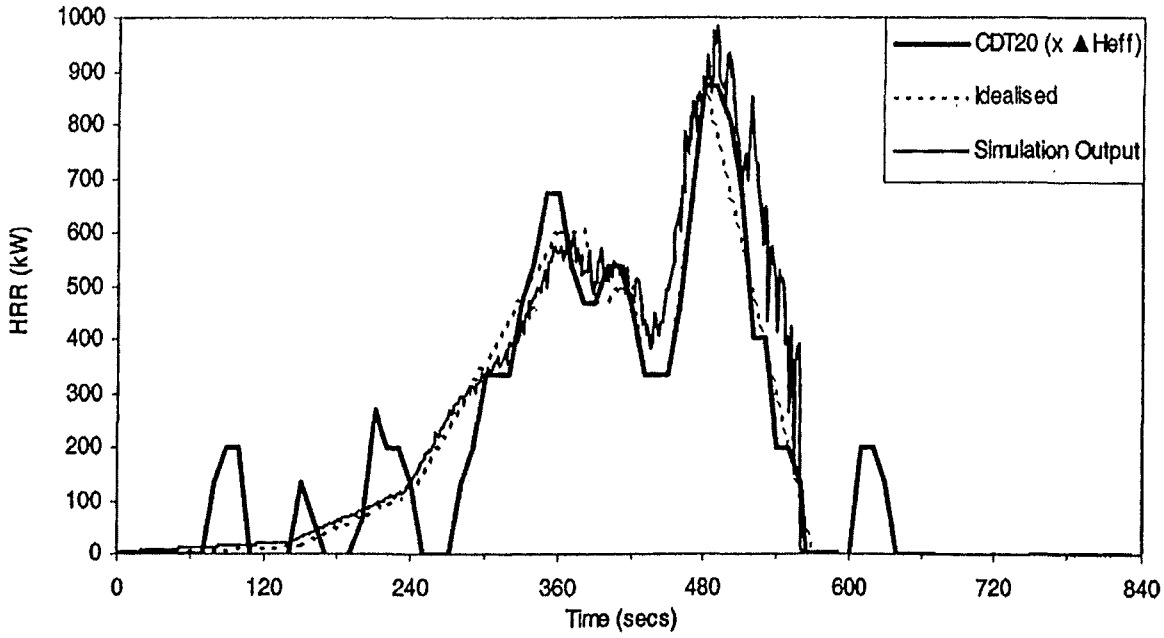

Figure 4-9. Derivation of HRR Curves – Test CDT20

Figures 4-8 and 4-9 show the same plots for CDT20. Because of the rather erratic mass loss curve, the family of curves for HRR does not match as well as the previous test.

With this method the heat of combustion can only be determined after a suitable match of temperatures has been attained. Karlsson et al. describe the relationship between HRR (Q) and heat of combustion as:

$$Q = \dot{m}\,\Delta H_{eff} \qquad \ldots(4\text{-}1)$$

where $\dot{m}$ = mass burning rate

This will derive the average effective heat of combustion. It was found that ΔH_{eff} was approximately 30 MJ/kg for test CDT17 and 34 MJ/kg for test CDT20. These values are consistent with the range of values of 30 - 38 MJ/kg that Girgis derived, as discussed earlier.

Figures 4-11 and 4-12 compare the HRR of tests CDT17 and CDT20 respectively with a medium t^2 growth curve after a 160 and 150 second incipient phases for test CDT17 and CDT20 respectively. Both tests show a good match for the medium t^2 growth curves. While the first peak in HRR for both tests occurs about the same time and has approximately the same magnitude, the second peak for CDT20 occurs earlier, and has an approximately 60% higher magnitude, and the duration of the fire is less compared to CDT17. While the two test fires have a lot of similarities, they had quite different outcomes as to detector response, as will be discussed later.

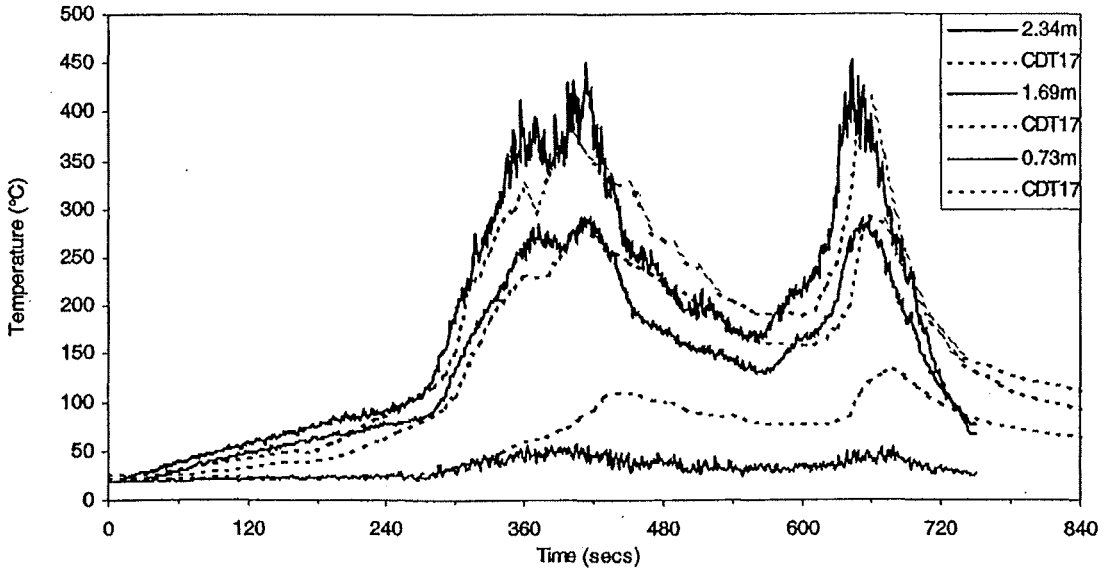

Figure 4-10. Uncorrected Lounge Temperatures - Test CDT17

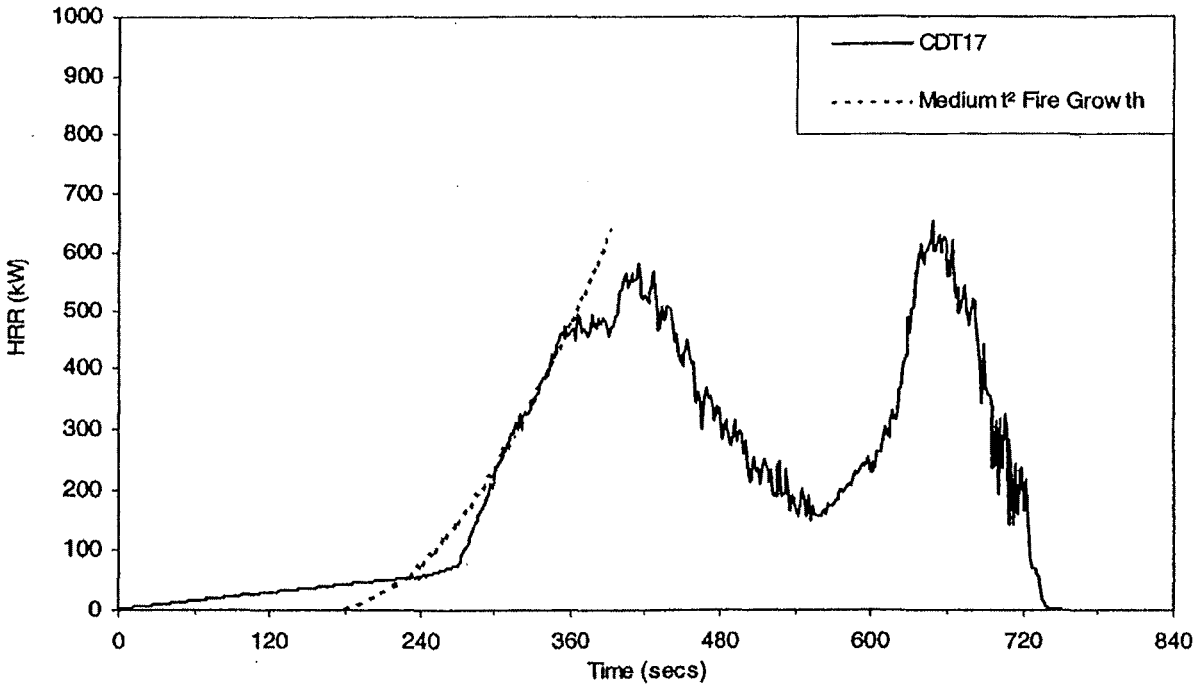

Figure 4-11. HRR Curve – Test CDT17

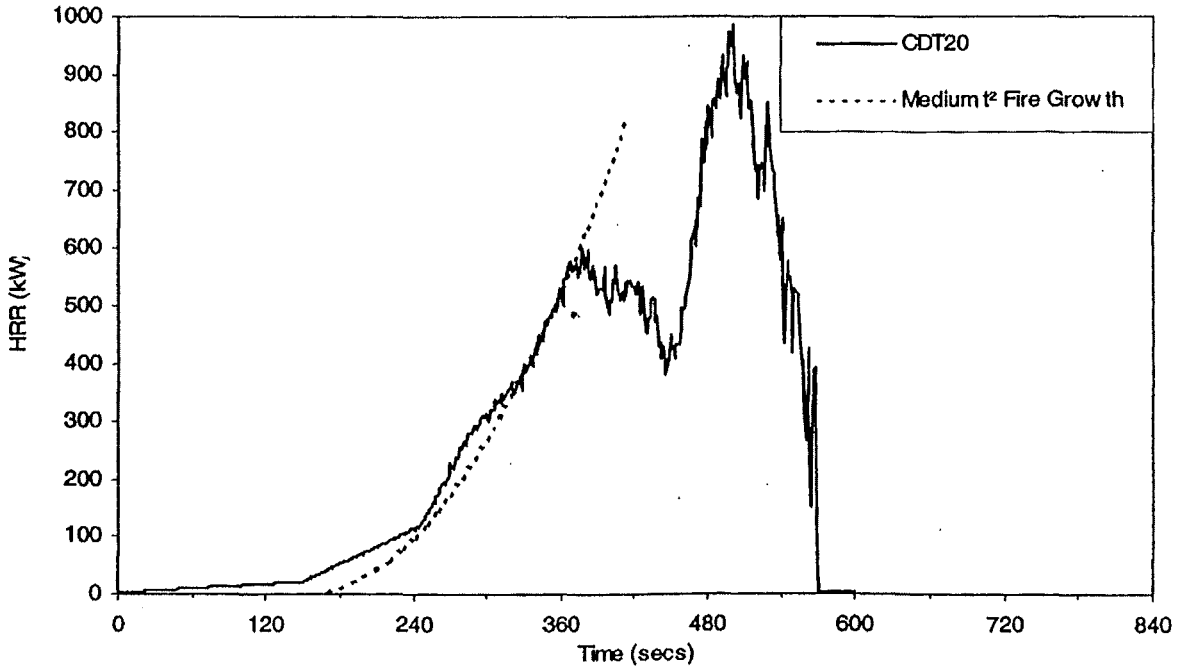

Figure 4-12. HRR Curve – Test CDT20

4.7 Correction of Time Error

Figure 4-10 presents the temperature plots in the lounge for test CDT17 at various thermocouple heights, as indicated by the key. It should be noted that the trace for the predicted temperatures are in advance of the test temperatures by a few seconds. As an electric igniter lit a timber crib on the seat of the chair to start the fire, it could be that there is some error between the recorded time for the start of the test and the actual test start time. In light of this some corrections were made to the test times to accommodate these differences.

Figure 4-13 compares the predicted and actual test temperature readings for test CDT17 after a correction of -10 seconds was applied to the test time. Figure 4-14 considers CDT20 with a -15 second correction included. These plots show a closer match between the two traces than the earlier plots. Note that this time correction was also applied to the detector activation times given in Figures 3-2 and 3-3.

4.8 Optical Density

The soot density in the environment around the detector D_{uo} is required by Heskestad's method. This is quantified by the optical density, which is a value derived by FDS after the input of a specific value for soot yield from combustion. As discussed in Section 4.5, extra simulations that did not include radiators were performed to assess the soot density throughout the house.

For this study a nominal value for the soot yield Y_s of 0.10 kg/kg was assumed. From this information, FDS calculates a distance that correlates with the visibility distance S as:

$$S = C.K \qquad \ldots (4\text{-}2)$$

where C = constant

K = light extinction coefficient

The constant C is related to the intensity of visibility of signs, and in FDS it has the default value of 3. As Mulholland discusses, this distance S is related to the optical density as follows:

$$D_{uo} = K / 2.3 \qquad \ldots (4\text{-}3)$$

The sensitivity of detectors is commonly reported in terms of obscuration O_{bs}. As Schifihiti (2001) discusses, obscuration is related to optical density in the following equations:

Percent obscuration per unit distance l:

$$\%O_{bs} = 100\left[1 - \left(\frac{I}{I_o}\right)^{1/l}\right]$$

Optical density per unit distance l:

$$D_{uo} = -\frac{1}{l} LOG\left(\frac{I}{I_o}\right)$$

where l = unit distance

I = intensity of light beam through smoke

I_o = initial intensity of light beam

In Heskestad's method, the value of D_{uo} found by FDS is equated to the optical density inside the detector D_{ui} after entry delays. D_{ui} is then compared against the preset activation density for the specific detector. In this study this activation density was the reasonably high figure of $0.14 m^{-1}$, as discussed by Mulholland for black smoke. As Brozovsky et al. states, Underwriters Laboratories (UL) require smoke detectors to respond within the range for optical density of 0.007 to $0.058 m^{-1}$.

4.9 Development of the House Domain Geometry

During the development of the house's computational domain, the effects of several different modelling functions of FDS and features of the house were investigated. This section discusses the ramifications of these differences.

The domain used to analyse the house was developed by initially creating a representation of the lounge (fire room) only. This was later extended to include the entire ground floor, and later the top floor was added. For the lounge computational domain only, it was found that the location of the chair within the room affected the HRR curve. The chair was located fairly close to the wall as shown in Figure 4-2, and its closeness had an effect on the HRR curve. This is undoubtedly because the closer the chair is to the wall the lesser volume of air can be entrained into the fire's plume. Furthermore, as the volume of the entire computational domain increased, the amount of ventilation into the analysis volume changed, which also affected the HRR curve. What can be determined from this is that any model should emulate the location of the fire as closely as possible, and that only modelling a single room in a multi-room enclosure does not necessarily adequately emulate the effects of a fire, even within the fire room.

There has already been some discussion earlier in this chapter about the difficulties of accommodating the balustrades within the domain. As the balustrades have to fit within the allocated grid layout, several different arrangements of balustrade elements were considered. The balustrade layout finally chosen was the one that most closely matched the temperature profile on the stairs that was attained during the actual fire test, based on a model of the ground floor only without the function of radiators. The results of this analysis are presented in Appendix B. This includes a comparison with a simulation where no balustrade was included in the domain at all, which demonstrates that the presence of balustrades cools temperatures down.

Also discussed earlier was the setting to disallow the creation of eddies within the sloped ceiling above the staircase. Consecutive simulations revealed that not allowing these eddies increases the temperatures within the upper floor by approximately 5°C. Another feature of the house that had an effect on temperatures was the incorporation of the internal walls as Gib board. This had the consequences of increasing the temperatures in the fire room by approximately 20°C, and had a lesser effect on the temperatures on the first floor.

Chapter 5 RESULTS AND DISCUSSION

5.1 Temperatures

Plots of predicted and actual test temperatures for tests CDT 17 and CDT20 were shown earlier in Figures 4-13 and 4-14 respectively after the correction of the time error as discussed earlier. These show a good match between predicted and actual temperatures at heights of 2.34m and 1.69m above the floor for the both fire tests. A lesser match was derived at a height of 0.73m, but a match at this lower height is of lesser importance for modelling the behaviour of detectors at ceiling level. These same plots are shown in Figures 5-1 and 5-2 at a larger scale over the initial 360 second time period, which is the time period in which most of the detectors in the house had activated. Once again these plots show a reasonably good match at height of 2.34m and 1.69m, with a lesser match at a height of 0.73m. A full family of curves of temperature for all five thermocouple trees that were modelled is presented in Appendix C for fire test CDT17 and Appendix D for test CDT20.

5.2 Grid Sizes

As stated earlier, most of this study was performed assuming a grid size of 100mm. To ascertain the significance that the choice of grid size has on the results, one fire test (CDT17) was also analysed with a grid size of 75mm. The match between the plots of HRR is shown in Figure 5-3. Unfortunately, the 75mm grid simulation overestimates the HRR. This is indicative of the fact that the input value for HRRPUA was slightly overestimated rather than an error is the results of FDS. Nonetheless there is a close match between the trends of the two plots.

Plots of temperatures in the lounge, entry hall and bedroom 2 are shown in Figures 5-4 to 5-6 respectively. While the overestimation in HRRPUA makes itself known at the height of 2.34m in Figure 5-4, this effect is much less obvious at the lower two heights in this figure. Moreover, in Figures 5-5 and 5-6 there is little difference between the results of the two grid sizes, particularly at the greater heights. From these results, and considering the overestimation in HRRPUA, it can be determined that there is little difference between the 75mm and 100mm grid sizes in

terms of the prediction of temperatures, which agrees with the findings of Friday et al. as discussed earlier.

It should be noted that while there is little difference between the two grid sizes in terms of temperature, there was a significant difference in computational resources. In fact the calculation time for the 75mm grid model was four times longer than the 100mm grid for the same analysis volume.

A full family of curves of temperature for all five thermocouple trees that were modelled with a 75mm gird size is presented in Appendix E for fire test CDT 17.

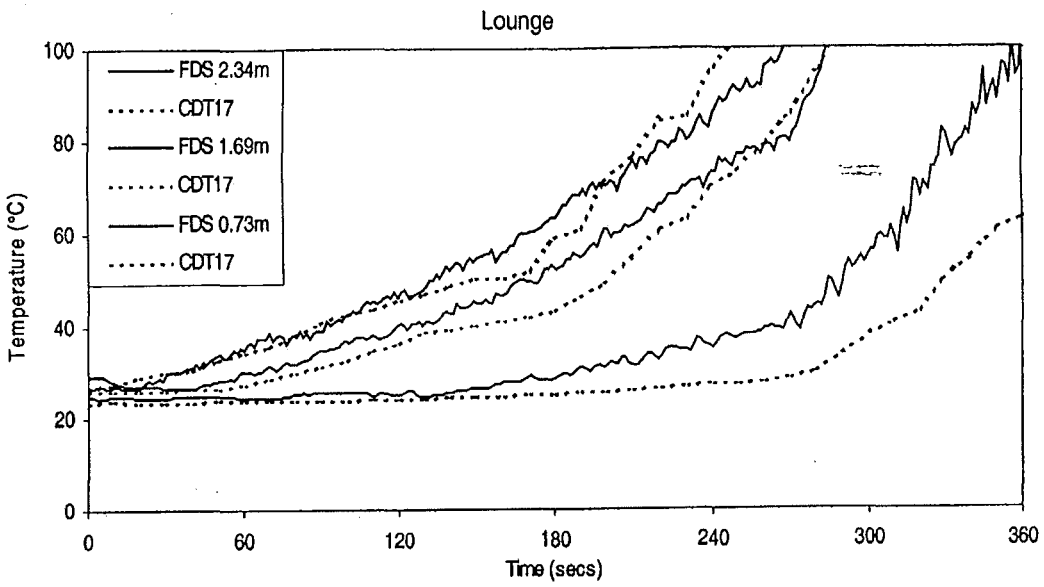

Figure 5-1. Lounge Temperatures – CDT17

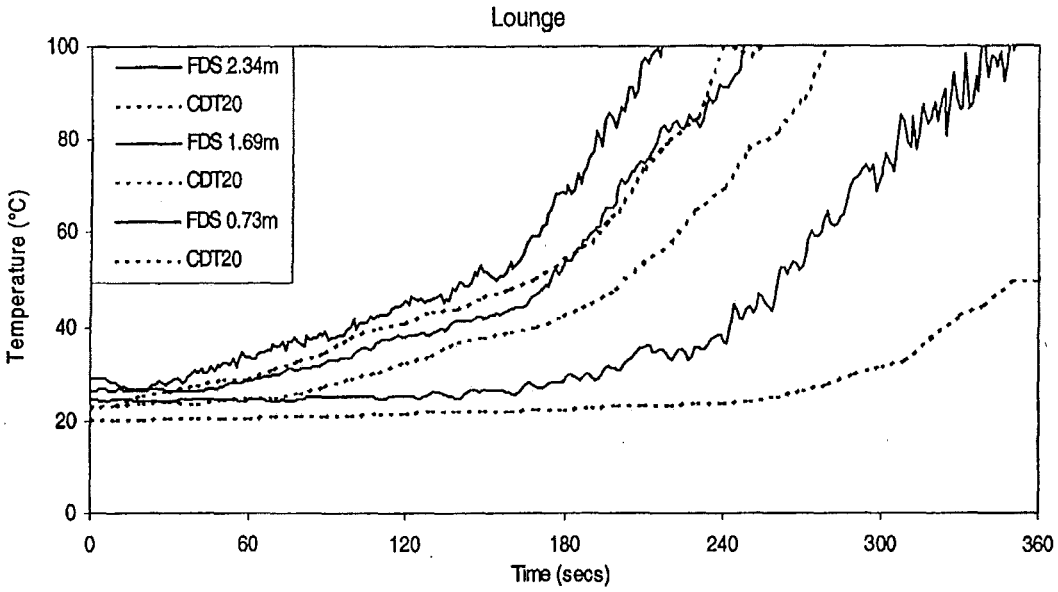

Figure 5-2. Lounge Temperatures – CDT20

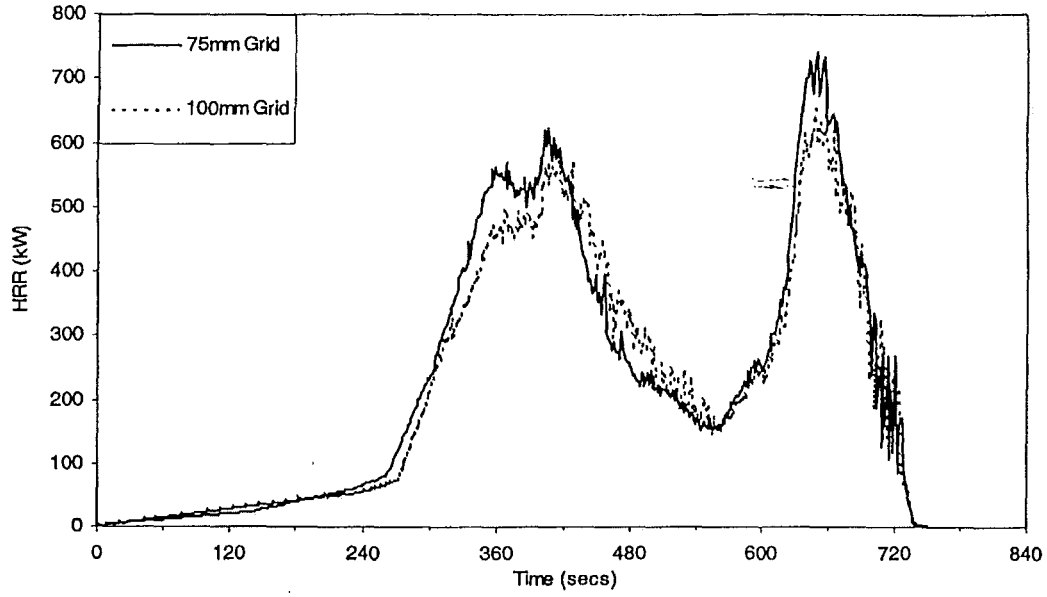

Figure 5-3. HRR Curves, Comparison of Grid Sizes – CDT17

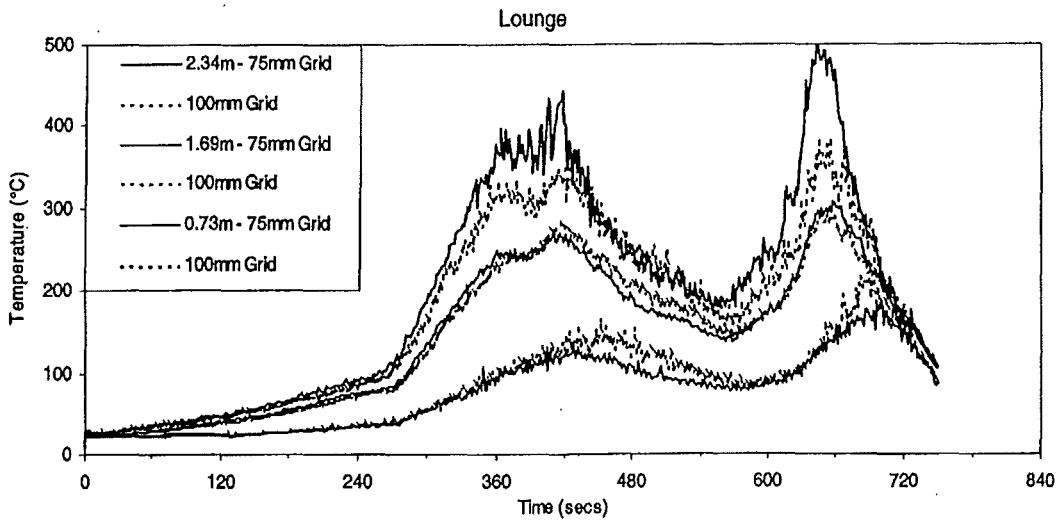

Figure 5-4. Lounge Temperatures, Comparison of Grid Sizes – CDT17

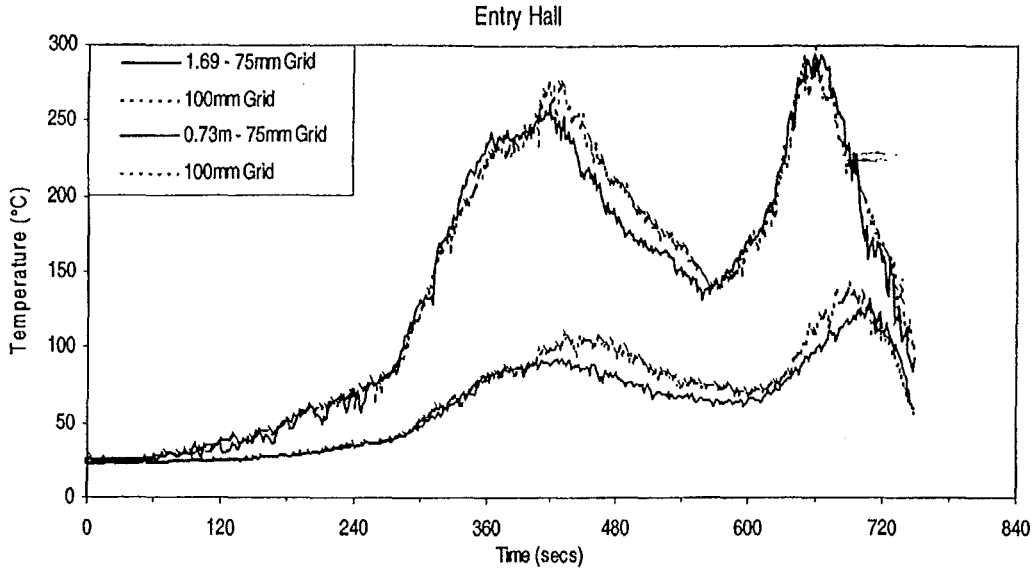

Figure 5-5. Entry Hall Temperatures, Comparison of Grid Sizes – CDT17

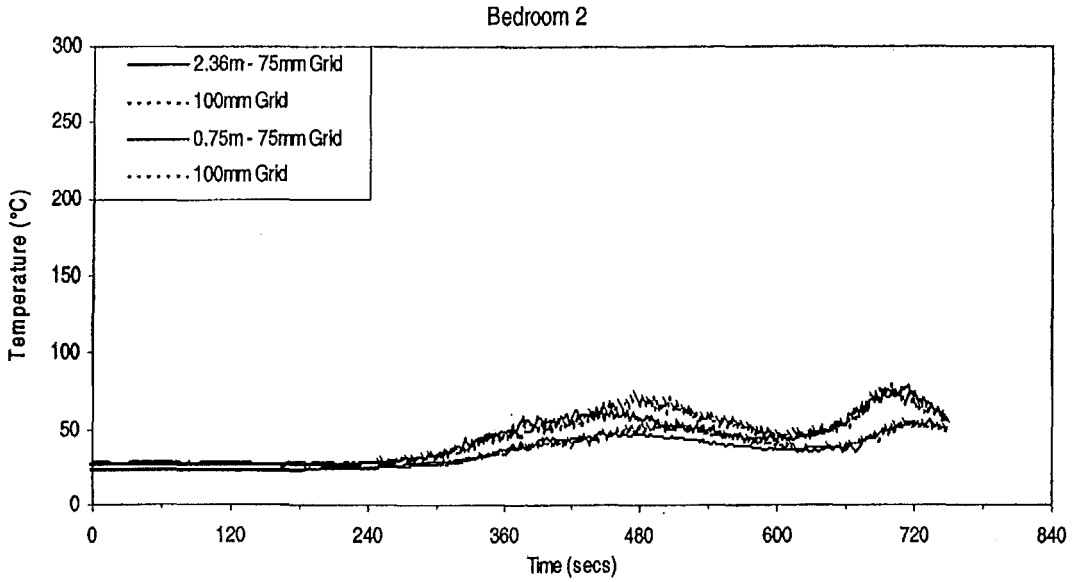

Figure 5-6. Bedroom 2 Temperatures, Comparison of Grid Sizes – CDT17

5.3 Optical Density

As discussed earlier, the simulations that attempted to model the production of smoke did not include the house's radiators because of the difficulties associated with these radiators producing their own smoke. The initial estimate for smoke yield was nominally taken as 0.10 kg/kg, and the results of these simulations are presented in Figures 5-7 and 5-8 within the lounge and bedroom 2 only for test CDT17, and Figures 5-9 and 5-10 for test CDT20. As expected the rise in optical density in the bedroom trails that in the lounge by about 120 seconds. For both tests, the trend of the increase in optical density is well modelled. Unfortunately, the prediction of density is overestimated in the first 300 seconds of each simulation, as these figures show. The significance of this inaccuracy is that this is the time at which most of the smoke detectors within the house had activated. A full family of curves of optical density for all four rooms within the house is presented in Appendix C for fire test CDT17 and Appendix D for test CDT20.

The inaccuracy in these predictions caused difficulties in applying Heskestad's method, as will be discussed later in this chapter. As a means of attempting to draw some useful conclusions about this particular prediction method, the results for optical density that were derived from FDS were arbitrarily halved. The results of this

factored reduction can be seen in Figures 5-11 to 5-14 for the same rooms and tests as the unfactored results discussed above. These figures show that the trends in increase of optical density does not match as well as previously, but the magnitudes of actual and predicted optical density are more equal near the actual activation times. These results were still used in an investigation into Heskestad' s method, as will be discussed later.

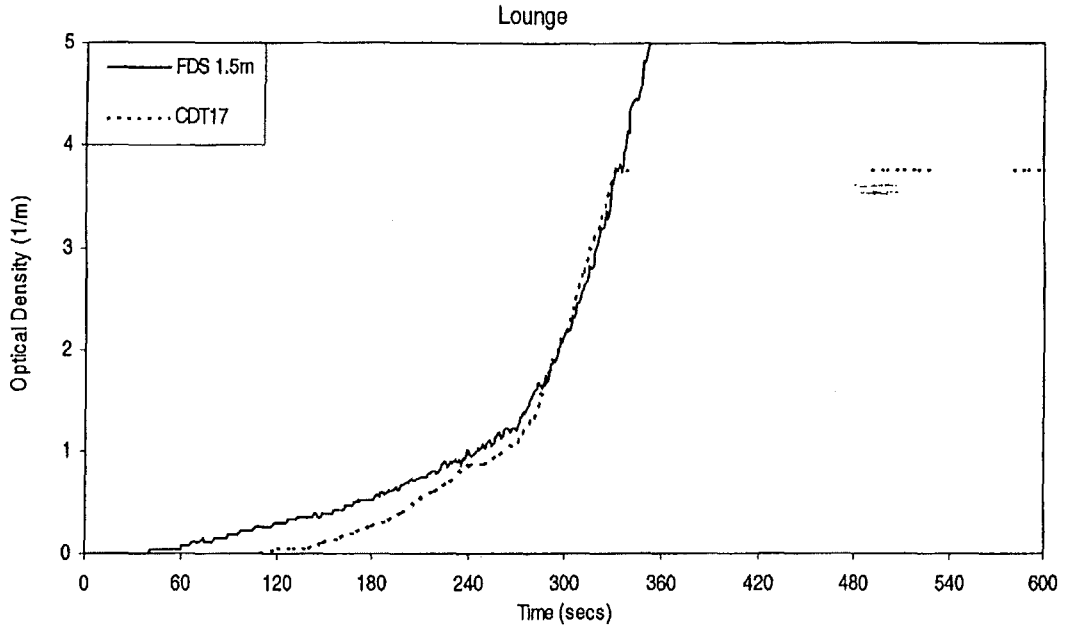

Figure 5-7. Lounge Optical Density – CDT17

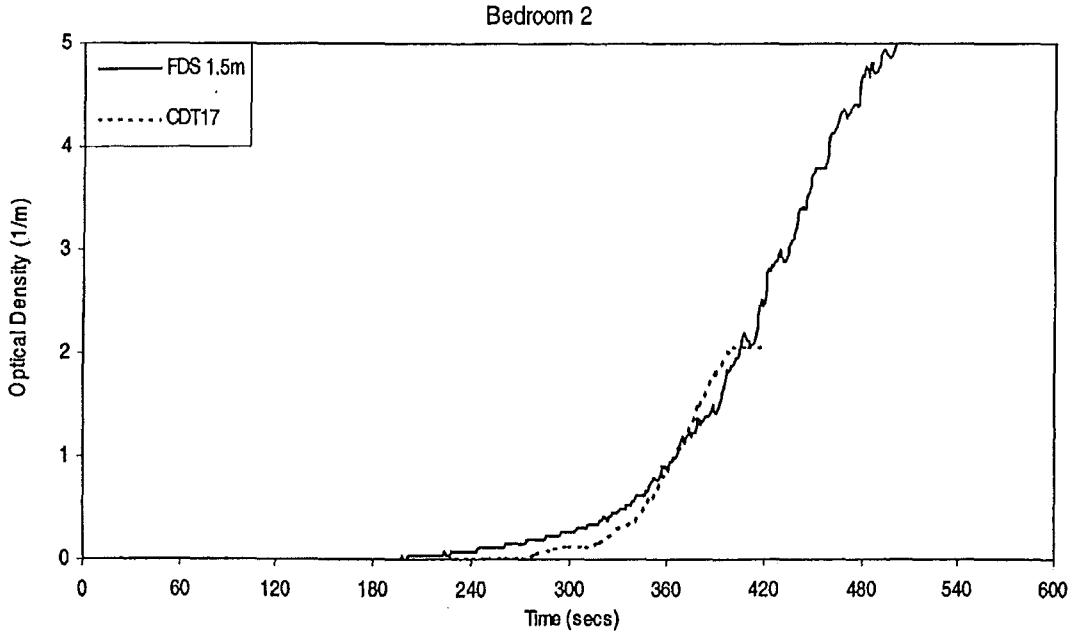

Figure 5-8. Bedroom 2 Optical Density – CDT17

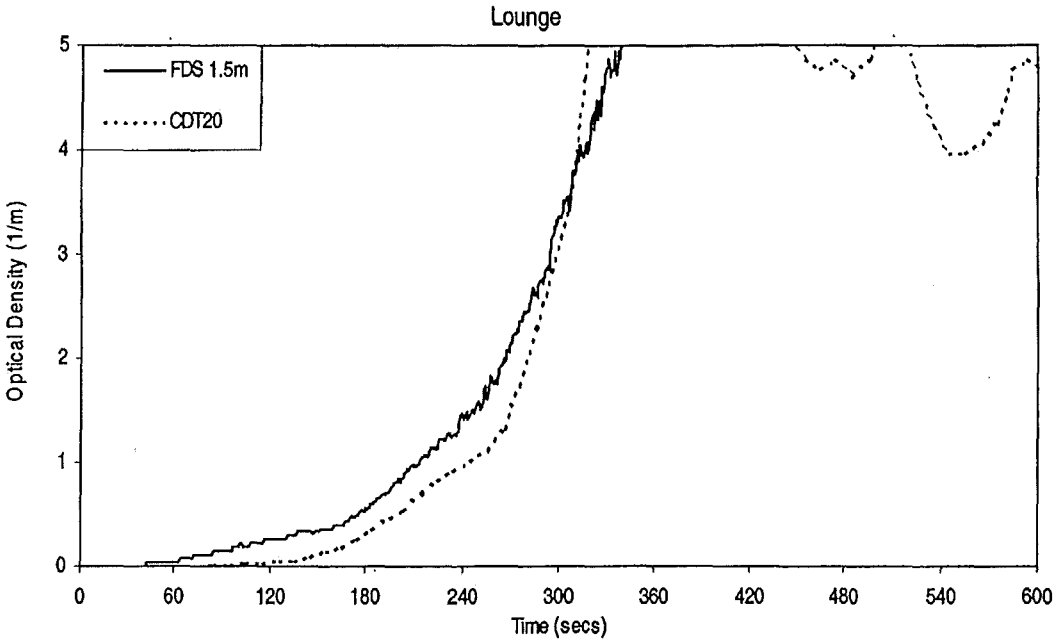

Figure 5-9. Lounge Optical Density – CDT20

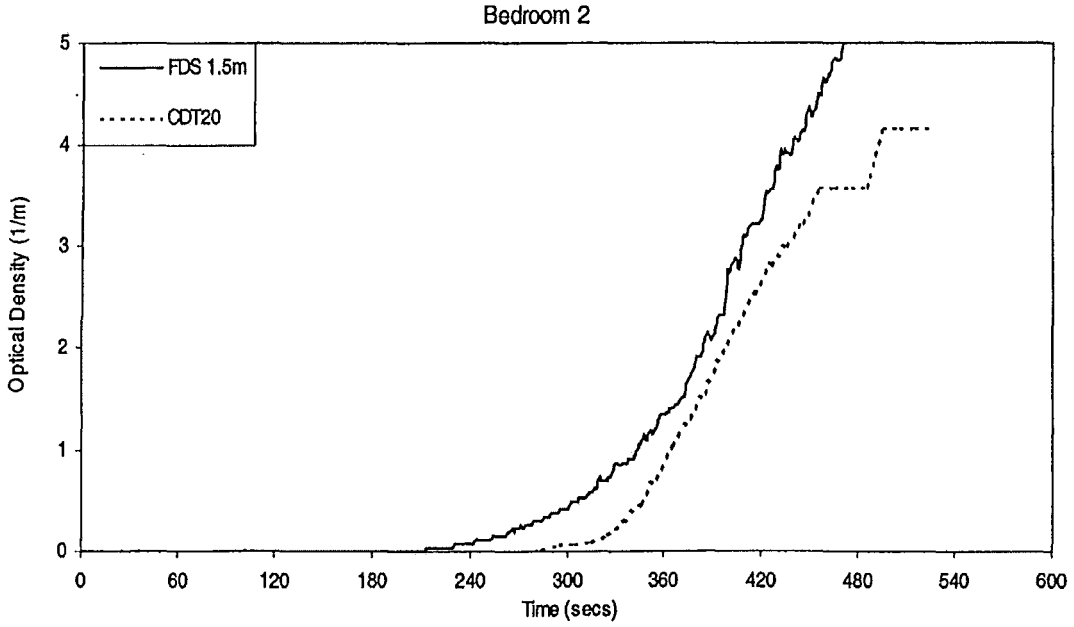

Figure 5-10. Bedroom 2 Optical Density – CDT20

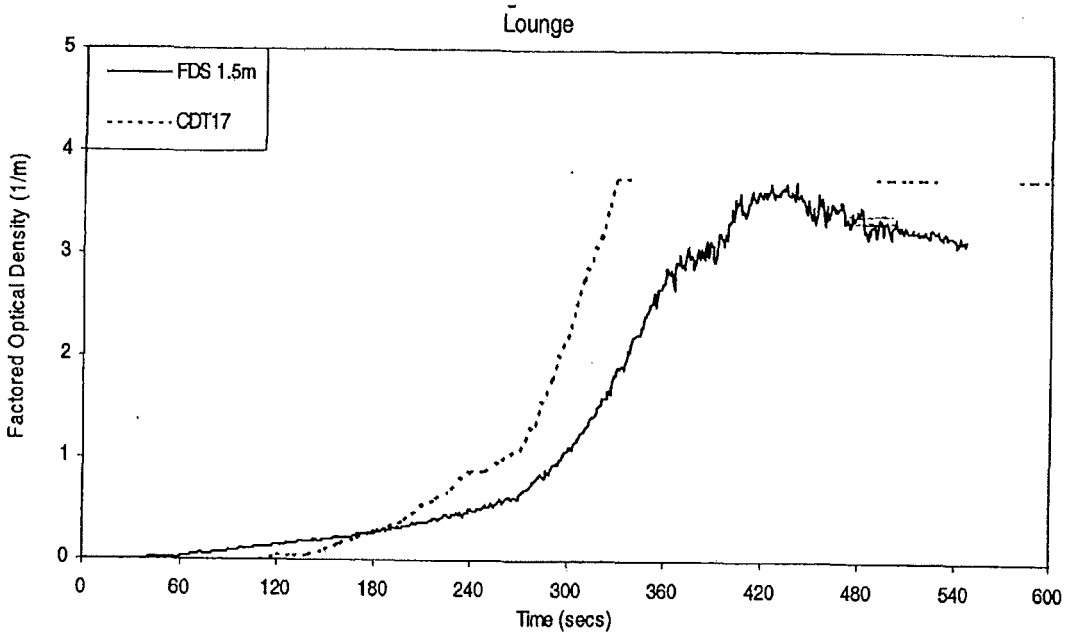

Figure 5-11. Factored Lounge Optical Density – CDT17

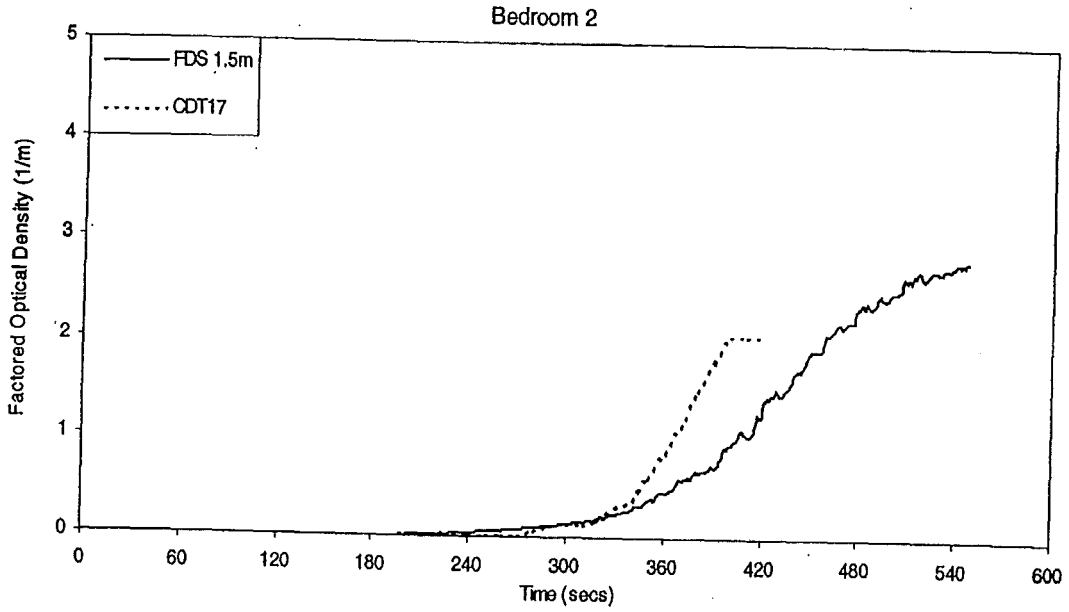

Figure 5-12. Factored Bedroom 2 Optical Density – CDT17

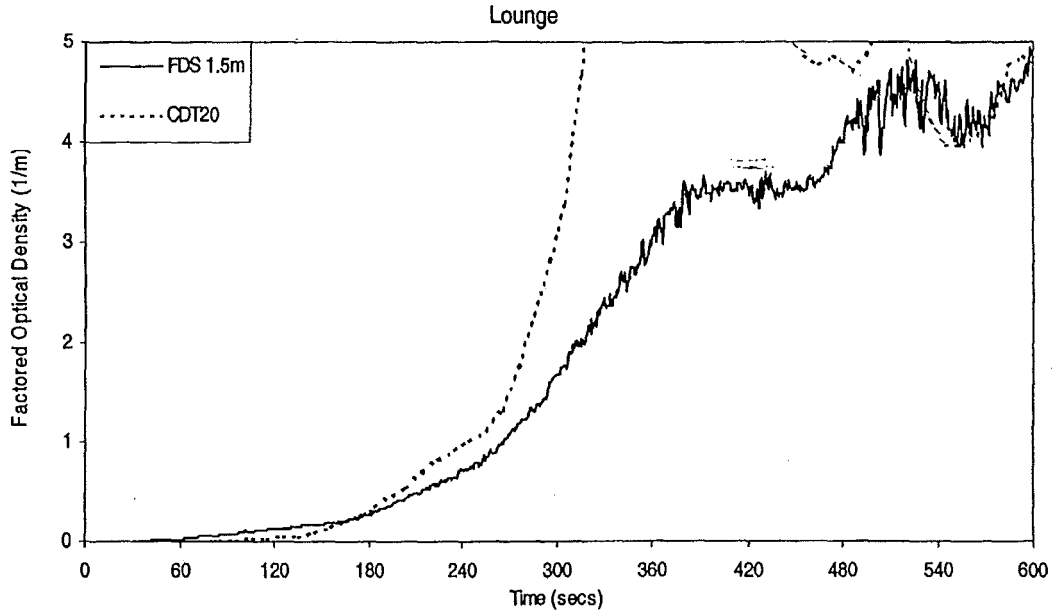

Figure 5-13. Factored Lounge Optical Density – CDT20

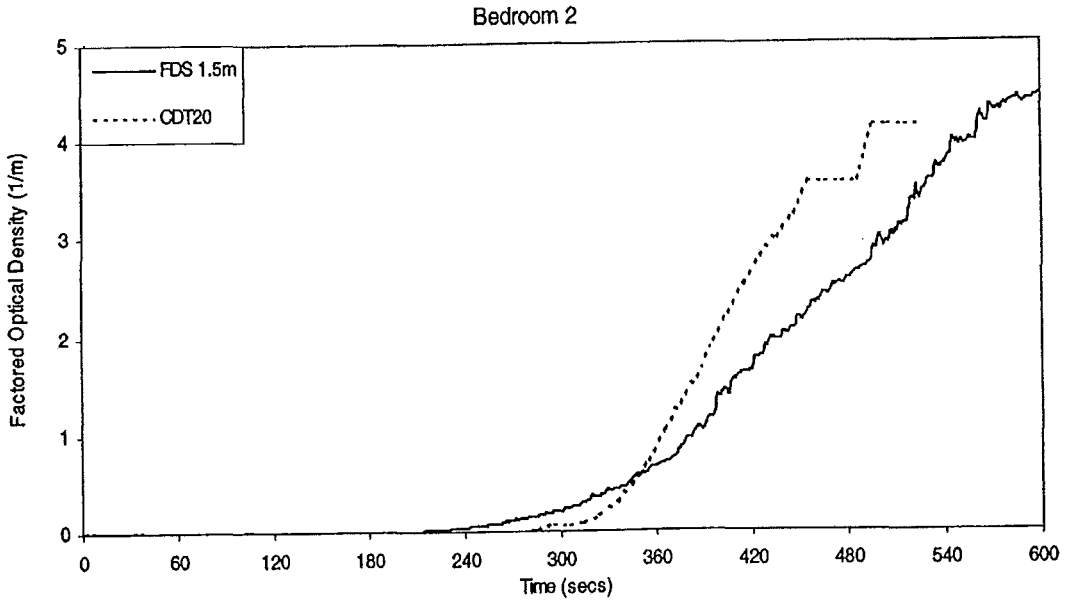

Figure 5-14. Factored Bedroom 2 Optical Density – CDT20

5.4 Modelling of Smoke Detector Behaviour

Three prediction methods were considered in this study as was discussed in Chapter 2. The results for the predictions of activation times are compared with the actual activation times for both fire tests.

5.4.1 Temperature Correlation

The results of the analysis of activation times for the ionisation detectors from test fire CDT 17 are shown in Figure 5-15 for the temperature correlation method. The ionisation and optical detectors were located in the lounge, entry hall, landing and bedroom 2. Taking the lounge as an example, if the activation temperature T_{act} is 4°C, then the predicted activation time is 64 seconds. If T_{act} is 13°C the prediction time is 129 seconds, and if 20°C then the time is 178 seconds. This is compared in Figure 5-15 with the test activation time of 110 seconds. Considering all four ionisation detectors, if T_{act} = 4°C then there is a significant error in the lounge, a lesser error in the entry hall, but a good match on the top floor. If T_{act} = 13°C then there is a reasonably good match for all detectors except the landing. Meanwhile the T_{act} = 20°C option would appear to be unreasonably high for this detector.

However, the situation is quite different for test CDT20 as shown in Figure 5-16. In this case the same options as to activation temperatures are given, but the option of T_{act} = 20°C goes from being too high in the previous test to not being high enough.

The predicted times for the optical detectors for test CDT1 7 is presented in Figure 5-17. In this case, T_{act} = 20°C provides a good match in the lounge and entry hall, but provides up to a 45% error on the upper floor of the house. Conversely, if T_{act} had the significantly lower value of 10°C, then while there will be a reasonably good match for the upper floor detectors, but errors of up to 30% in the lounge. But for test CDT20 in Figure 5-18 the activation temperature of 20°C will underestimate the activation times in every case.

From the results of this method, and more particularly from the results of test CDT20, it will be hard to justify an activation temperature of less than 20°C. This value is significantly higher than the 2-4°C range of values given by Collier, and the types of fires cannot explain the significant difference between these two values. Figure 5-19 compares the HRR curve from Collier's fire with a fast t^2 growth fire, whereas Figure 5-20 compares CDT20 with a medium t^2 growth fire. From these two figures it can be seen that both fires had a t^2 growth, although while CDT20 was vitiated and extinguished itself, sprinklers that were manually operated at approximately 260 seconds extinguished the Collier fire. The only other significant difference between the two fires was the fact that CDT20 had airflow currents setup within the test house before the fire started. This is presumed not to have occurred in the Collier test. Collier did not specify the type of foam in the chair that was burnt.

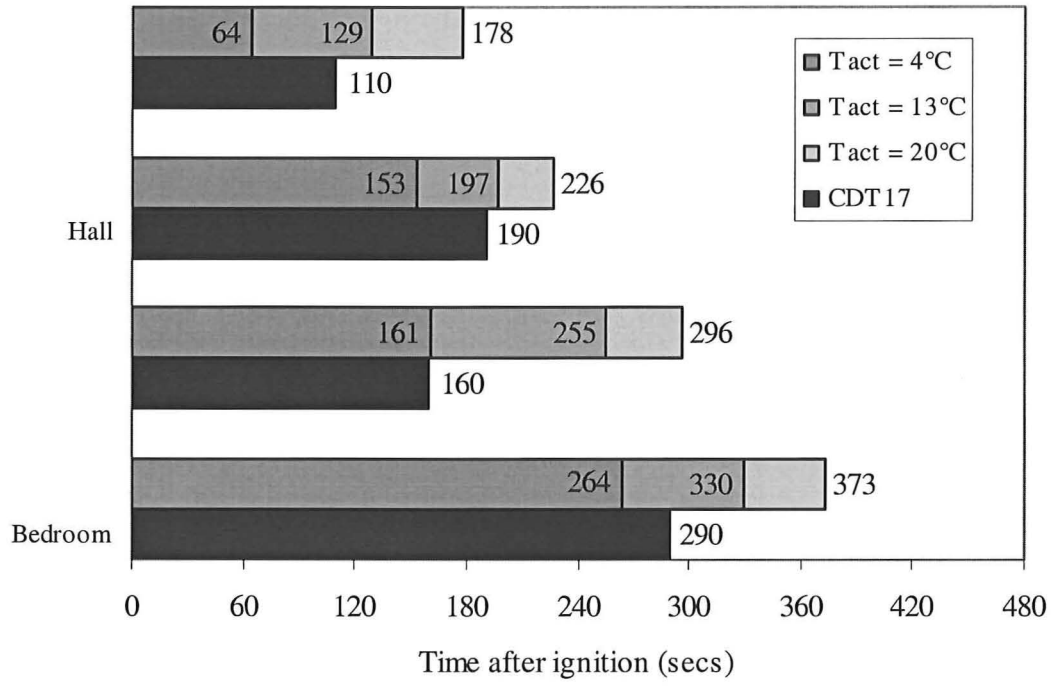

Figure 5-15. Temperature Correlation Method for Ionisation Detector – CDT17

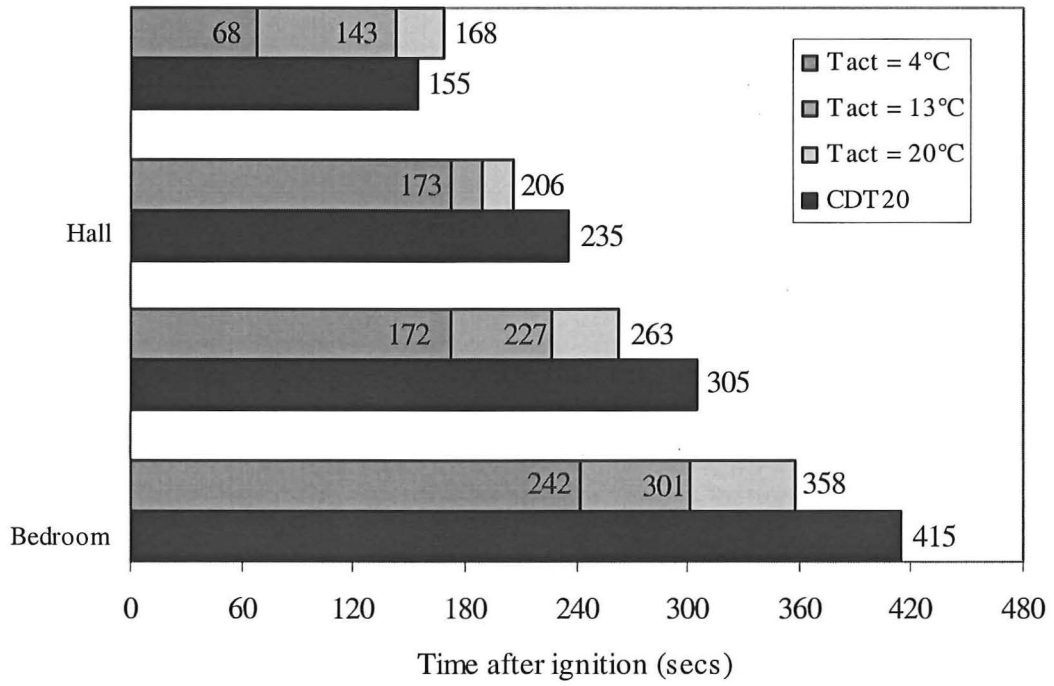

Figure 5-16. Temperature Correlation Method for Ionisation Detector – CDT20

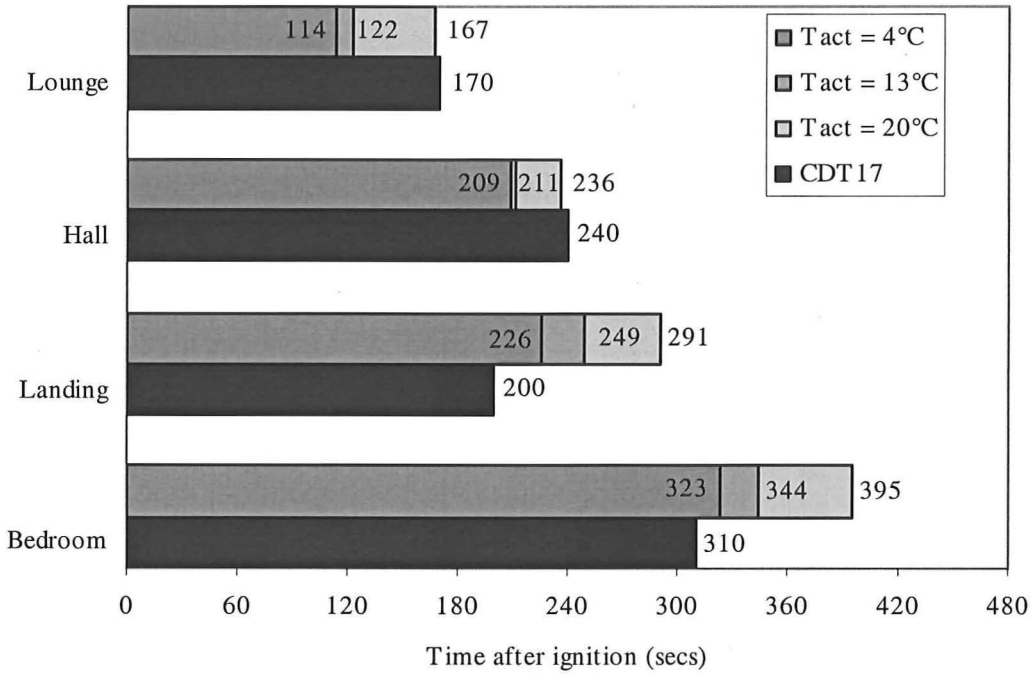

Figure 5-17. Temperature Correlation Method for Optical Detector – CDT17

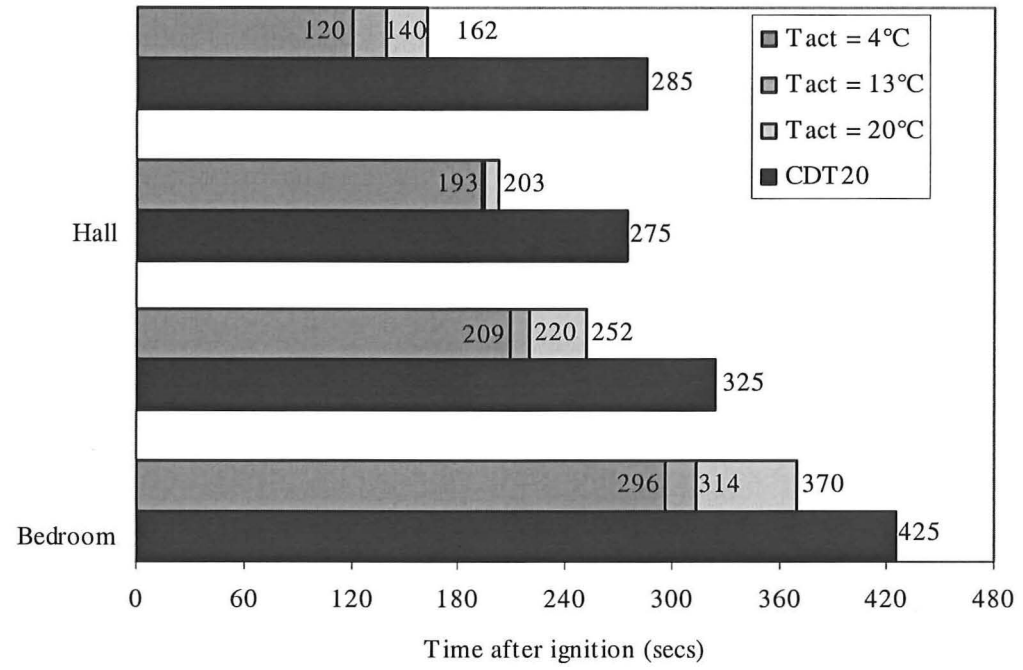

Figure 5-18. Temperature Correlation Method for Optical Detector – CDT20

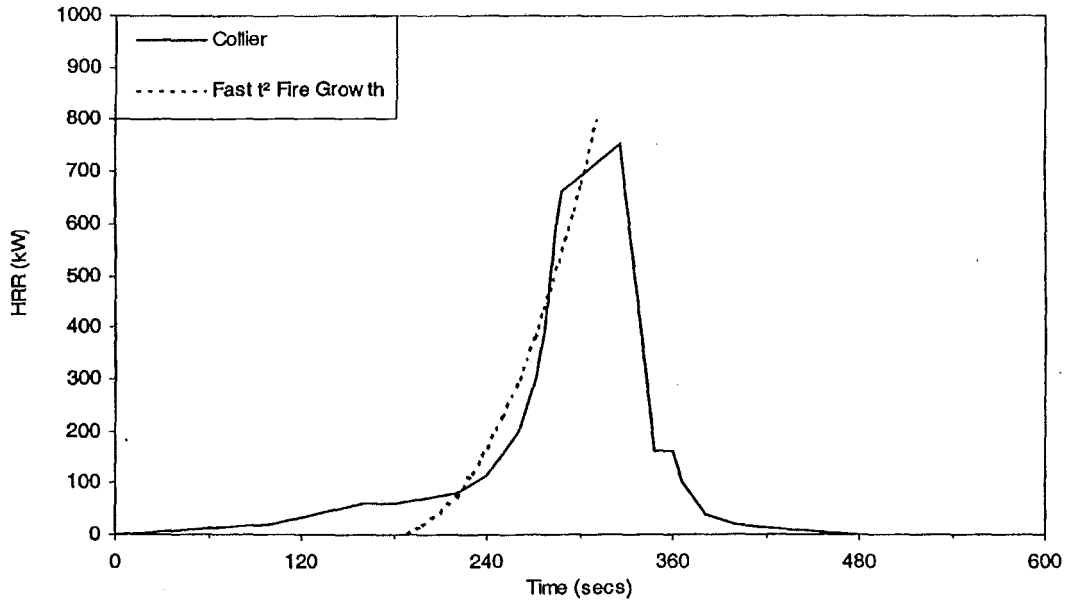

Figure 5-19. HRR Curve for Collier's House Fire Test

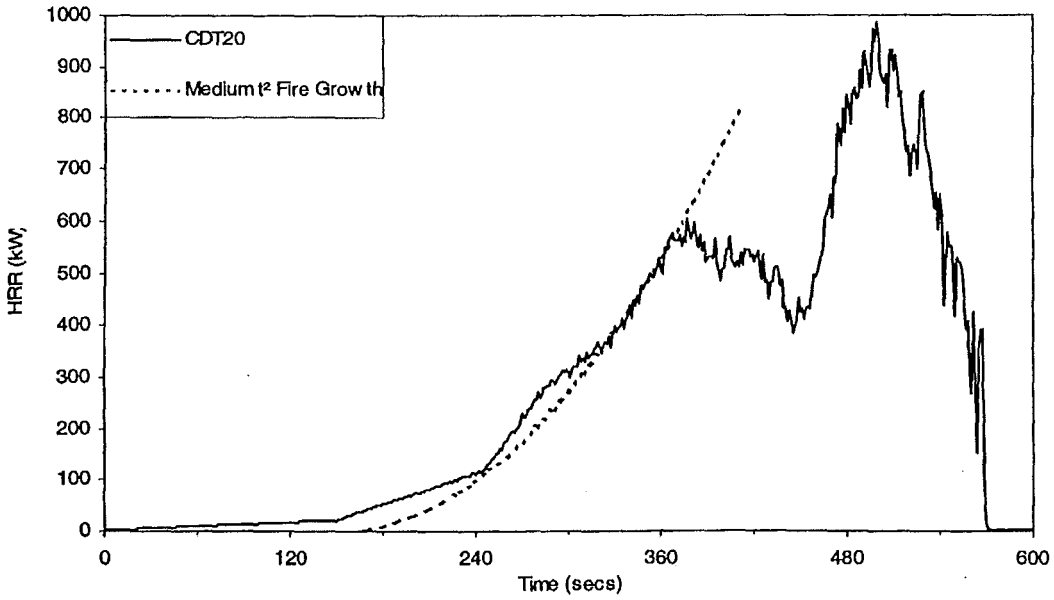

Figure 5-20. HRR Curve for Test CDT20

5.4.2 Pseudo-Heat Detector Method

The results of the analysis of activation times for the ionisation detectors from the fire test CDT17 and CDT20 are shown in Figure 5-21 and 5-22 respectively for the pseudo-heat detector method. All of the investigations in this method were performed with a value of RTI = 1 $m^{½} s^{½}$. It is interesting to note that the times predicted from

this method are within 5 seconds of those predicted from the temperature correlation method, which are shown in Figures 5-15 and 5-16.

The predicted activation times for the optical detectors from tests CDT 17 and CDT20 shown in Figures 5-23 and 5-24 respectively. The results for these two tests follow a similar trend to the results of the temperature correlation method, in that for T_{act} = 20°C a good match is attained for the ground floor during test CDT17, but provides up to 45% errors on the top floor. But for CDT20, this activation temperature will underestimate the activation times in each case.

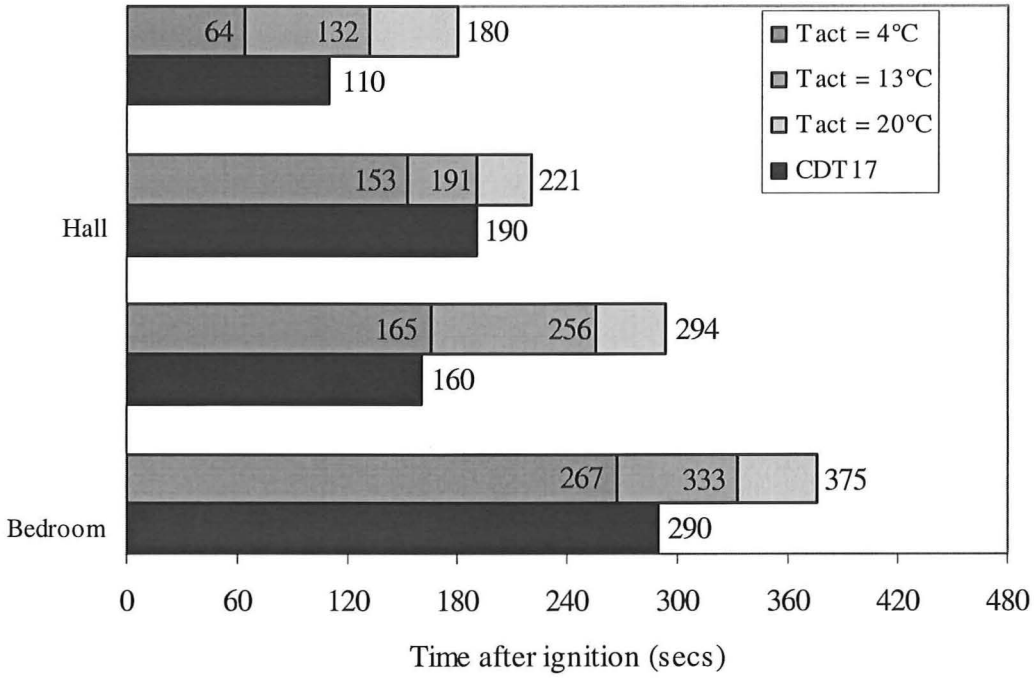

Figure 5-21. Pseudo-Heat Detector Method for Ionisation Detector – CDT17

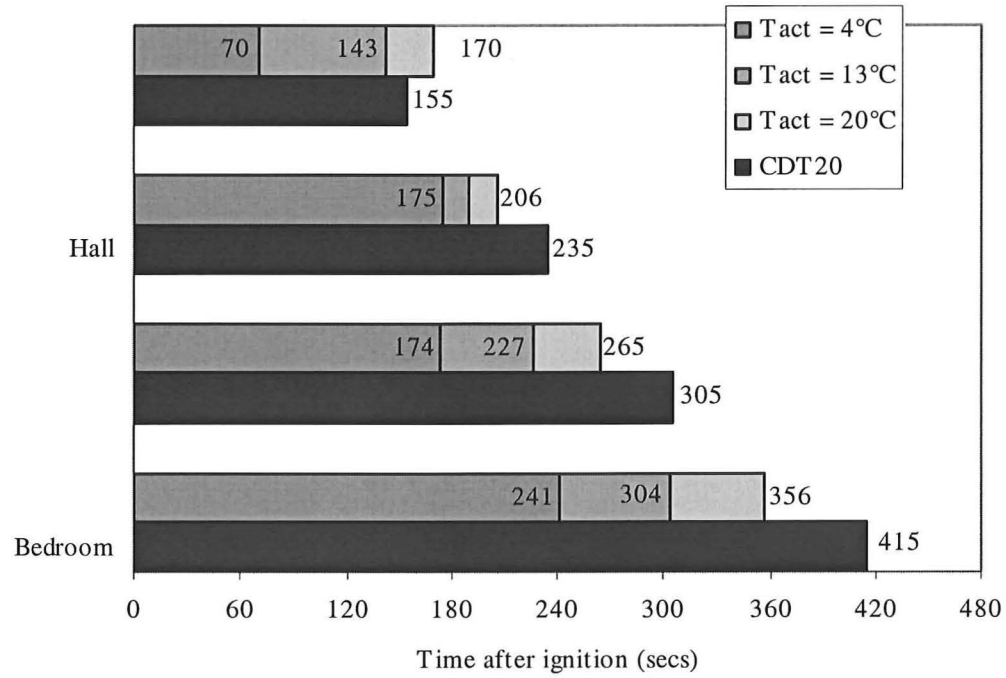

Figure 5-22. Pseudo-Heat Detector Method for Ionisation Detector – CDT20

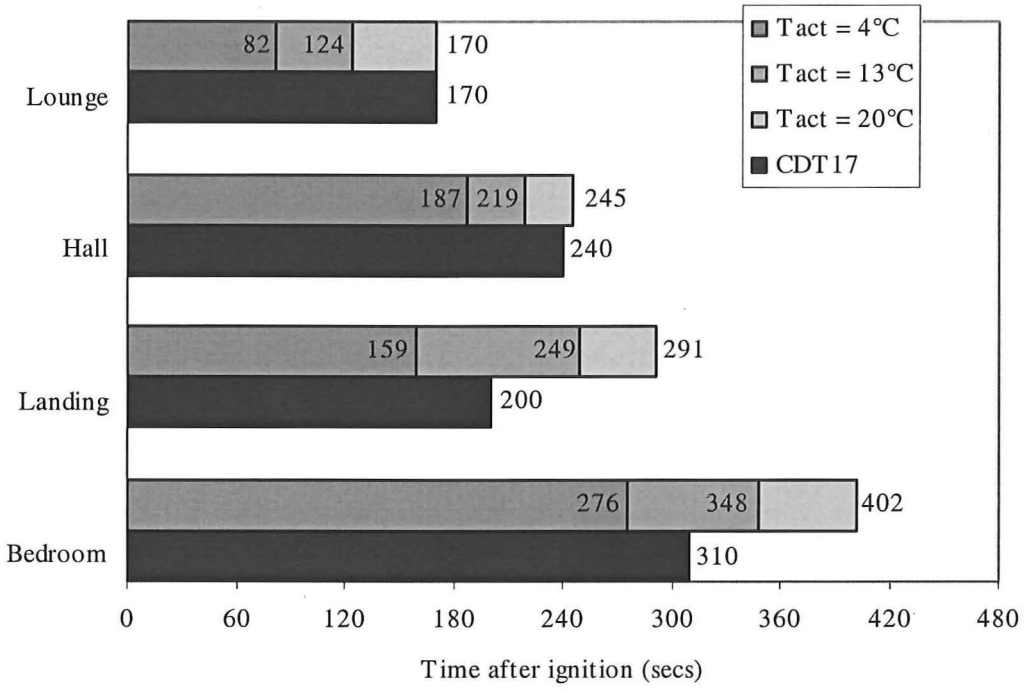

Figure 5-23. Pseudo-Heat Detector Method for Optical Detector – CDT17

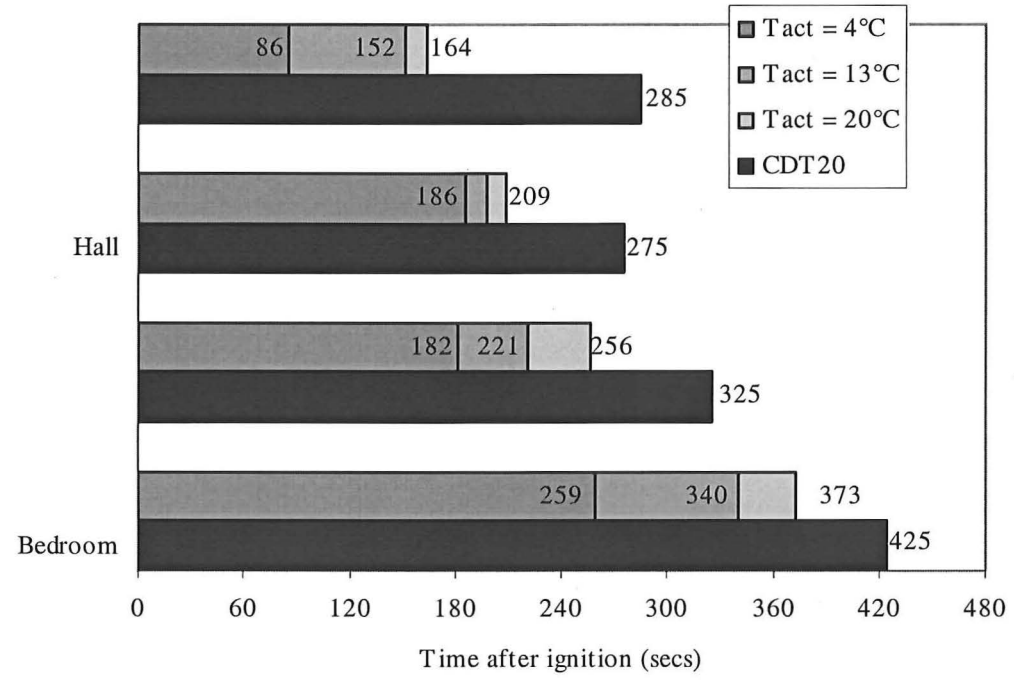

Figure 5-24. Pseudo-Heat Detector Method for Optical Detector – CDT20

5.4.3 Heskestad's Method

As discussed earlier, there were difficulties in applying the results of the FDS simulations to this method because of the overestimation of optical density in the early stages (first 300 seconds) of both fire tests. This overestimation led to the predicted activation times being extremely low compared to the actual times. But in order to proceed with some level of investigation of Heskestad's method, the values for the predicted optical density were arbitrarily halved.

The values for optical density that FDS calculates are derived from the value for smoke yield Y_s that was input by the user. In this study Y_s was given the value of 0.10 kg/kg, which is slightly lower than the range of values given by Tewarson for flexible polyurethane foams. However, the upholstery in the chairs for these test fires was a type of combustion-modified foam, and Tewarson's values might not be suited to these types of foams. In addition to this, the slope of the optical density curve in Figures 5-11 to 5-14 is quite flat at the early stages, which means that the predicted activation times will be highly sensitive to the environment over this initial period.

As discussed in Chapter 4, the value for the activation density for the detectors is 0.14 m^{-1} as discussed by Mulholland for black smoke. This value was applied to both types of detectors. The values for effective length L are based on the values presented in Table 2-1.

Given the level of deviations that have gone into the simulation data while investigating this method, there is little point in trying to compare the results of this investigation with the other two. However, it should be noted that the trend in the activation times of these results is similar to those of the other methods.

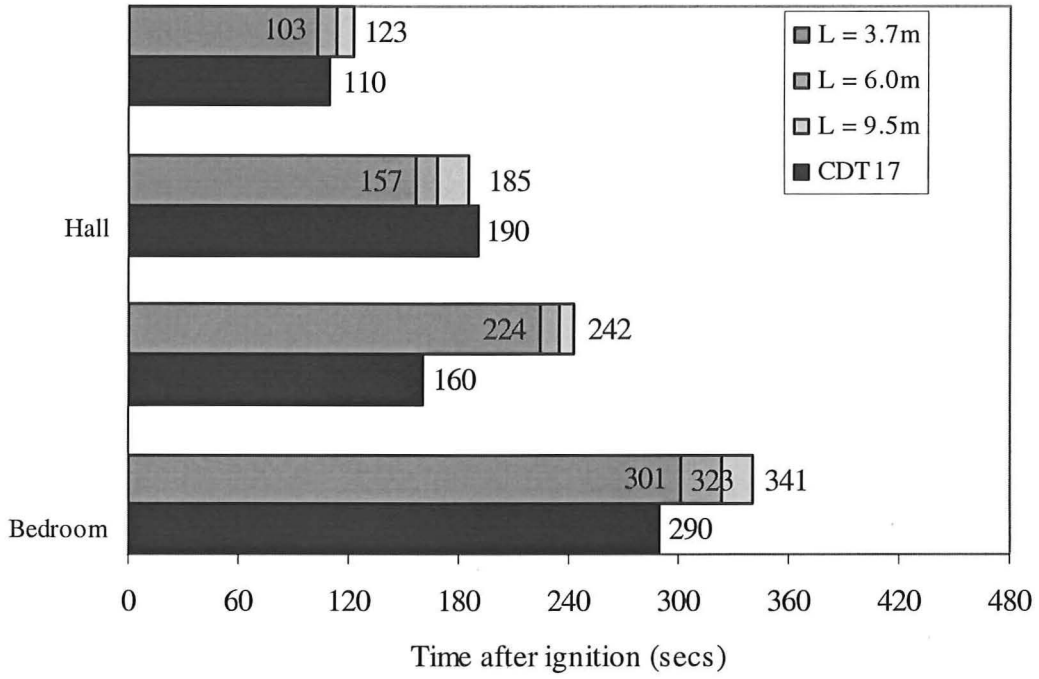

Figure 5-25. Heskestad's Method for Ionisation Detector – CDT17

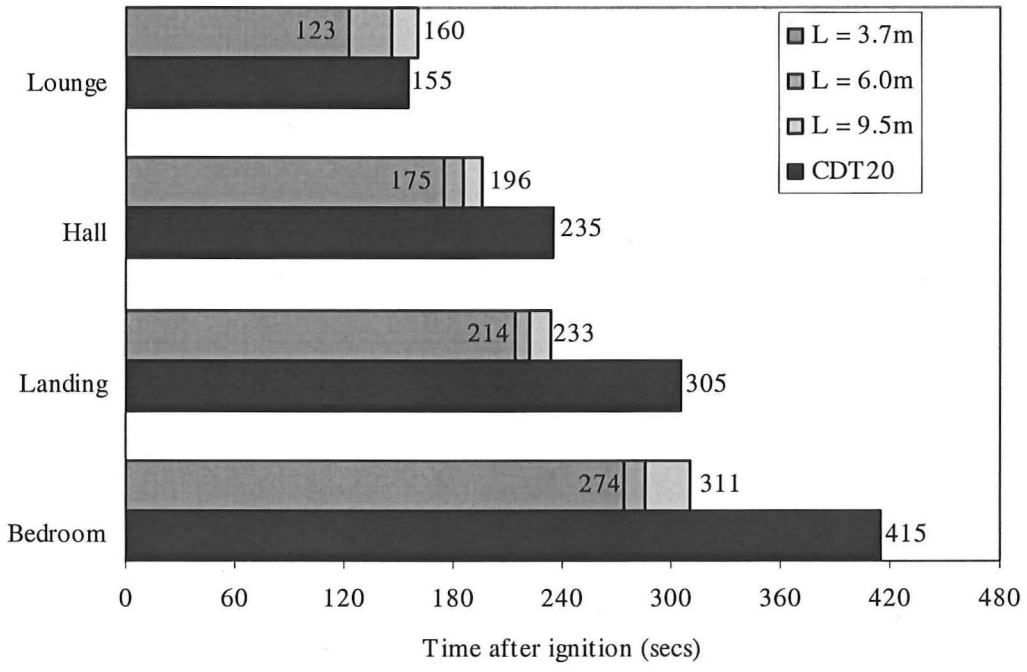

Figure 5-26. Heskestad's Method for Ionisation Detector – CDT20

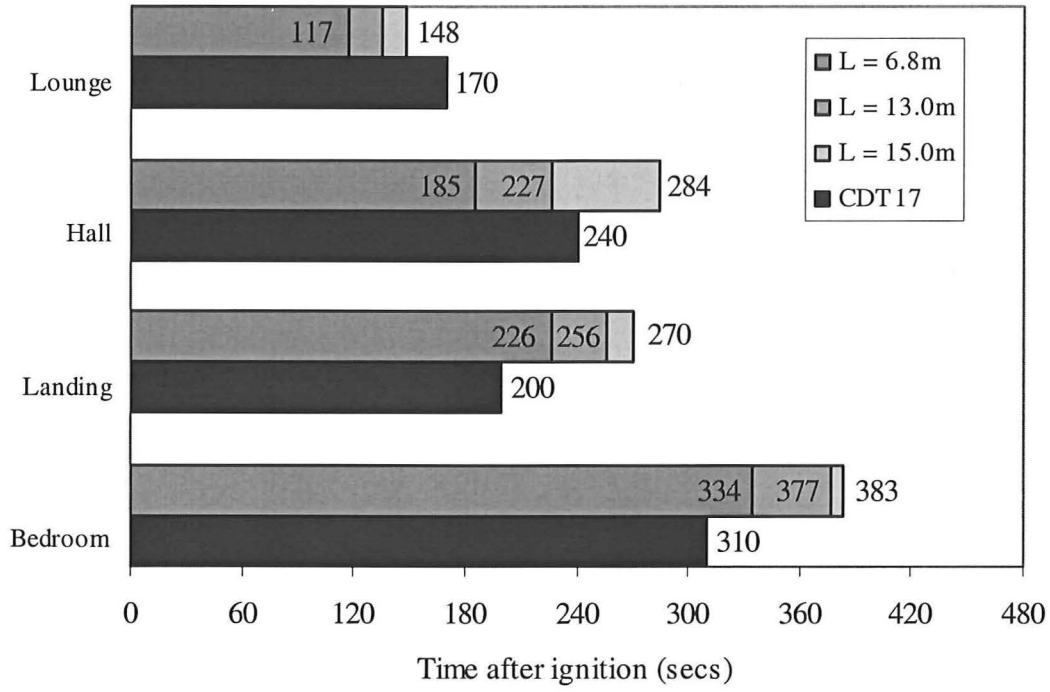

Figure 5-27. Heskestad's Method for Optical Detector – CDT17

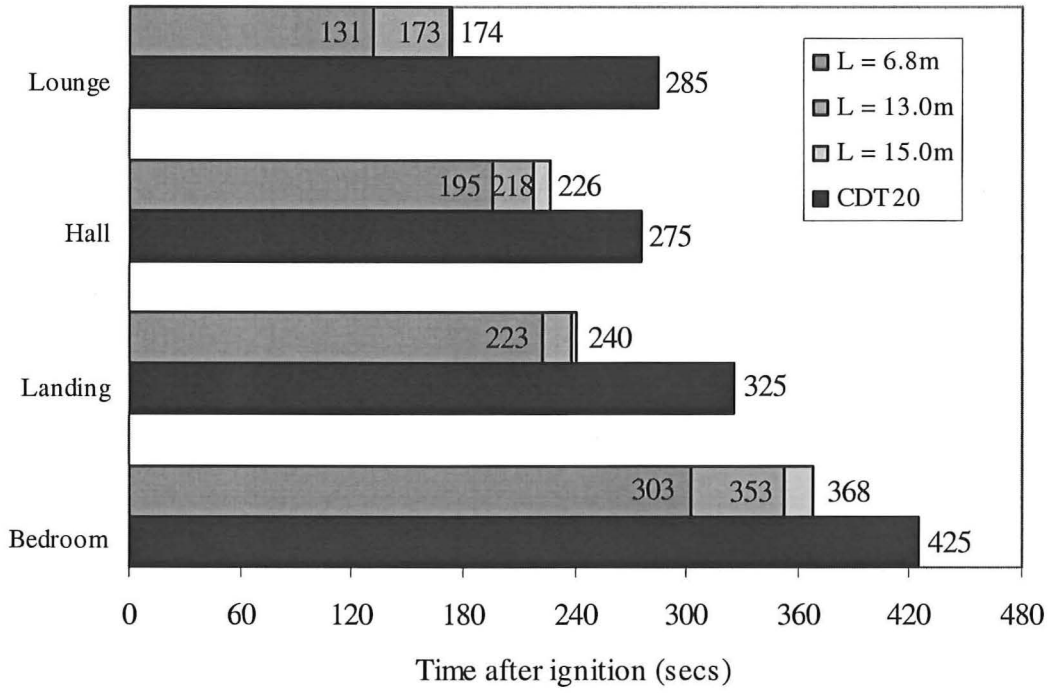

Figure 5-27. Heskestad's Method for Optical Detector – CDT20

5.5 Observations About Smoke Detector Modelling

It is interesting to note that two chair-fire scenarios, where the chairs' upholstery and fabric cover, mass, and location within the fire room are the same, as is the level of ventilation into the fire room, can yield quite different results in terms of the behaviour of the fire. This is indicative of the unpredictability of fire, and hence of the smoke generated.

Other researchers have reported the significance of a critical velocity, below which the lag times for the detectors increase markedly. This phenomenon will affect both the pseudo-heat detector and Heskestad's methods. As Brozovsky et al reports, the magnitude of this critical velocity is in the order of 0.16 m/s. The velocities predicted in this study are presented in Appendices C and D, which show that generally the velocities at the actual activation times are generally above 0.2 m/s. The only exception is the ionisation detector in bedroom 2 during test CDT17 (the longer duration fire), where the velocity is around this critical value. Therefore, as the predicted velocities are generally higher than the critical value, the concept of critical velocity has no significance in these analyses.

Looking at Figures 5-15 to 5-28, for test CDT20 (the high HRR, short duration fire), the detector activation times were longer than those for CDT17. However, for the temperature correlation method the predicted activation times are longer for CDT17 then they are for CDT20. This trend is repeated for the pseudo-heat detector method. Heskestad's method exhibits a similar trend for the top floor, but not the ground floor where the trend is the reverse. All three methods tend to over predict the activation times for CDT17 and under predict those for CDT20.

Another interesting feature of the results is the trend in the activation times for the different rooms. For test CDT17 the detectors on the landing activated before those in the entry hall, whereas for CDT20 the reverse occurred. However, for all three methods for predicting the detectors' behaviour, the general trend was for the activation times to be commensurate with the distance that the particular detector was from the source of the fire.

There is little difference between the results of the temperature correlation method and the pseudo-heat detector method where RTI has the value of 1 $m^{½}$ $s^{½}$. In other words, the simpler temperature correlation method is not significantly less accurate than the pseudo-heat detector method. Looking at Figures 5-15 to 5-18 it seems that the most prudent prediction approach would be to use the temperature correlation method with an activation temperature of 20°C, as this will tend to provide a predicted time somewhere between the two fire scenarios considered in this study. As this value is higher than the values recommended by other researchers, it can be hypothesised that the air currents in the house that were set up by the radiators have a significant effect on the behaviour of the detectors. This should not be surprising considering that it is generally accepted that smoke detectors should not be positioned immediately adjacent to grilles for HVAC systems.

While it may seem amiss to apply the same value for T_{act} to both the ionisation and optical detectors, given the debatable nature of the results, it is difficult to justify a more refined approach.

Chapter 6 CONCLUSIONS

This study modelled the results of an earlier investigation into two chair fires in the ground floor of a two-storey house to assess firstly whether the effects of these fires could be modelled with a field model, and secondly whether the behaviour of the domestic smoke detectors could also be satisfactorily predicted. The conclusions drawn from this study are collated below:

6.1 House Domain Geometry

- From the results of this study it can be seen that the house could be successfully modelled by FDS using the geometry discussed in this report.
- The allocation of the physical properties of Gib board to the internal walls, the corrugated sloped ceiling over the stairs, and the inclusion of balustrades all had some impact on the gas temperatures and behaviour within the house.
- The location of the chair within the fire room, and the creation of only part of the house for modelling had a more significant effect on the gas and fire behaviour. This is indicative of the importance of including the entire collection of rooms when modelling multi room enclosures.
- There was little difference between the results of the 100mm and 75mm grid size geometries.

6.2. Comparisons With Fire Behaviour

- It was difficult to achieve good matches for temperature and optical density at the early stages of the fires. Unfortunately this is the time when smoke detectors are expected to activate.
- There were reasonably good matches between the predicted and actual temperatures for the duration of the tests as a whole. These matches were better at the upper levels within each room.
- FDS was able to predict the trends for optical density, although there were significant errors in magnitude.

6.3. Comparisons With Smoke Detector Behaviour

- The general trend of the activation sequences of the detectors throughout the house was emulated.
- In the modelling of houses, it could be non-conservative to assume that there will not be any heating system regardless of the occupancy, or to assume that its effects will be negligible.
- There is little difference between the temperature correlation and pseudo-heat detector methods of predicting smoke detector behaviour with a low value of RTI.
- Activation times for both ionisation and optical detectors can be predicted by the use the temperature correlation method with T_{act} = 20°C.

It is important to note that these conclusions relate to flaming fires and domestic ionisation and optical smoke detectors.

6.4. Further Research

In terms of the FDS modelling software:

- The estimations for soot yield should have the ability to differentiate between the sources of the total HRR. This will avoid the difficulty of the radiators producing soot.
- Models should be developed to emulate particle coagulation, and the change in particle size and shape.
- As modelling software has developed in the past, it has evolved in ways that have not been useful to researchers into detector behaviour. Fire and detection models should progress together, so that useful detection models are derived.

With this particular series of fire tests:

- Investigate the results of the Cardington tests to investigate whether the inconsistent results between the two fire scenarios considered in this study for

the domestic detectors are also apparent for the commercial detectors that were monitored during the same tests, or was one of the tests studied a flawed test.

- Consider other tests with domestic detectors to investigate whether more definite findings develop.
- Further investigate the soot yield to see if better predictions of optical density can be attained.
- If better results are derived, reinvestigate Heskestad's method to see if more consistent results can be found by this method.

REFERENCES

Bjorkman, J, Kokkala, M A and Ahola, H 1992. "Measurements of the Characteristic Lengths of Smoke Detectors". *Fire Technology,* Vol 28, No 2, pp 99- 106.

Brozovsky, E, Motevalli, V and Custer, R L P 1995. "A First Approximation Method for Smoke Detector Placement Based on Design Fire Size, Critical -Velocity, and Detector Aerosol Entry Lag Time". *Fire Technology Fourth Quarter,* pp 336 - 354.

BRE, CD Rom of Cardington Test Results, Fire Research Station, Building Research Establishment, UK.

Bukowski, R W and Averill, J D 1998. "Methods for Predicting Smoke Detector Activation". *Fire Suppression and Detection Research Application Symposium, Research and Practice: Bridging the Gap.* National Fire Protection Research Foundation, USA, pp64 - 72.

Cleary, T, Chernovsky, A, Grosshandler, W and Anderson, M 2000. "Particulate Entry Lag in Spot Type Smoke Detectors". *Proceedings, Sixth International Symposium on Fire Safety Science.* International Association for Fire Safety Science, USA.

Cleary,T, Donnelly, M, Mulholland, G and Farouk, B 2001. "Fire Detector Performance Predictions in a Simulated Multi-Room Configuration". *Proceedings, AUBE '01, Twelfth International Conference on Automatic Fire Detection.* National Institute of Standards and Technology, USA, pp 455 — 469.

Collier, P C R 1996. "Fire in a Residential Building: Comparisons Between Experimental Data and a Fire Zone Model". *Fire Technology,* Vol 32, No 3, pp 195 - 217.

Friday, P A and Mowrer, F W 2001. *Comparison of FDS Model Predictions With FMJSNL Fire Test Data.* NIST Report OCR 01-8 10. National Institute of Standards and Technology, USA.

Girgis, N 2000. *Full-Scale Compartment Fire Experiments on Upholstered Furniture.* Fire Engineering Research Report, University of Canterbury, NZ.

Heskestad, G 1975. "Generalized Characteristics of Smoke Entry and Response for Products-of-Combustion Detectors". *Proceedings,* 7th *International Conference on Problems of Automatic Fire Detection.* Rheinish-Westfalischen Techischen Hochschule Aachen, pp 267-310.

Karlsson, B and Quintiere, J G 2000. *Enclosure Fire Dynamics.* CRC Press, Boca Raton, FL USA.

McGrattan, K B, Forney, G P. Floyd, J E and Hostikka, 5 2001. *Fire Dynamics Simulator (Version 2) - User's Guide.* Report NISTIR 6784 (Draft). National Institute of Standards and Technology, USA.

Mulholland, G W 1995. "Smoke Production and Properties". Section 2/Chapter 15, *SFPE Handbook of Fire Protection Engineering,* Second Edition, Society of Fire Protection Engineers, USA.

Newman, J S 1994. "Modified Theory for the Characterization of Ionization Smoke Detectors". *Proceedings, Fourth International Symposium on Fire Safety Science.* International Association for Fire Safety Science, USA, pp 785 - 792.

Peacock, R D, Reneke, P A, Jones, W W, Bukowski, R W and Forney, G P 1997. *A User's Guide for FAST: Engineering Tools for Estimating Fire Growth and Smoke Transport.* NIST Special Publication 921, National Institute of Standards and Technology, USA.

Purser, D A, Rowley, J A, Fardell, P J and Bensilum, M 1999. "Fully Enclosed Design Fires For Hazard Assessment In Relation to Yields of Carbon Monoxide and Hydrogen Cyanide". *Proceedings, Eighth International Conference.* Interscience Communications, UK, pp 1163 - 1169.

Qualey, J R, Desmarais, L and Pratt, J 2001. "Response-Time Comparisons of Ionization and Photoelectric/Heat Detectors". *Proceedings, AUBE '01, Twelfth International Conference on Automatic Fire Detection.* National Institute of Standards and Technology, Gaithersburg, Maryland, USA, pp 283 - 299.

Schifiliti, R P 2001. "Fire Detection Modeling — The Research-Application Gap". *Proceedings, AUBE '01, Twelfth International Conference on Automatic Fire Detection.* National Institute of Standards and Technology, USA, pp 529 - *560.*

Schifiliti, R P, Meacham, B J and Custer, L P *1995.* "Design of Detection Systems" Section 4/Chapter 1, *SFPE Handbook of Fire Protection Engineering,* Second Edition, Society of Fire Protection Engineers, USA.

Snegirev, A Y, Makhviladze, G M and Roberts, J P 2001. "The Effect of Particle Coagulation and Fractal Structure on the Optical Properties and Detection of Smoke". *Fire Safety Journal,* Vol 36, No 1, pp 73 - 95.

Spearpoint, M J 1996. *The Response of Domestic Smoke Alarms to Fires in a Typical Dwelling.* FRDG Publication No 16/96, Home Office Fire Research and Development Group, UK.

Tewarson, A 1995. "Generation of Heat and Chemical Compounds in Fires". Section 3/Chapter 4, *SFPE Handbook of Fire Protection Engineering,* Second Edition, Society of Fire Protection Engineers, USA.

Appendix A HOUSE DIMENSIONS, LOCATIONS OF INSTRUMENTATION

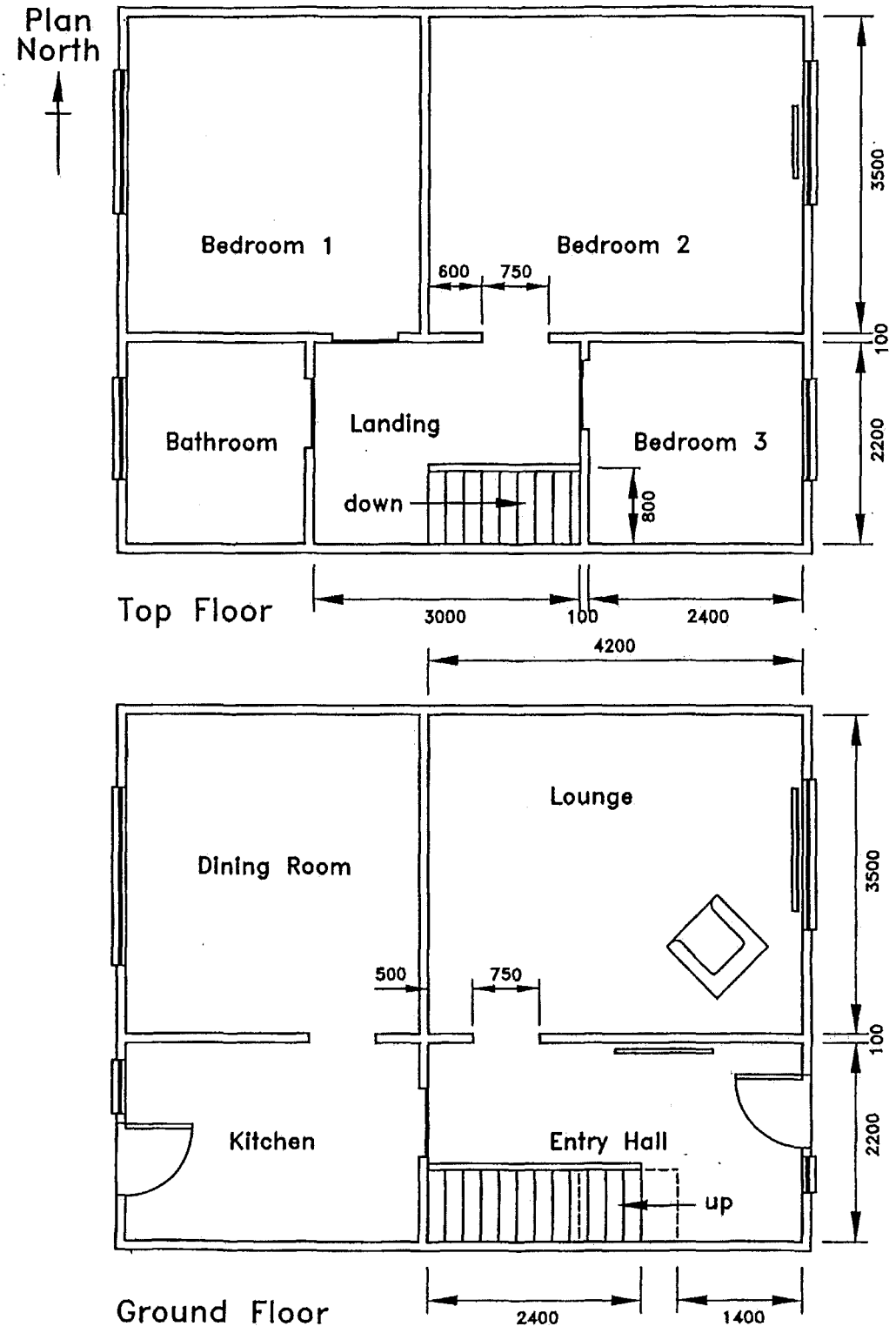

Figure A1. House Plans - Dimensions

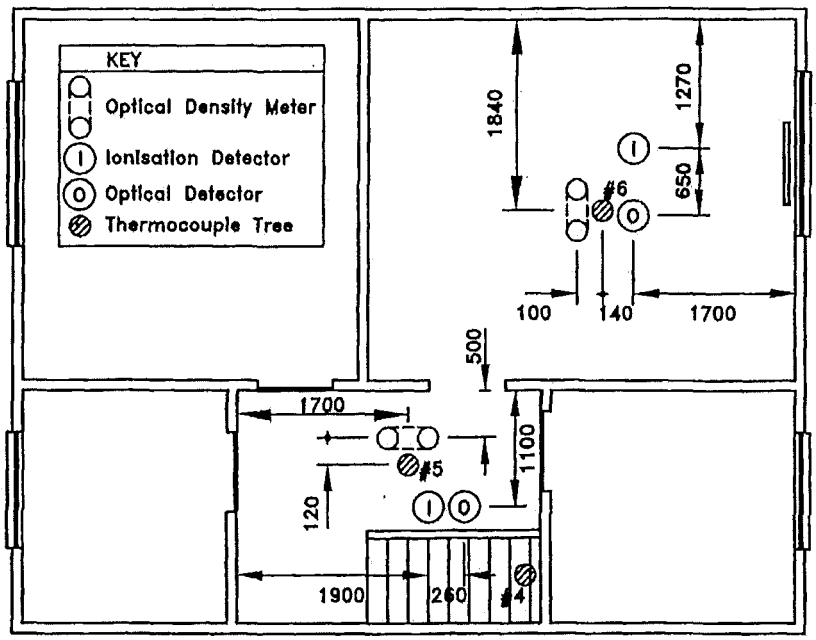

Top Floor

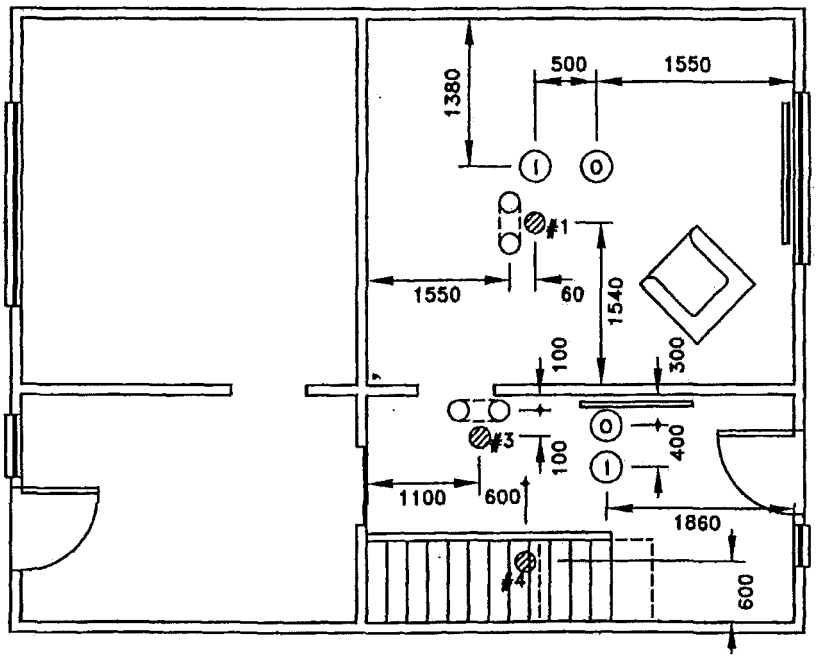

Ground Floor

Figure A2. House Plans – Locations of Instrumentation

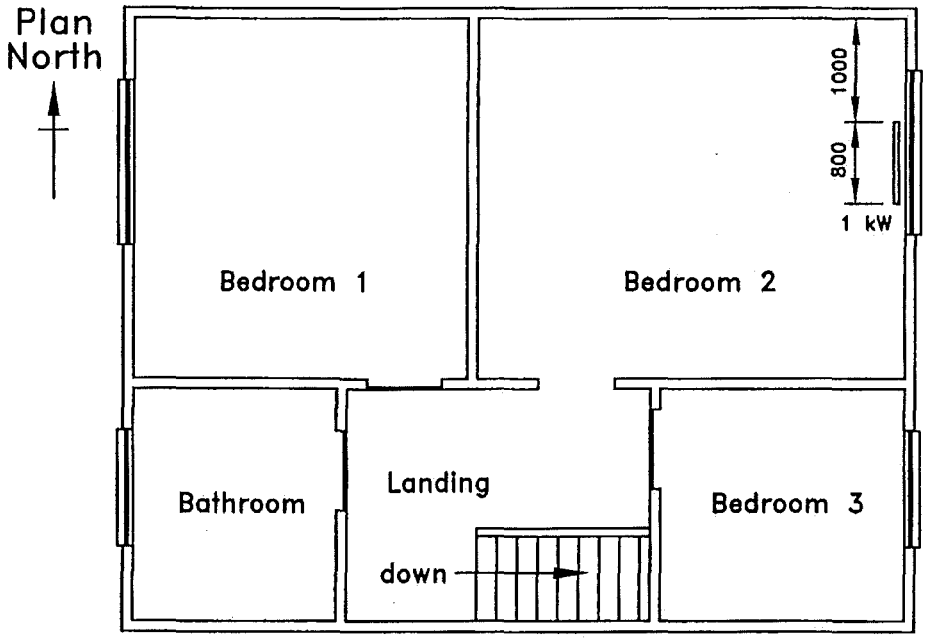

Top Floor

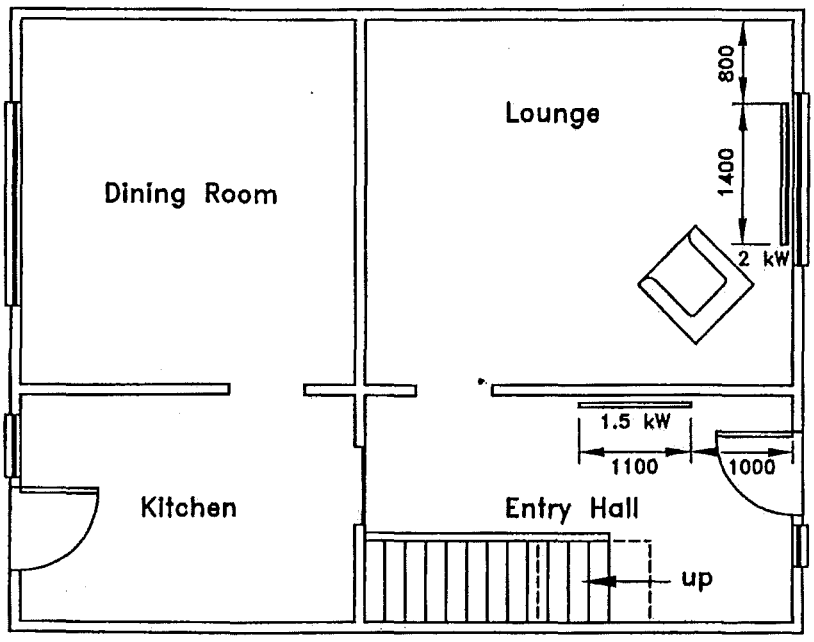

Ground Floor

Figure A3. House Plans – Locations and Ratings of Radiators

Appendix B INVESTIGATION INTO TYPES OF BALUSTRADES

Section 4.4 discusses difficulties with accommodating the balustrades into the house domain geometry. As the balustrades have to fit within the allocated grid layout, several different arrangements of balustrade elements were considered. The balustrade layout finally chosen was the one that most closely matched the temperature profile on the stairs that was attained during the actual fire test, based on a model of the ground floor only without the function of radiators. This section presents the results of the investigation into the types of balustrades.

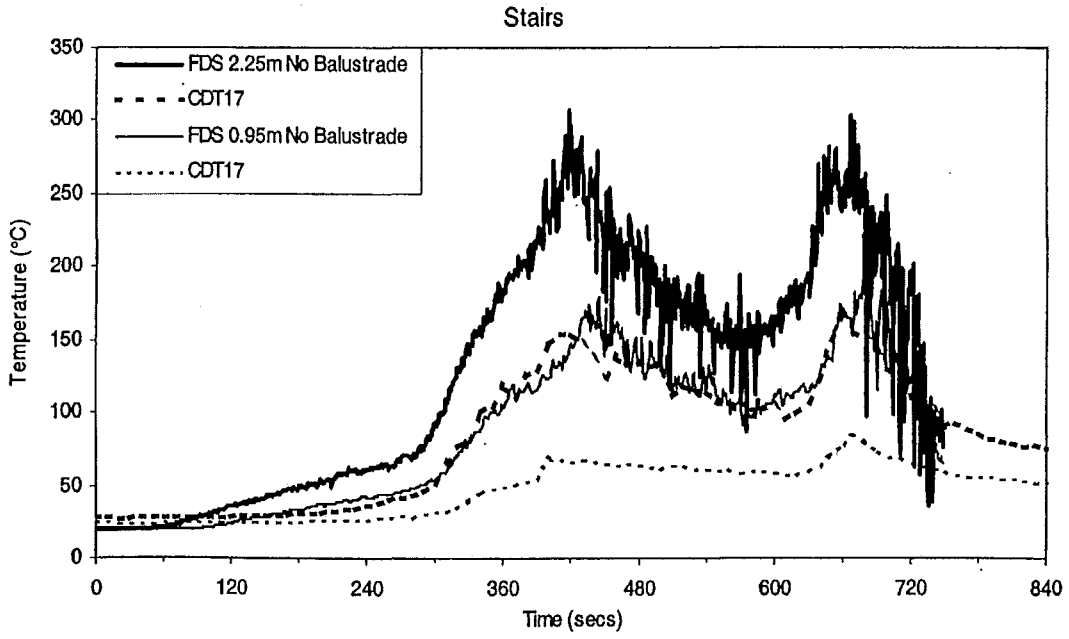

Figure B1. Temperature Curve – No Balustrade

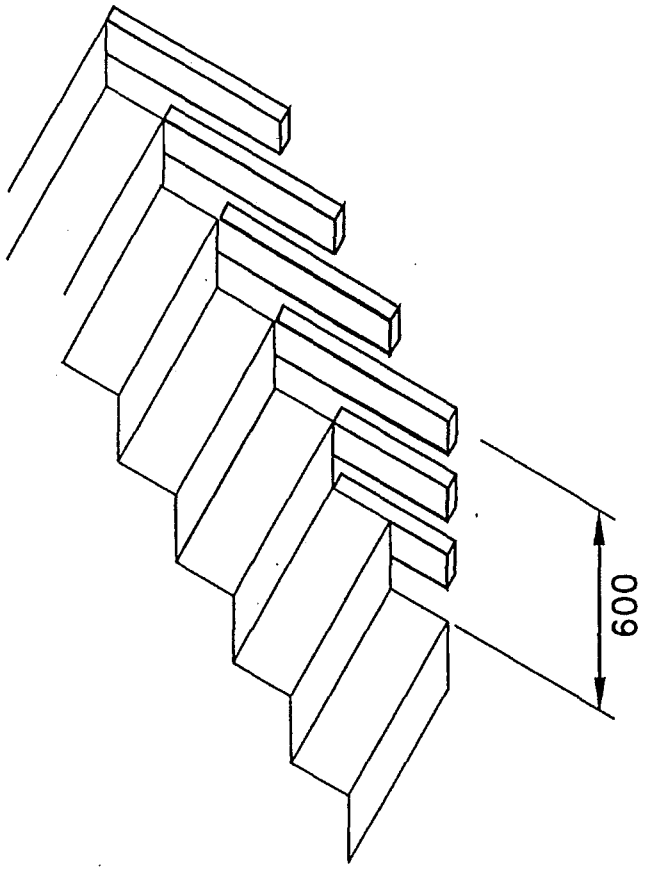

Figure B2. Diagram of Balustrade – 600mm High Horizontal

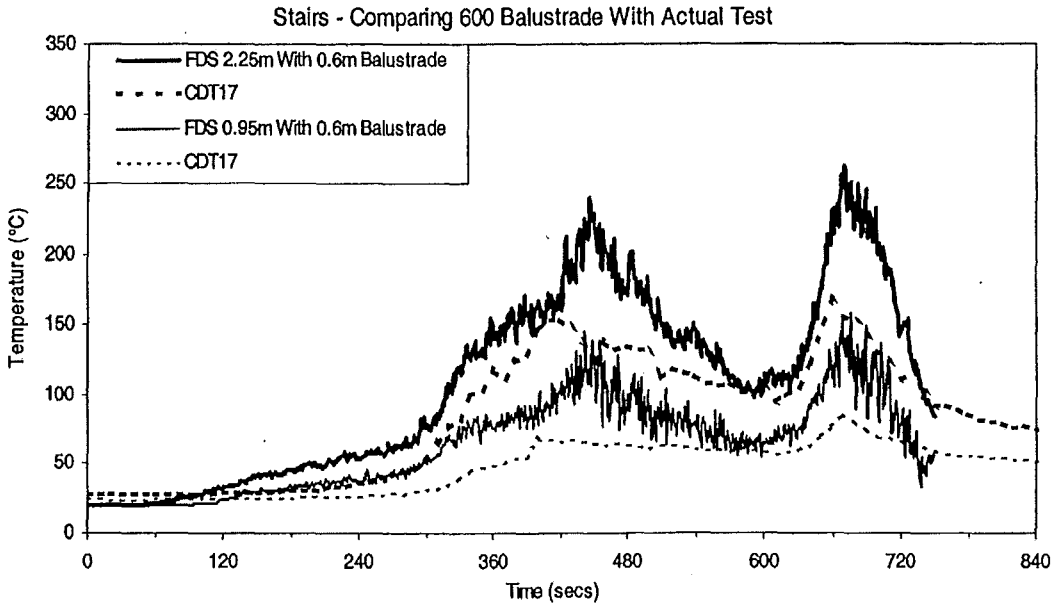

Figure B3. Temperature Curve – 600mm High Horizontal

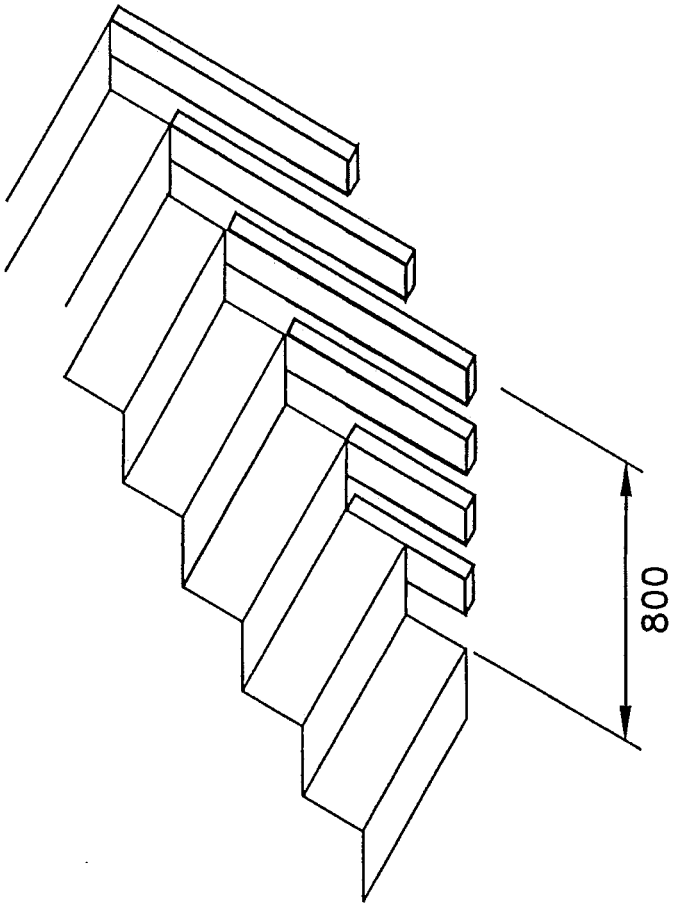

Figure B4. Diagram of Balustrade – 800mm High Horizontal

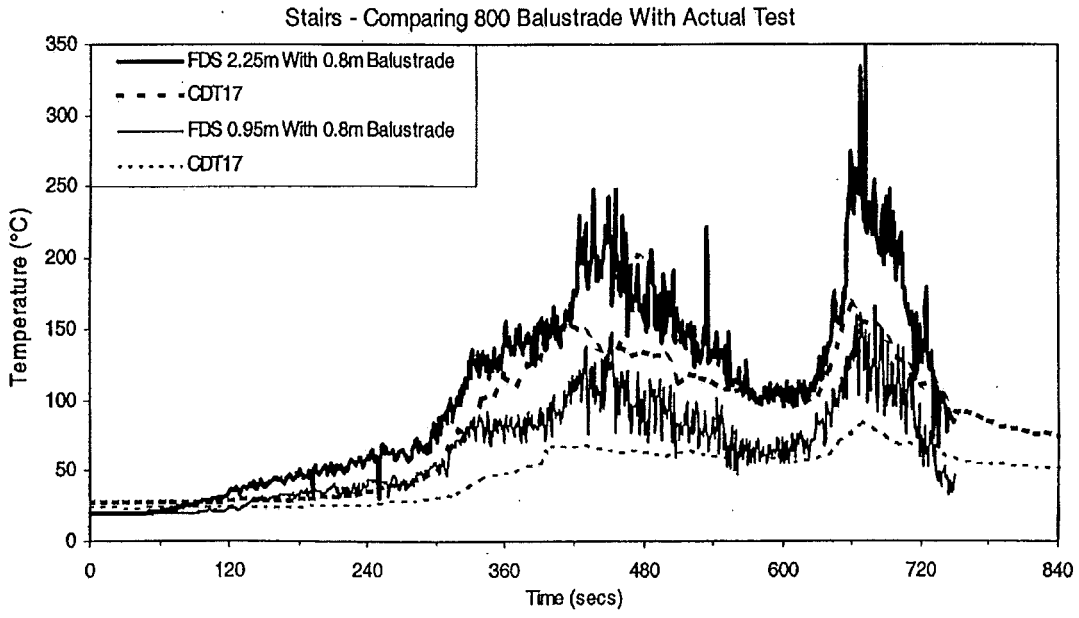

Figure B5. Temperature Curve – 800mm High Horizontal

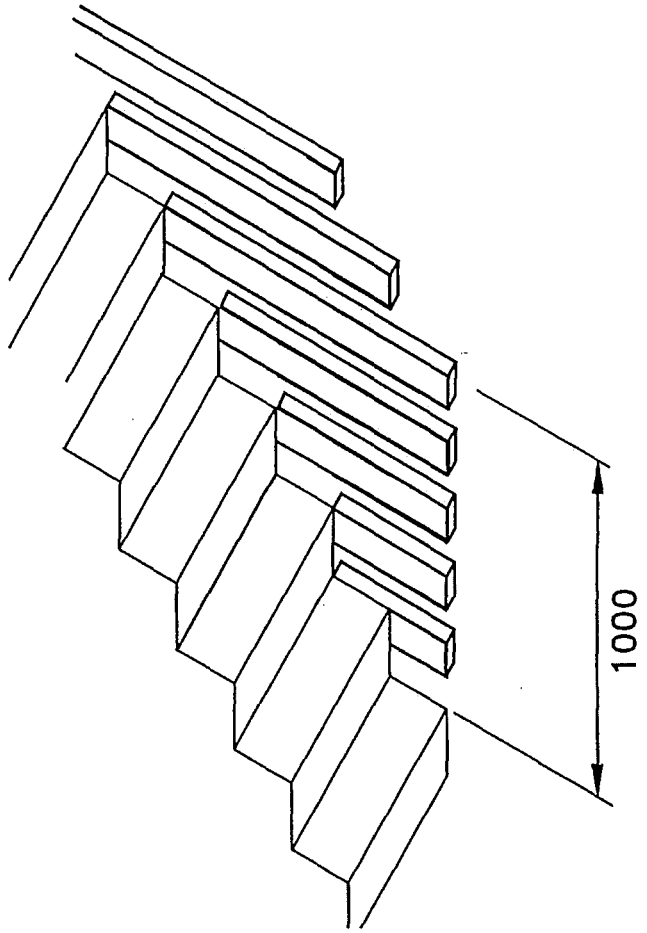

Figure B6. Diagram of Balustrade – 1000mm High Horizontal

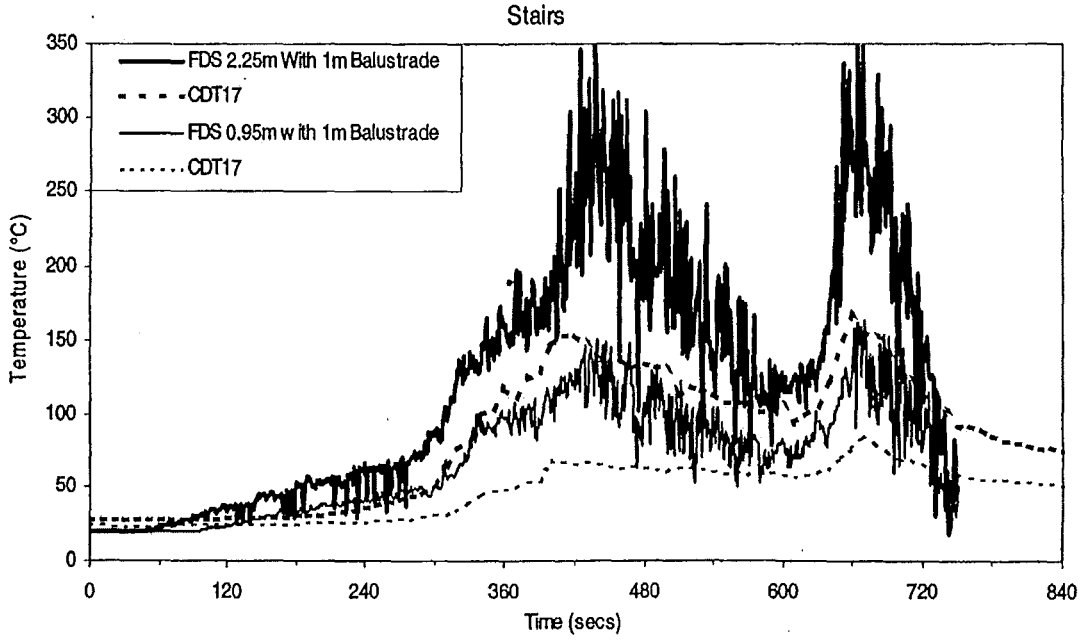

Figure B7. Temperature Curve – 1000mm High Horizontal

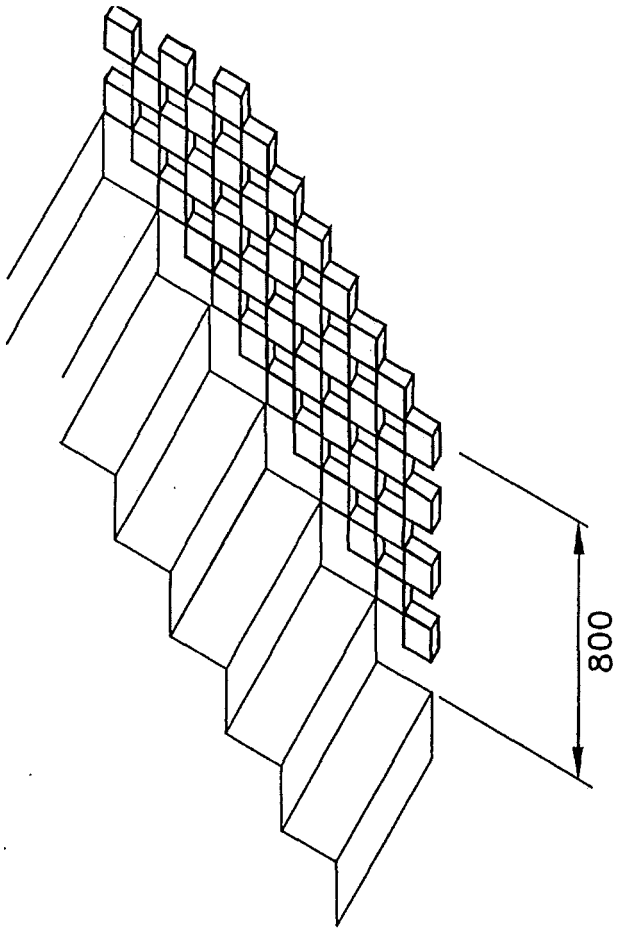

Figure B8. Diagram of Balustrade – 800mm High Cheque Pattern

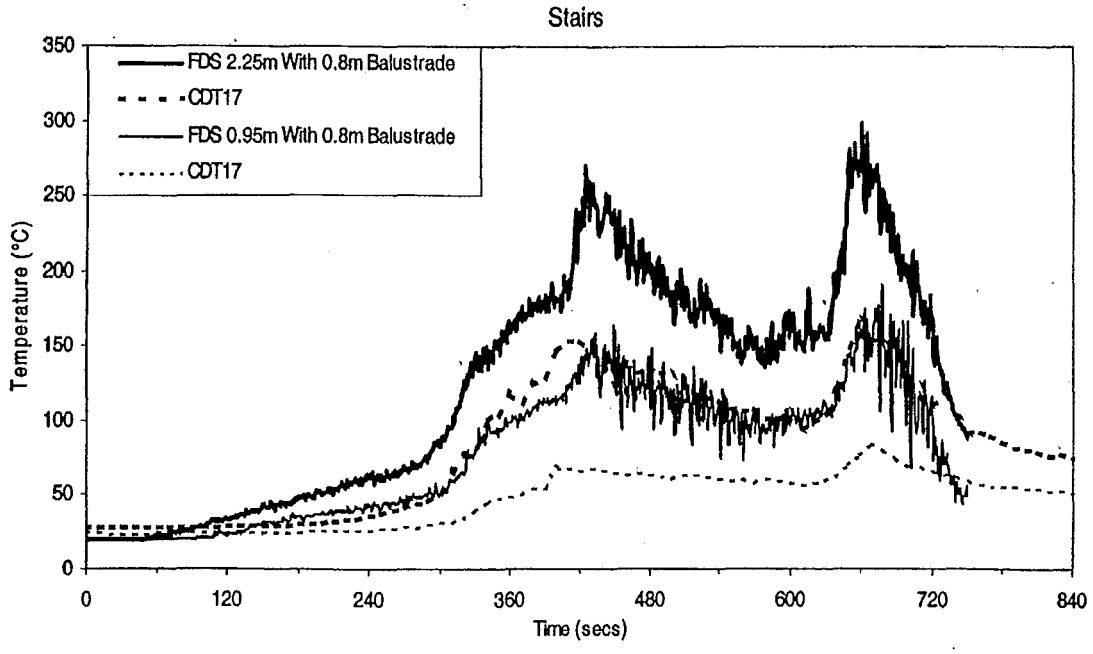

Figure B9. Temperature Curve – 800mm High Cheque Pattern

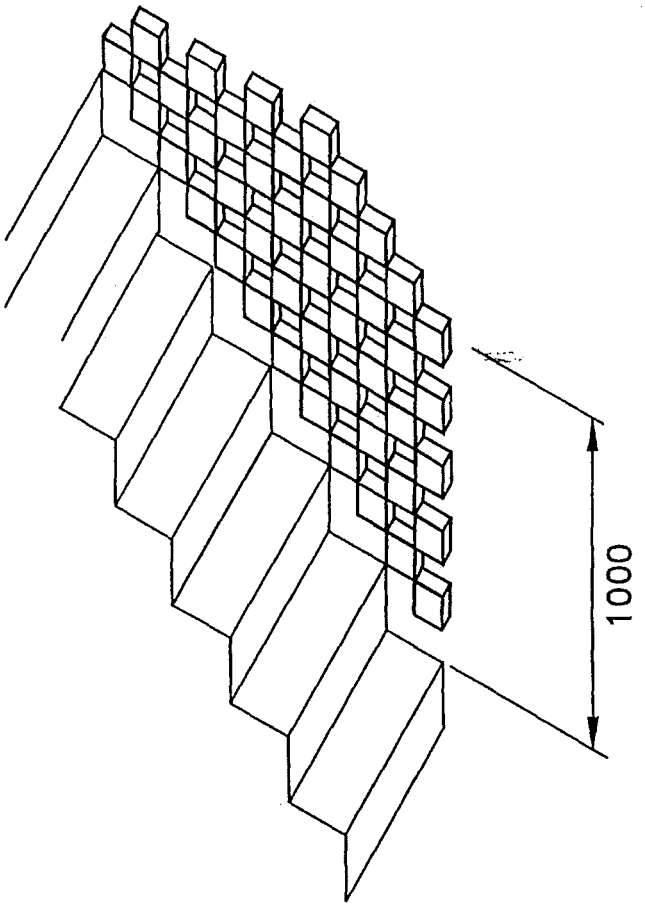

Figure B10. Diagram of Balustrade – 1000mm High Cheque Pattern

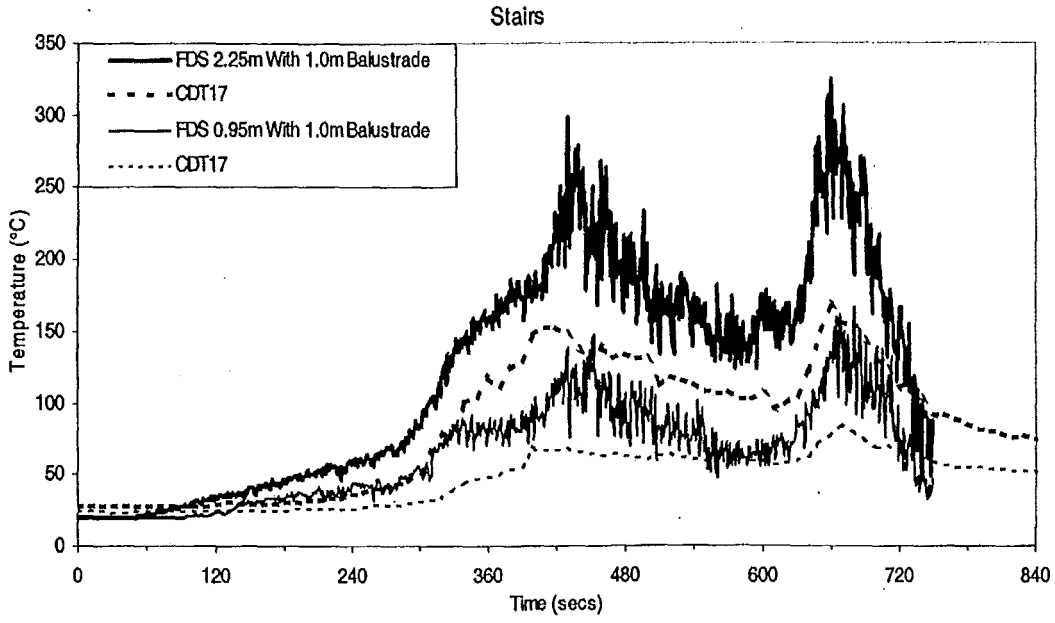

Figure B11. Temperature Curve – 1000mm High Cheque Pattern

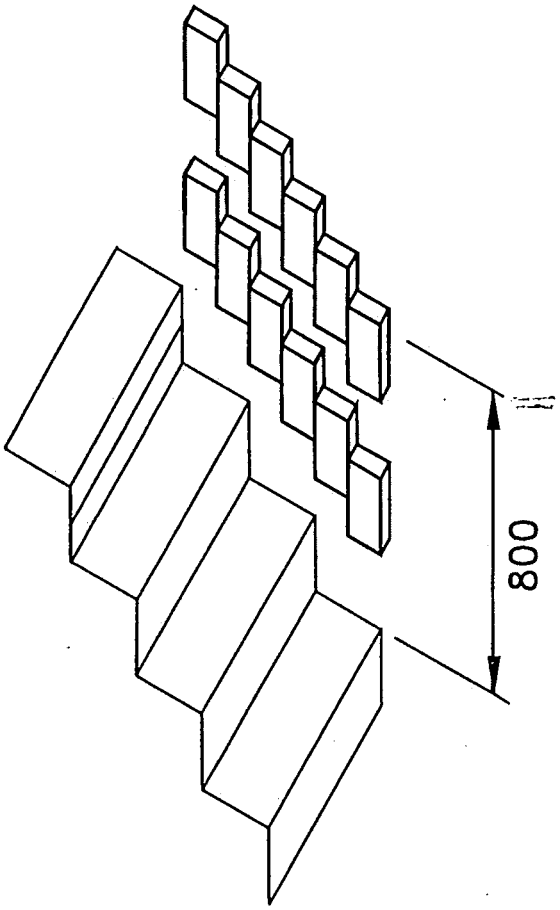

Figure B12. Diagram of Balustrade – 200mm High Soldiers

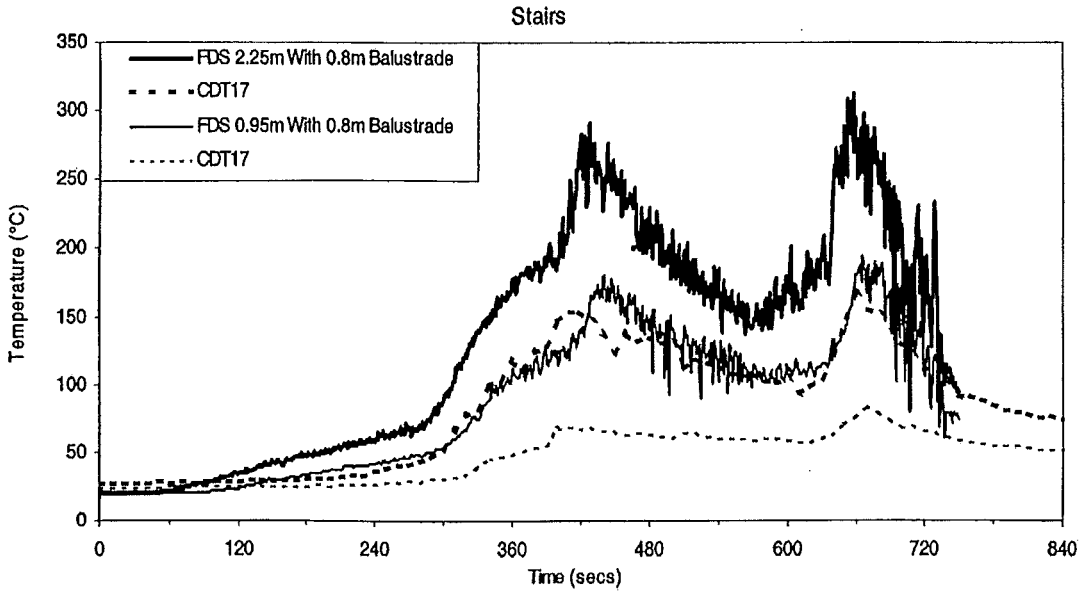

Figure B13. Temperature Curve – 200mm High Soldiers

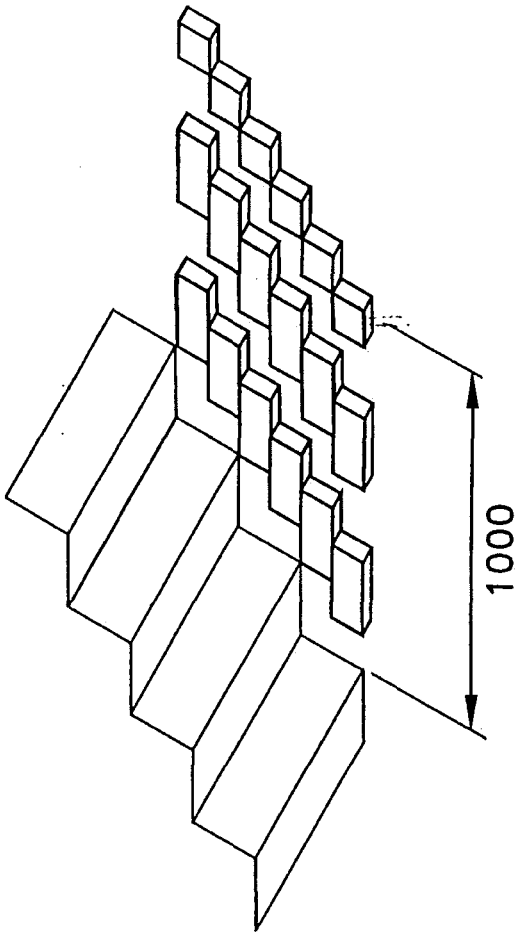

Figure B14. Diagram of Balustrade – 200mm High Soldiers with Handrail

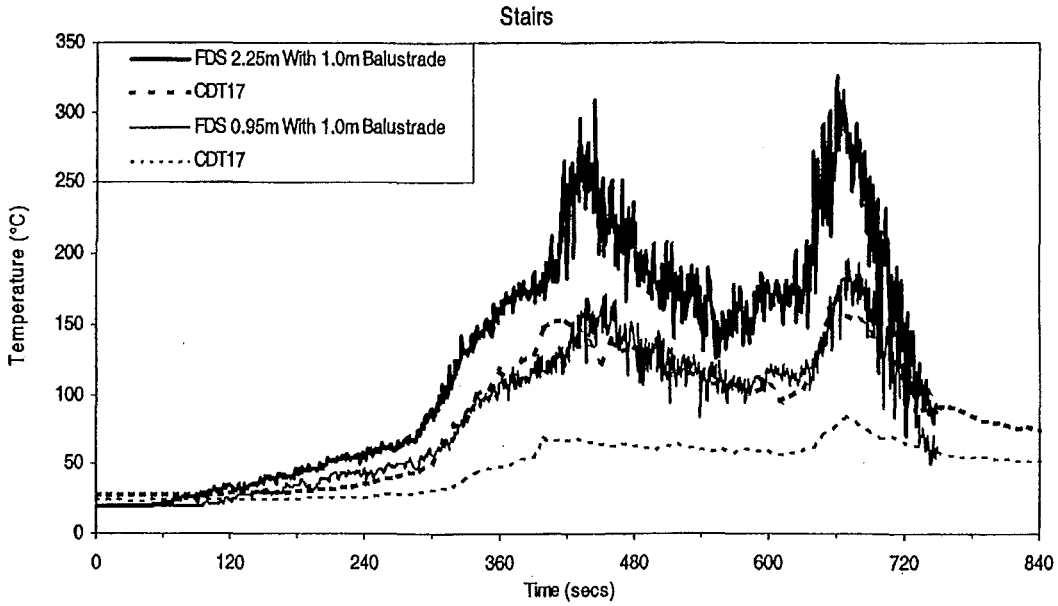

Figure B15. Temperature Curve – 200mm High Soldiers Plus Handrail

Appendix C FAMILIES OF CURVES FOR SIMULATIONS OF TEST CDT17

Throughout this report, graphs have been presented for predicted HRR, temperature, optical density, and discussions have taken place about predicted velocity. This section presents the full family of curves for test CDT17.

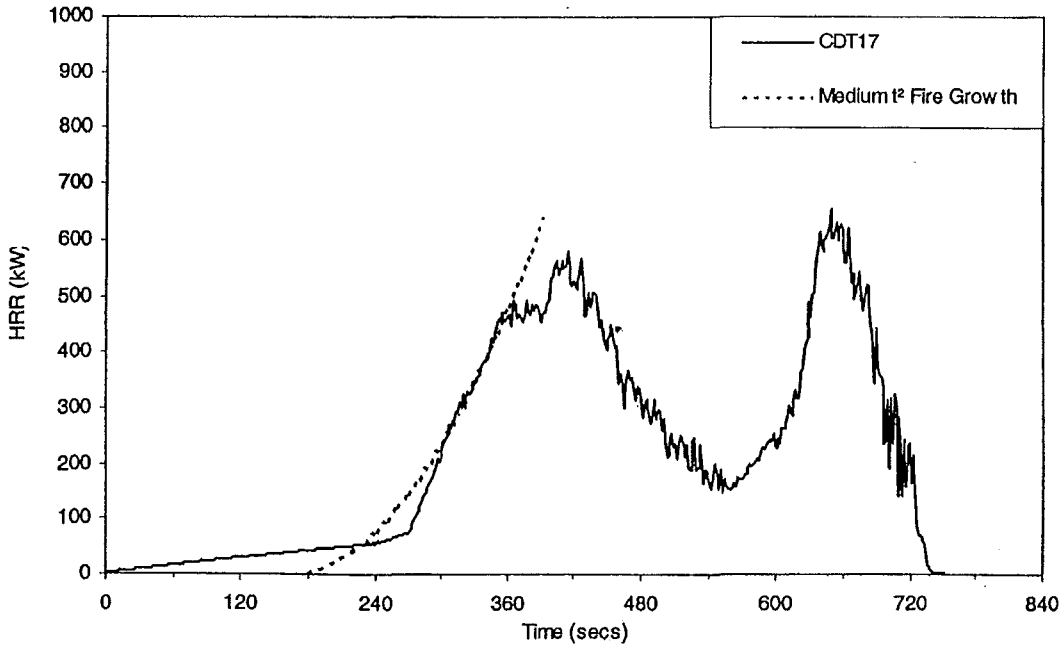

Figure C1. HRR Curve – TestCDT17

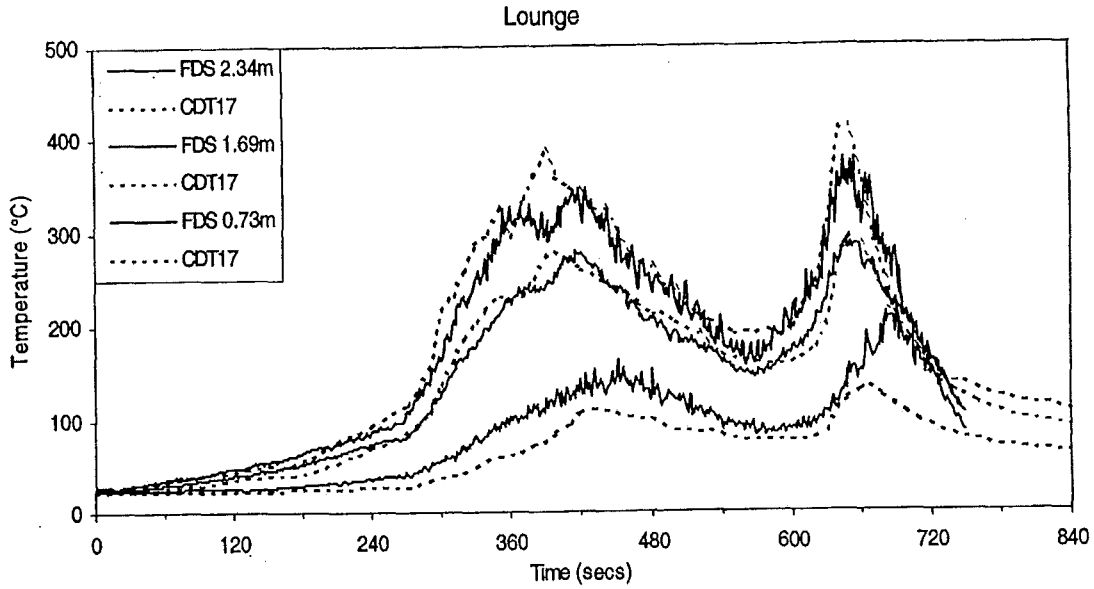

Figure C2. Lounge Temperatures – Test CDT17

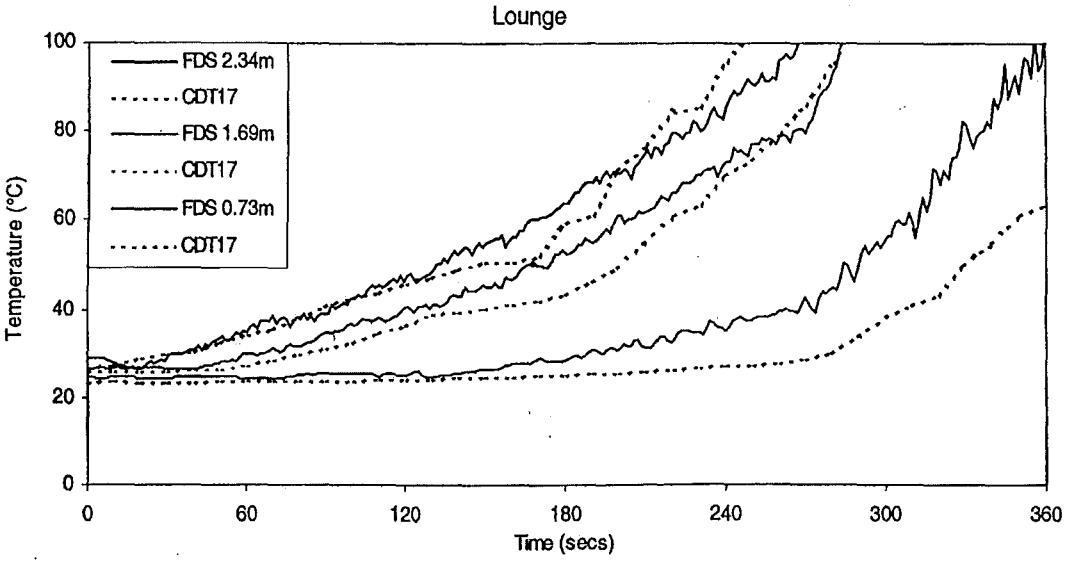

Figure C3. Lounge Temperatures – Test CDT17

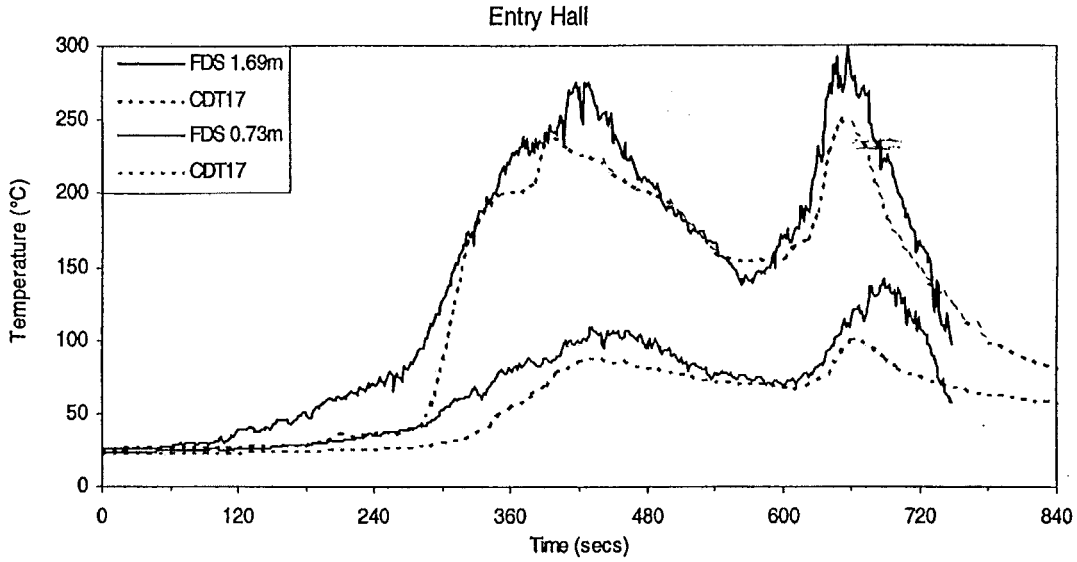

Figure C4. Entry Hall Temperatures – Test CDT17

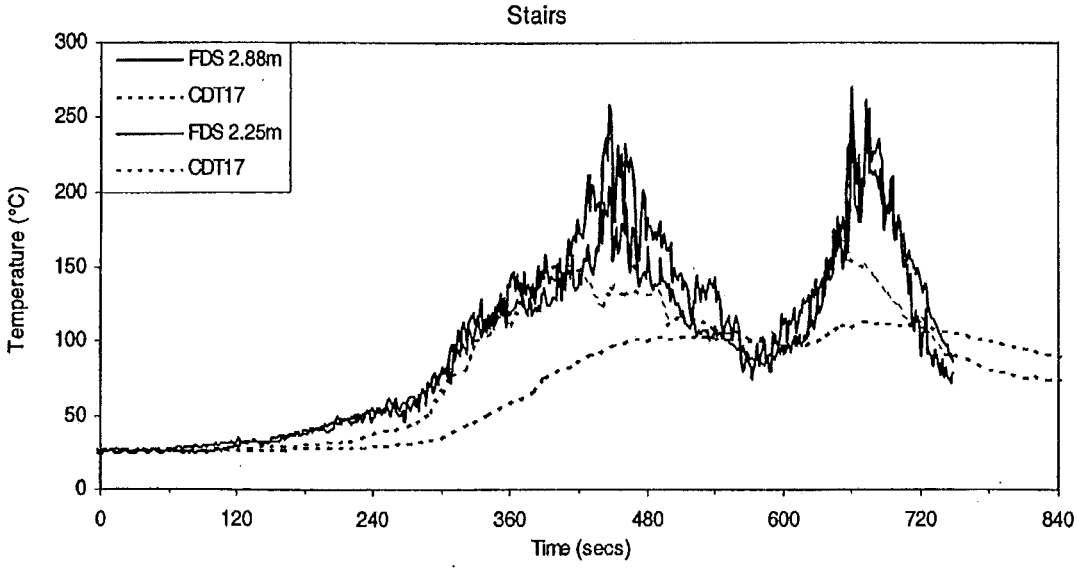

Figure C5. Stairs Temperatures – Test CDT17

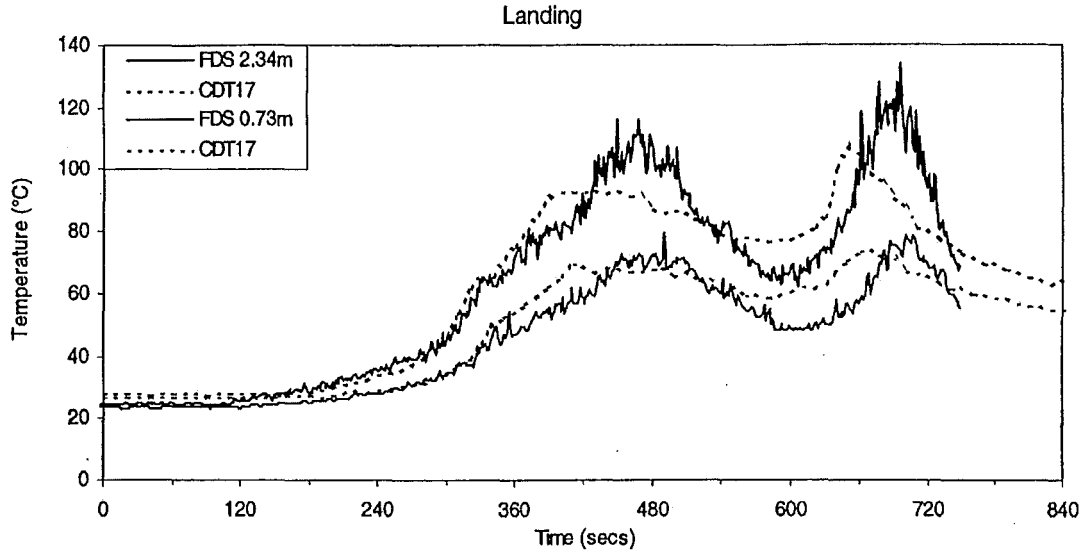

Figure C6. Landing Temperatures – Test CDT17

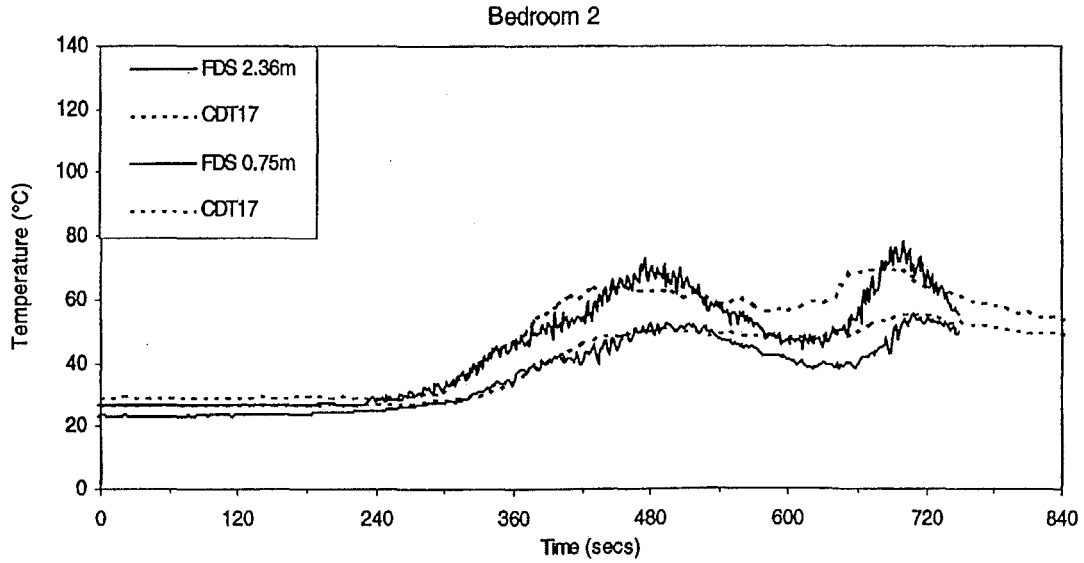

Figure C7. Bedroom 2 Temperatures – Test CDT17

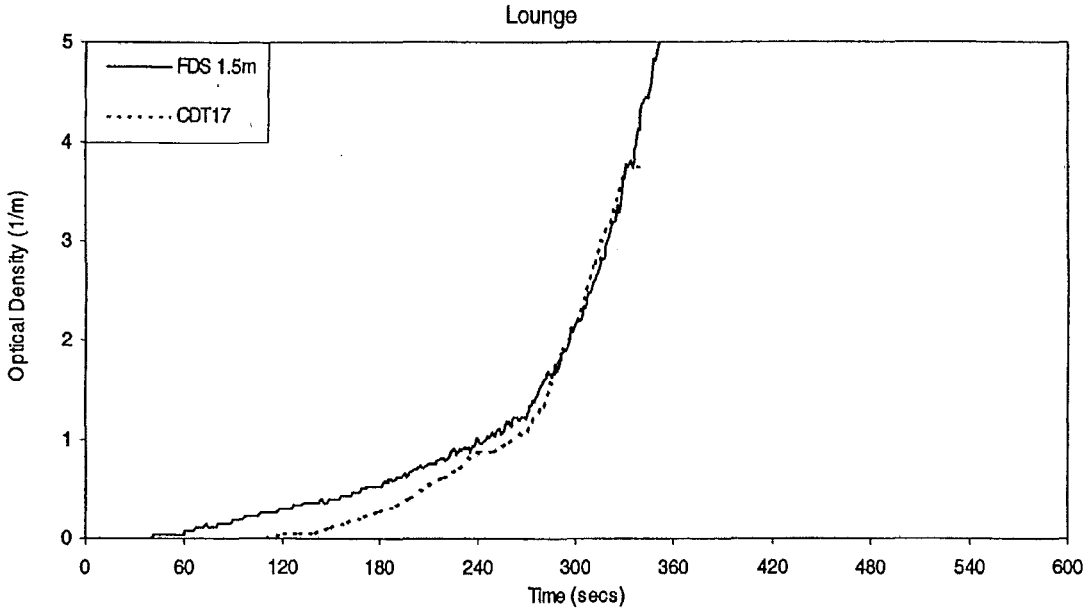

Figure C8. Lounge Optical Density – Test CDT17

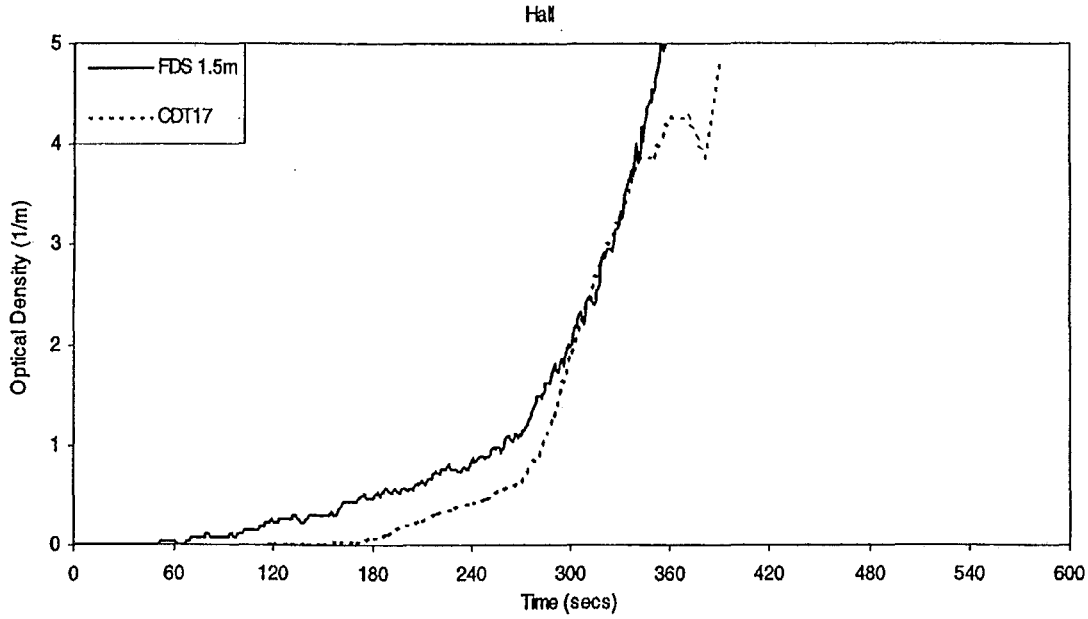

Figure C9. Entry Hall Optical Density – Test CDT17

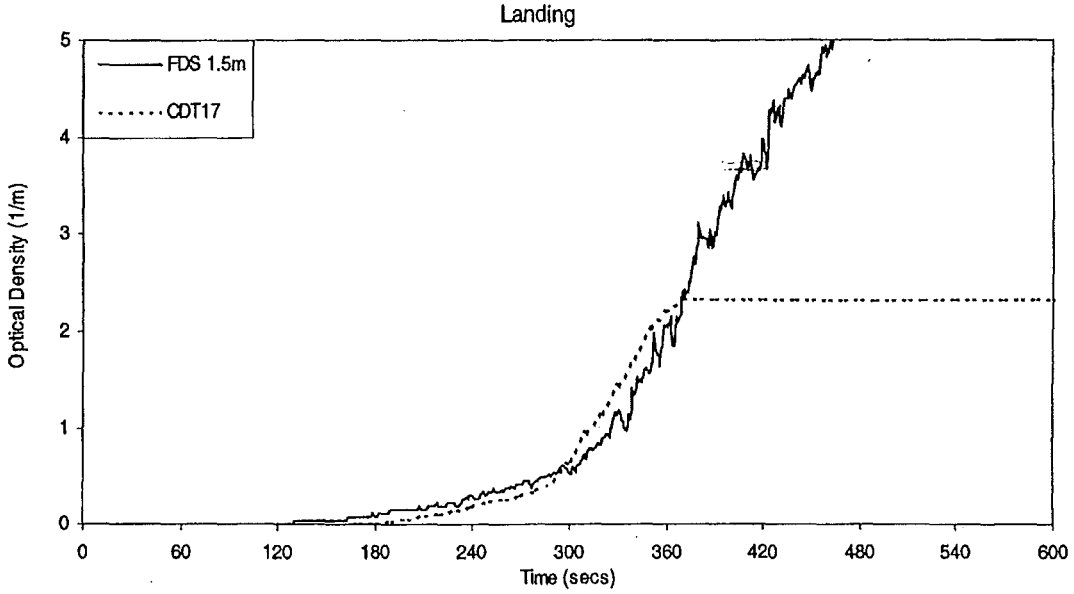

Figure C10. Landing Hall Optical Density – Test CDT17

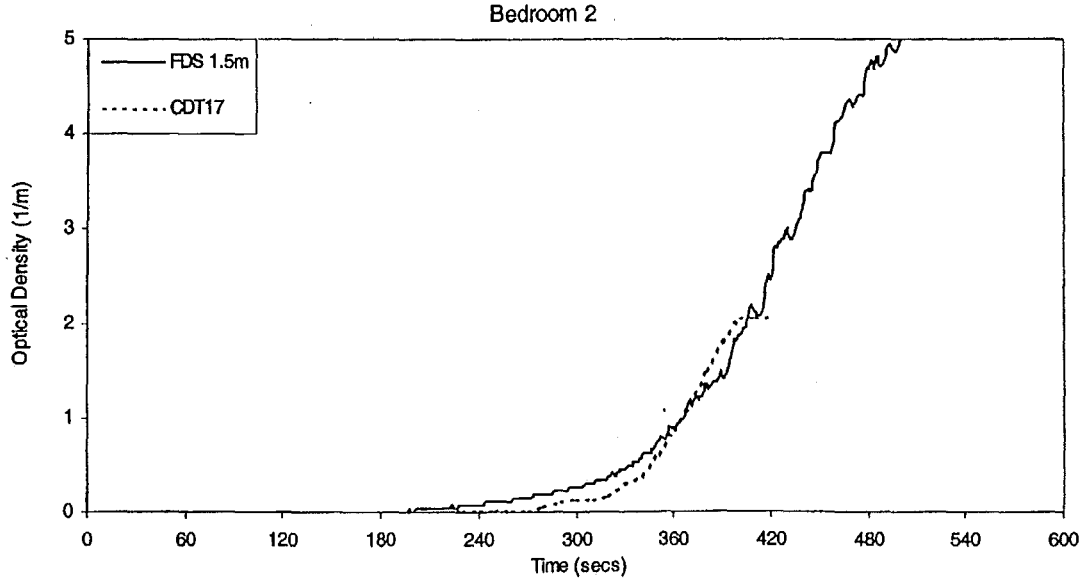

Figure C11. Bedroom 2 Optical Density – Test CDT17

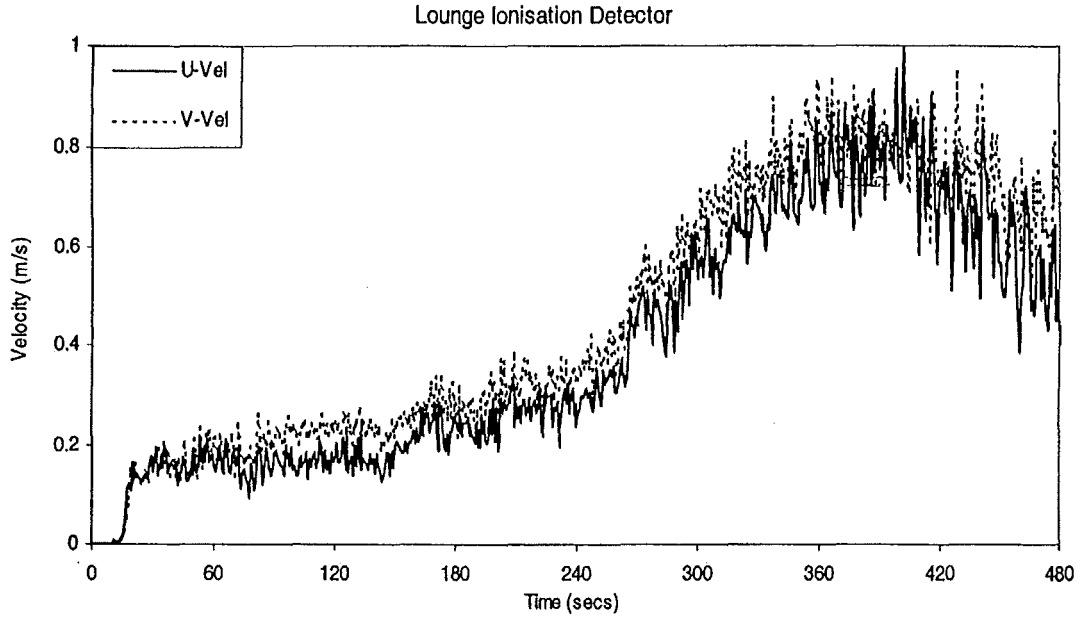

Figure C12. Lounge Ionisation Detector Velocity – Test CDT17

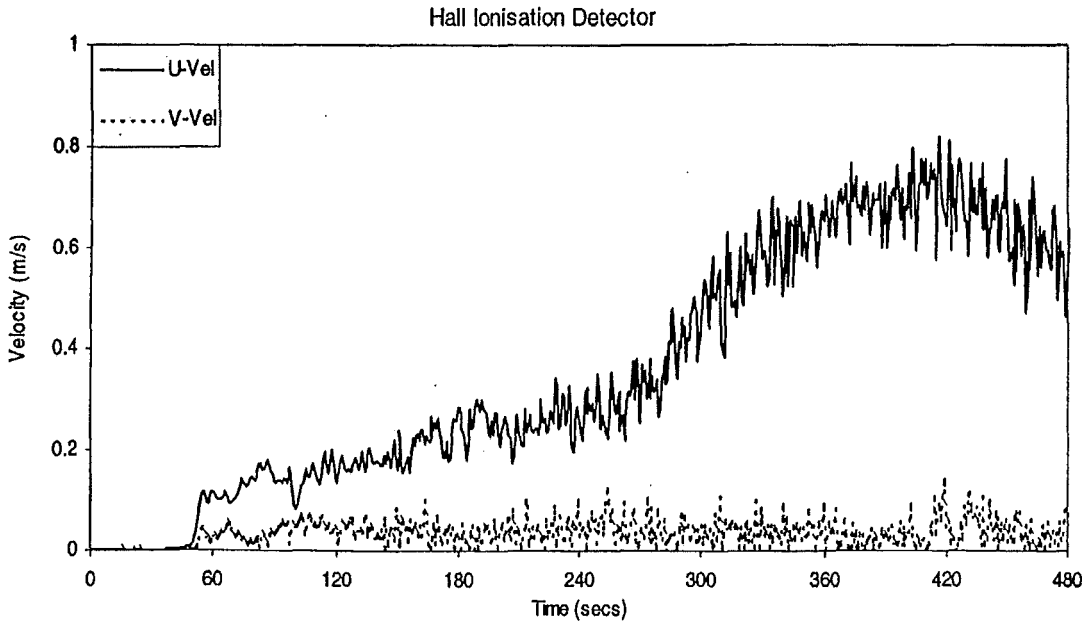

Figure C13. Hall Ionisation Detector Velocity – Test CDT17

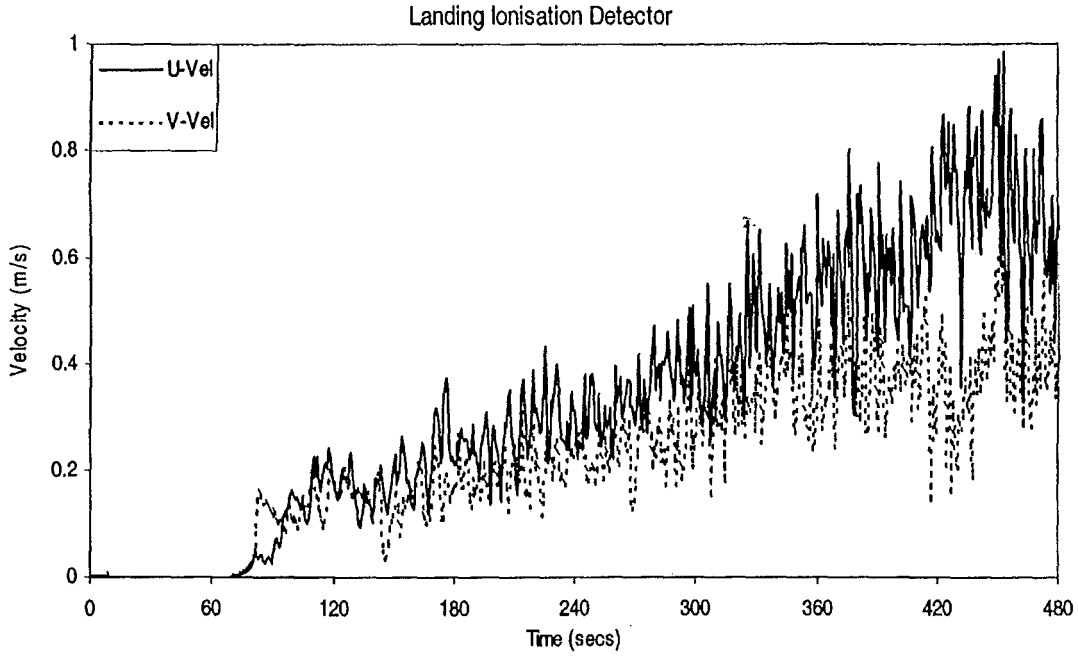

Figure C14. Landing Ionisation Detector Velocity – Test CDT17

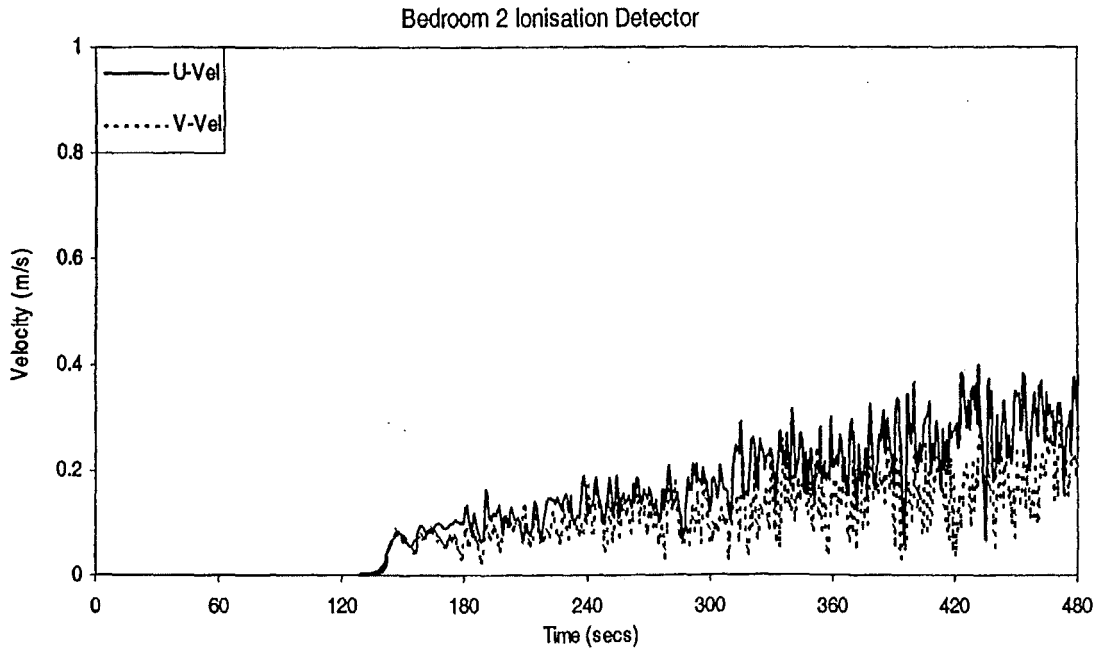

Figure C15. Bedroom 2 Ionisation Detector Velocity – Test CDT17

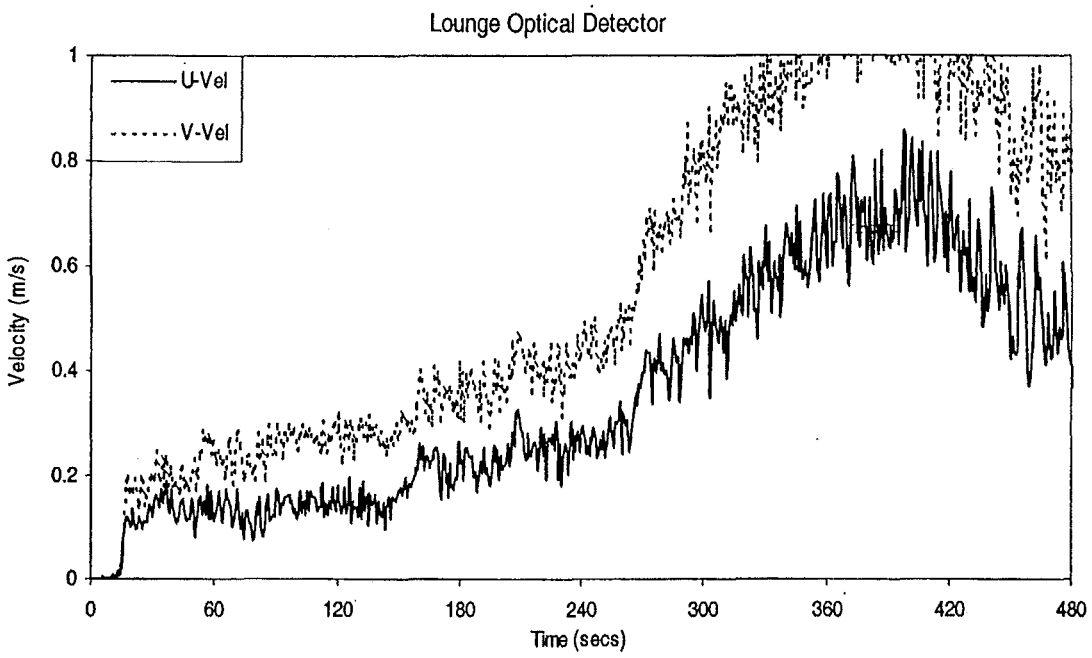

Figure C16. Lounge Optical Detector Velocity – Test CDT17

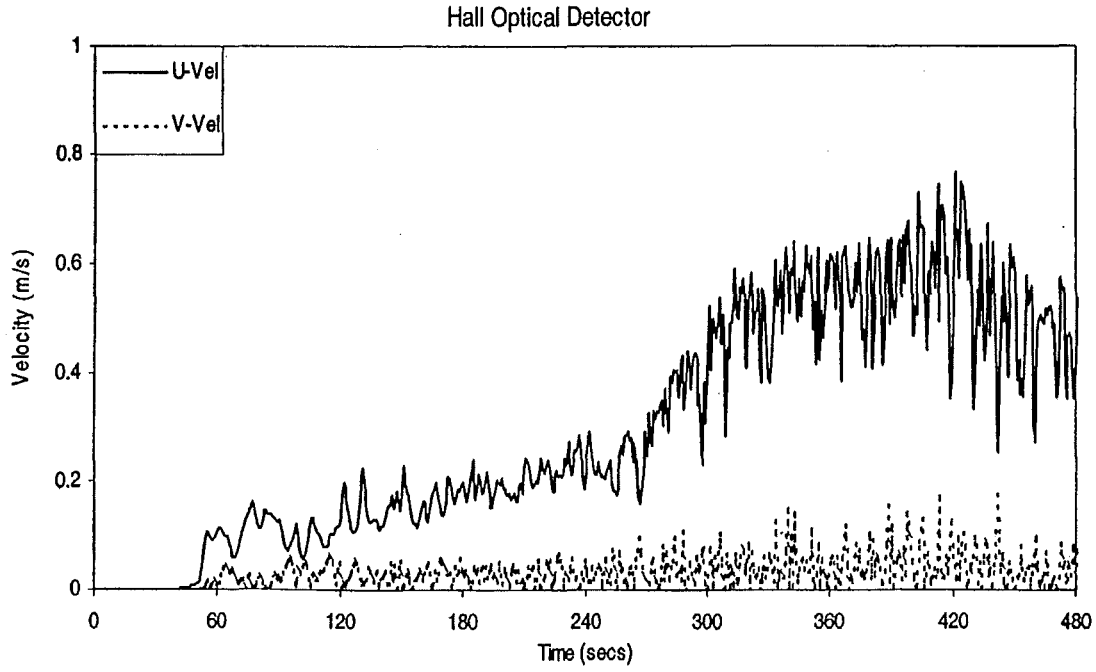

Figure C17. Hall Optical Detector Velocity – Test CDT17

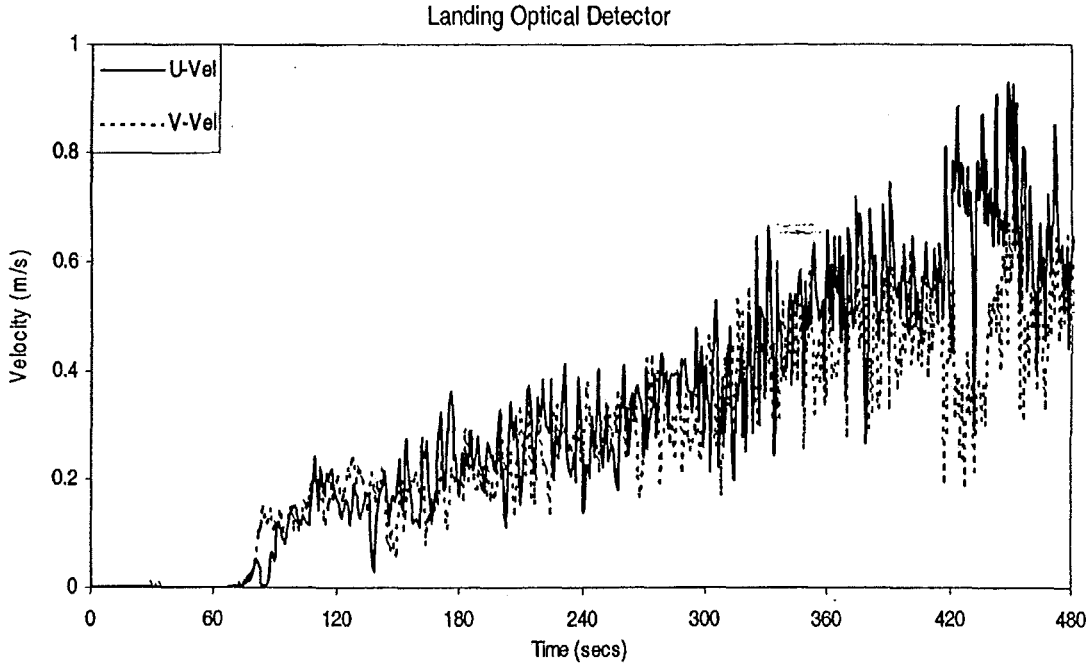

Figure C18. Landing Optical Detector Velocity – Test CDT17

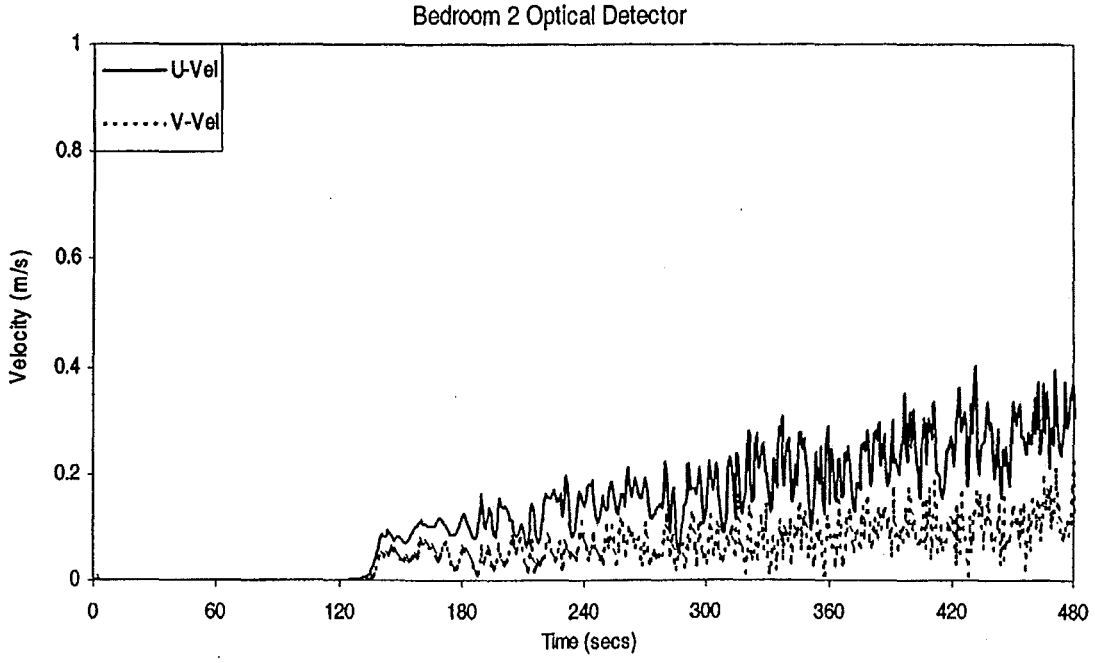

Figure C19. Bedroom 2 Optical Detector Velocity – Test CDT17

Appendix D FAMILIES OF CURVES FOR SIMULATIONS OF TEST CDT20

Throughout this report, graphs have been presented for predicted HRR, temperature, optical density, and discussions have taken place about predicted velocity. This section presents the full family of curves for test CDT20.

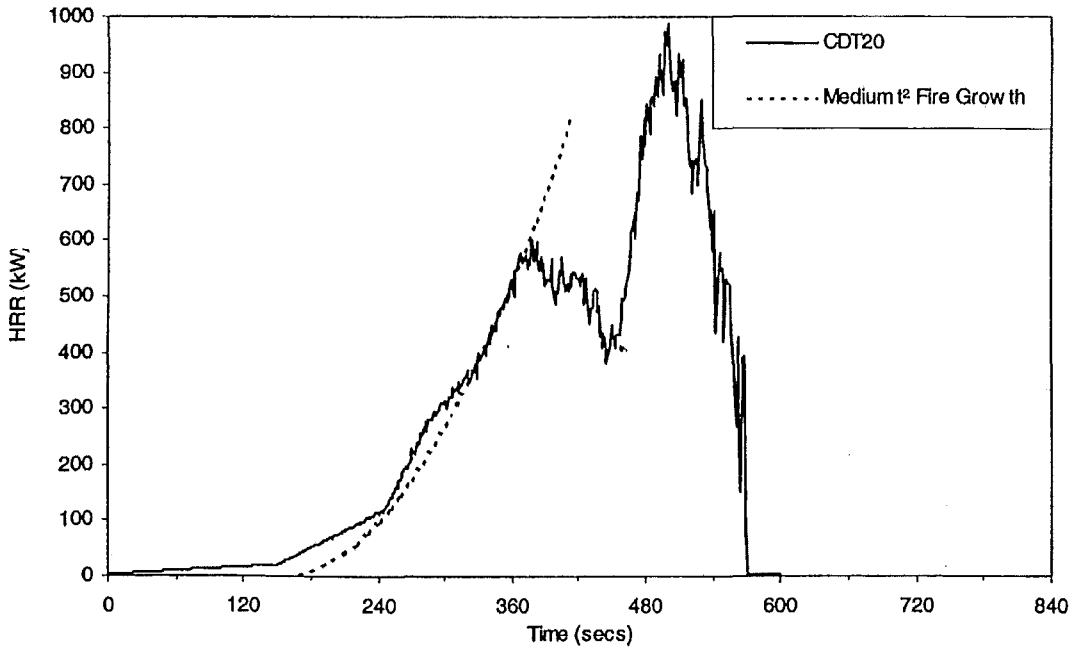

Figure D1. HRR Curve – TestCDT20

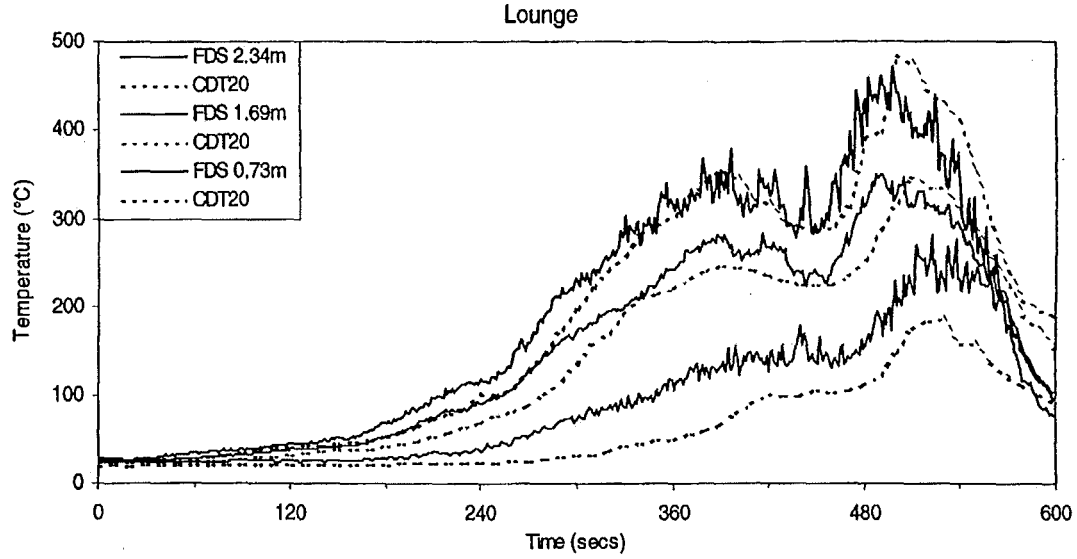

Figure D2. Lounge Temperatures – Test CDT20

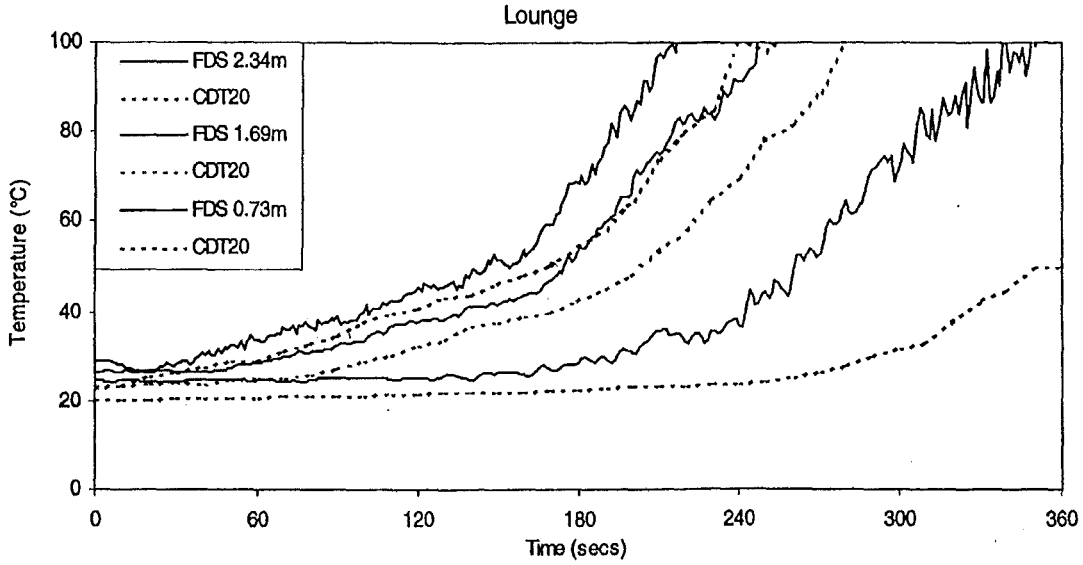

Figure D3. Lounge Temperatures – Test CDT20

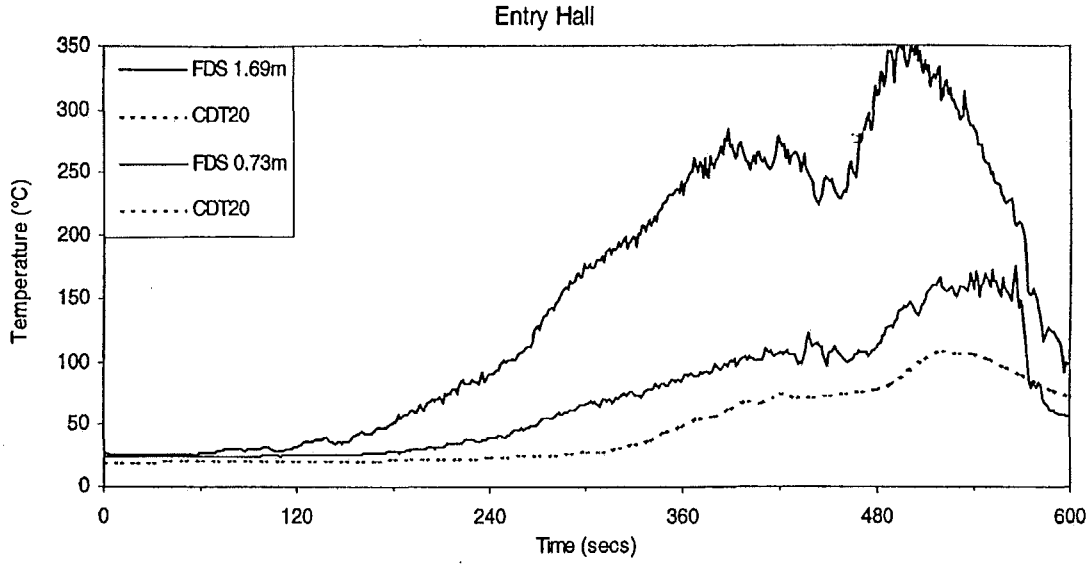

Figure D4. Entry Hall Temperatures – Test CDT20

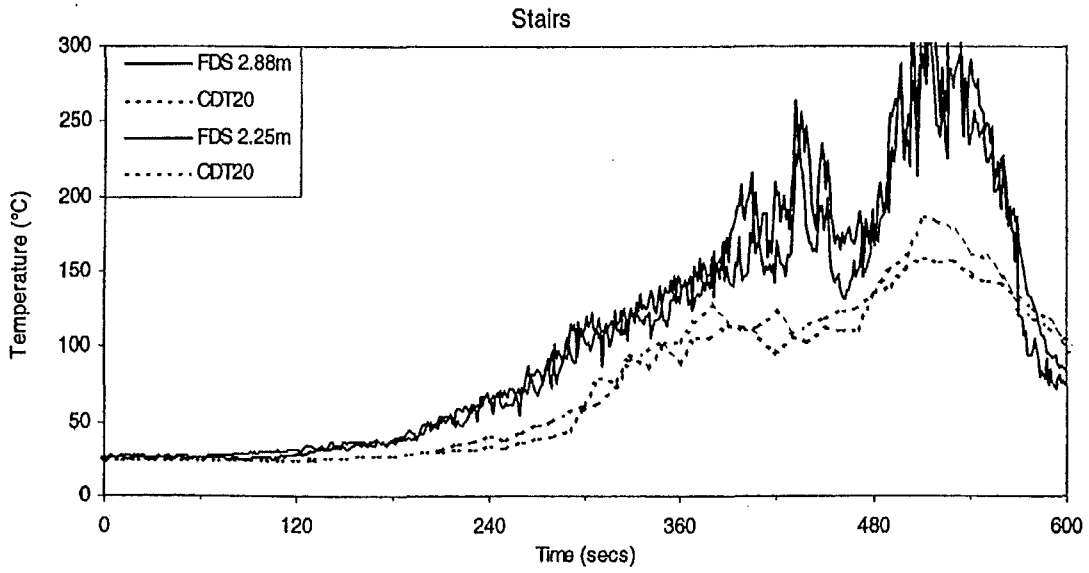

Figure D5. Stairs Temperatures – Test CDT20

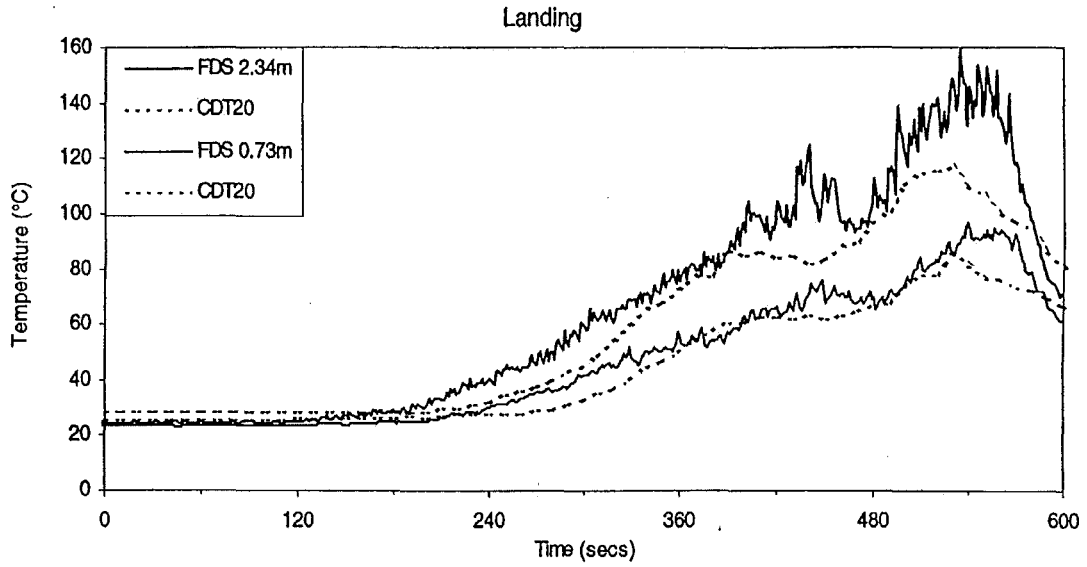

Figure D6. Landing Temperatures – Test CDT20

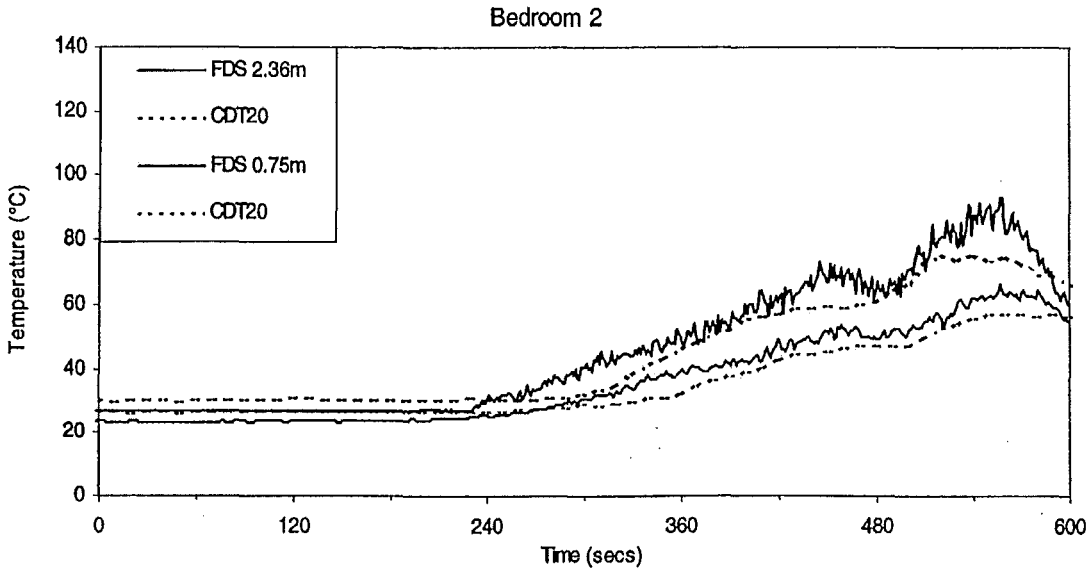

Figure D7. Bedroom 2 Temperatures – Test CDT20

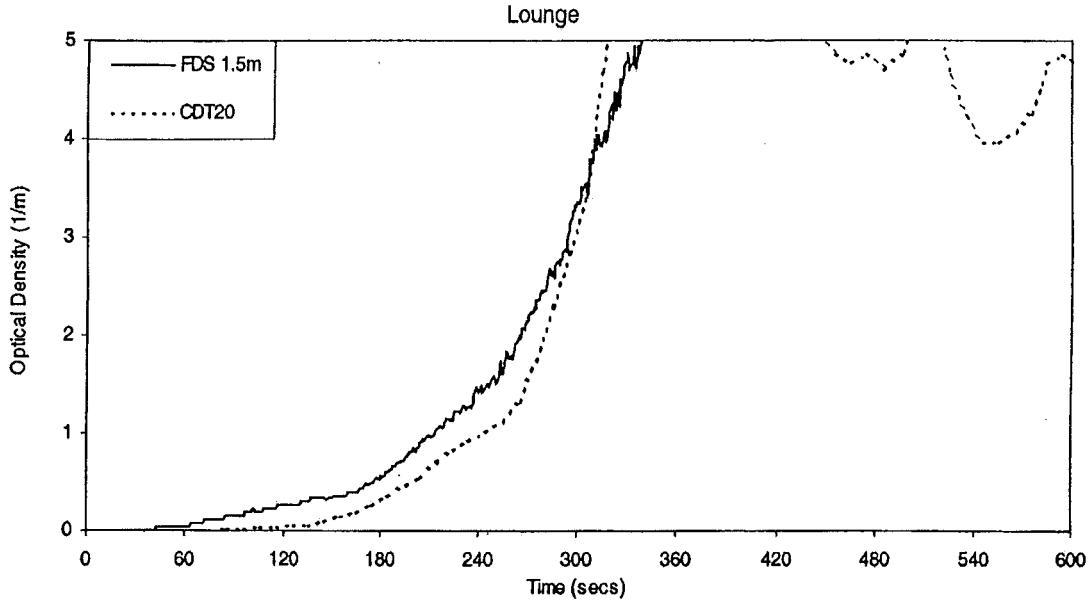

Figure D8. Lounge Optical Density – Test CDT20

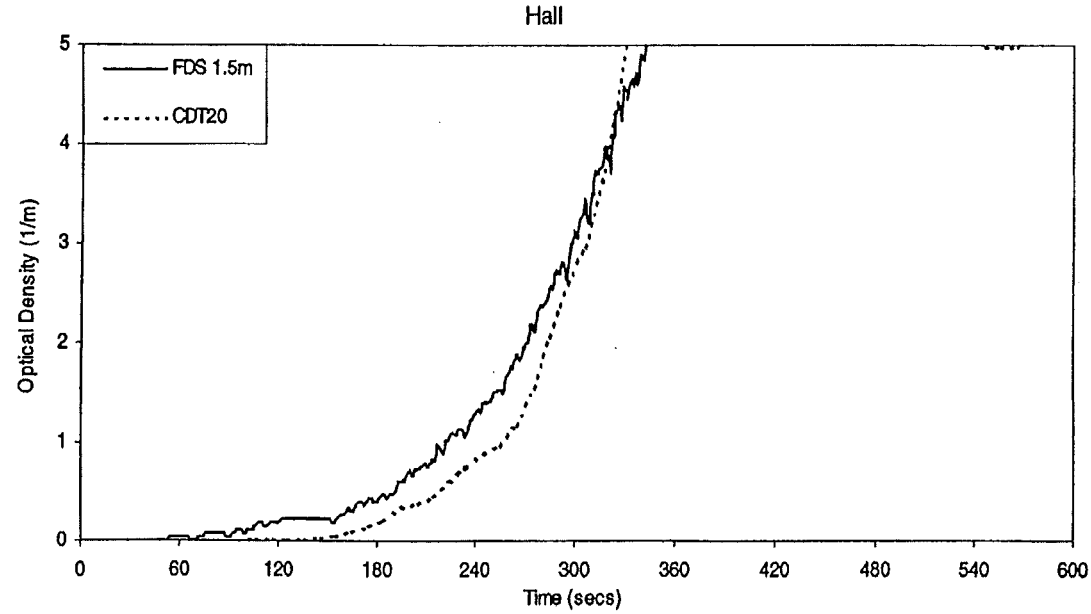

Figure D9. Entry Hall Optical Density – Test CDT20

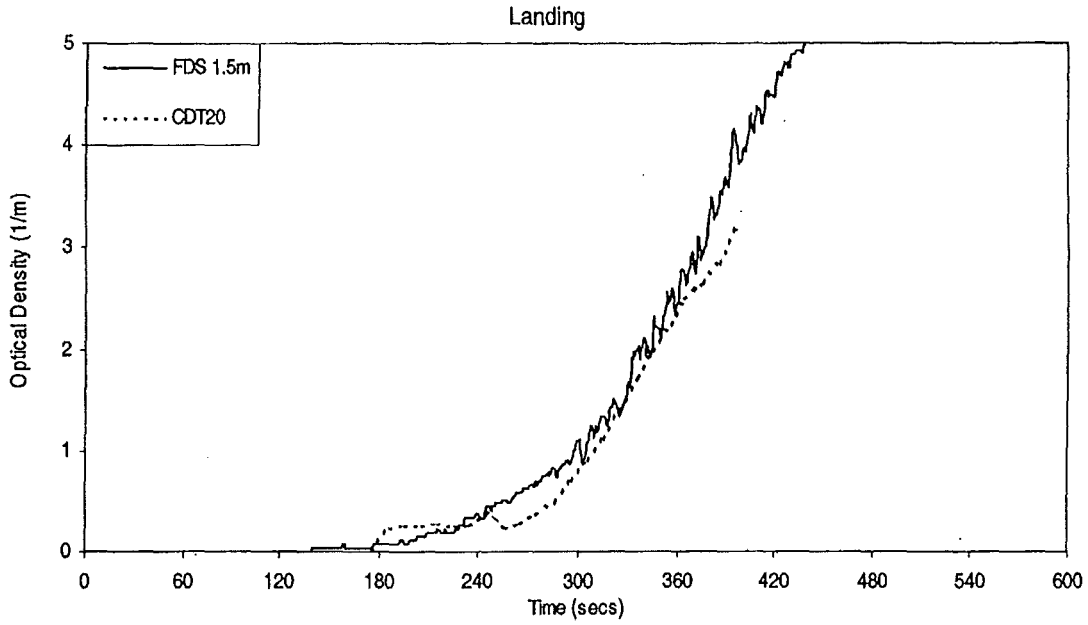

Figure D10. Landing Hall Optical Density – Test CDT20

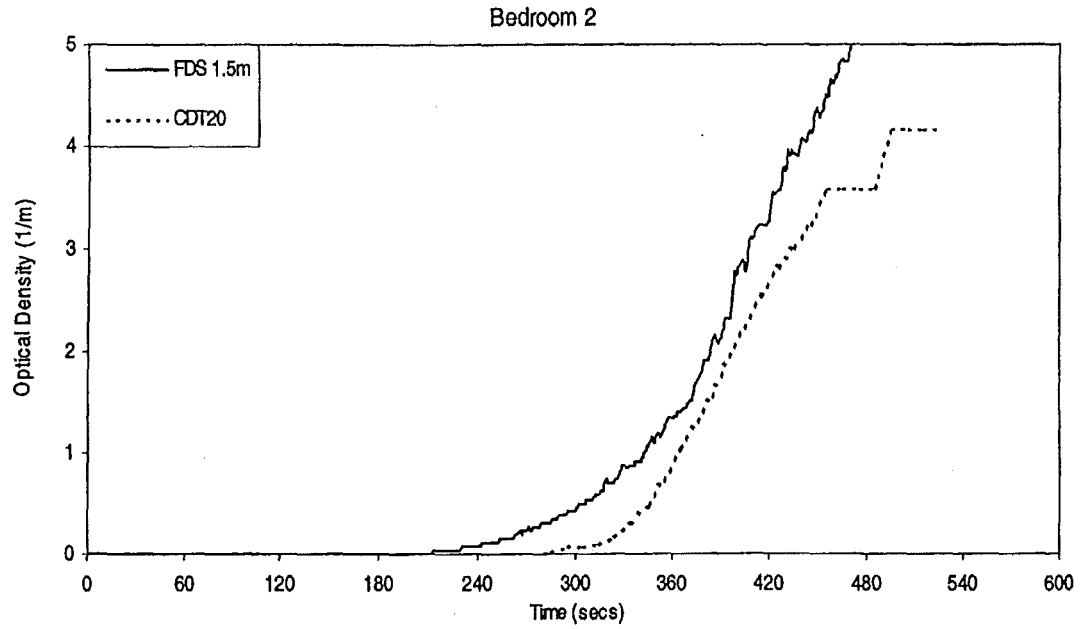

Figure D11. Bedroom 2 Optical Density – Test CDT20

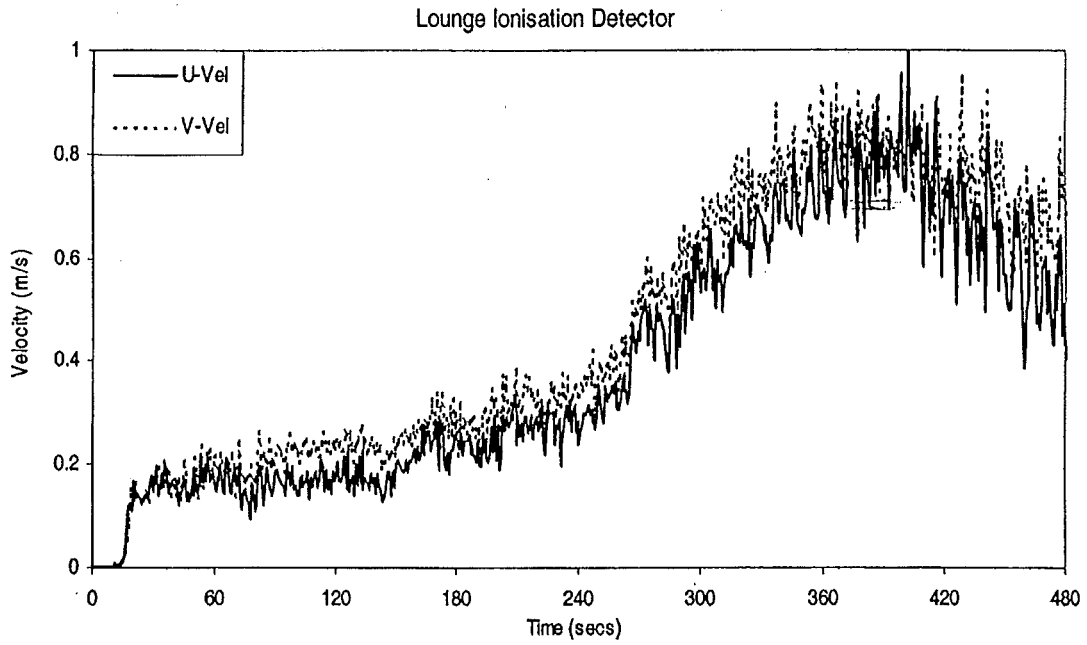

Figure D12. Lounge Ionisation Detector Velocity – Test CDT20

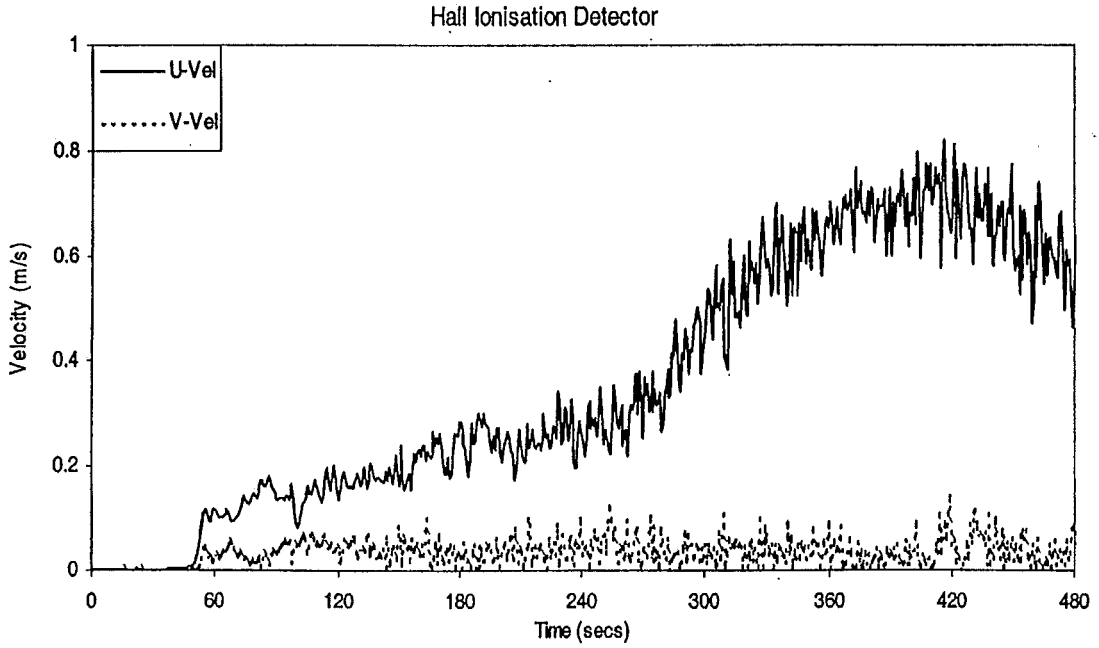

Figure D13. Hall Ionisation Detector Velocity – Test CDT20

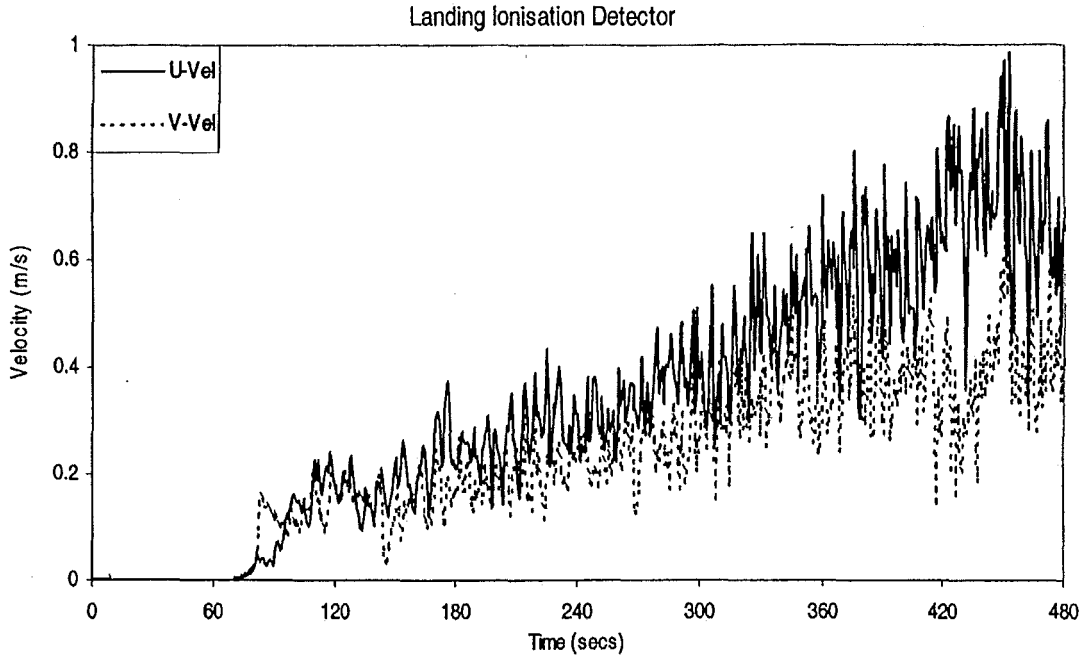

Figure D14. Landing Ionisation Detector Velocity – Test CDT20

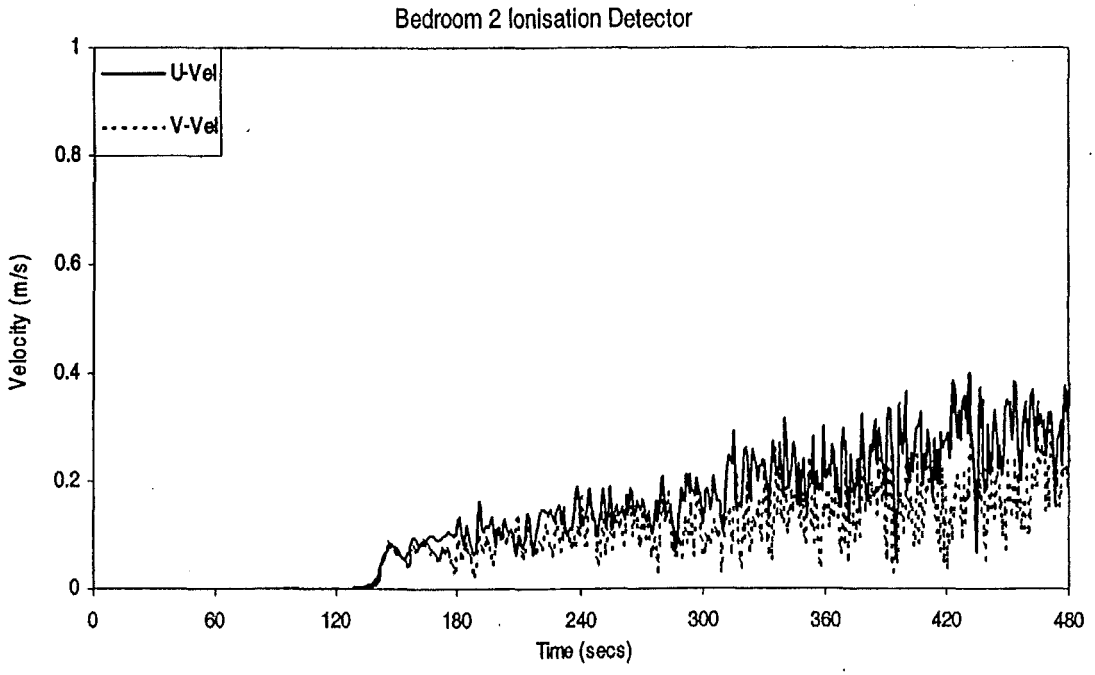

Figure D15. Bedroom 2 Ionisation Detector Velocity – Test CDT20

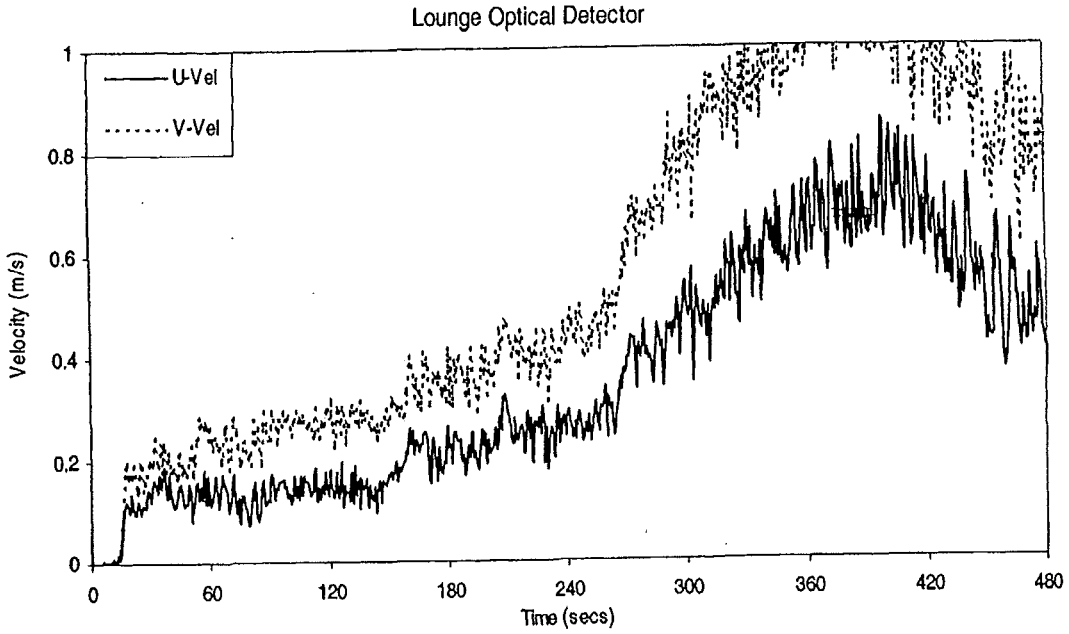

Figure D16. Lounge Optical Detector Velocity – Test CDT20

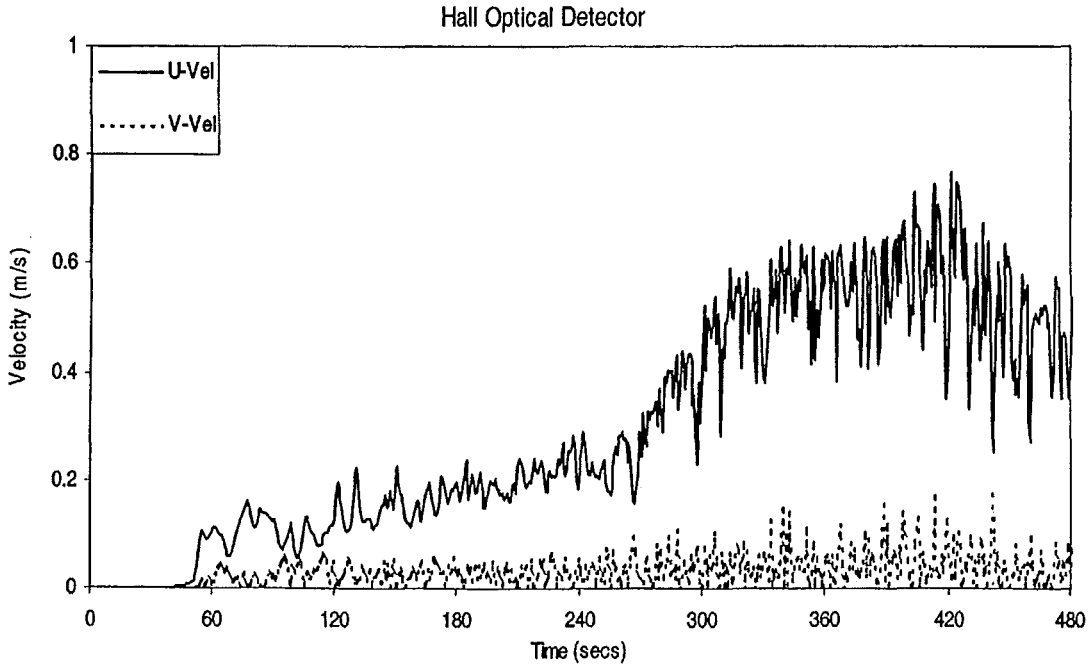

Figure D17. Hall Optical Detector Velocity – Test CDT20

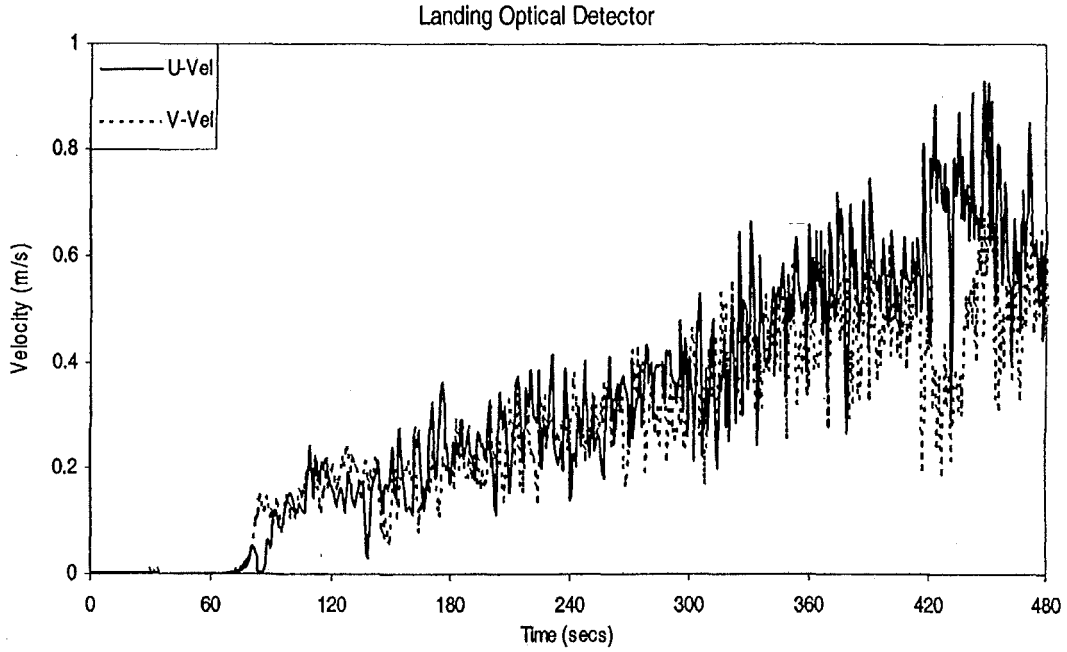

Figure D18. Landing Optical Detector Velocity – Test CDT20

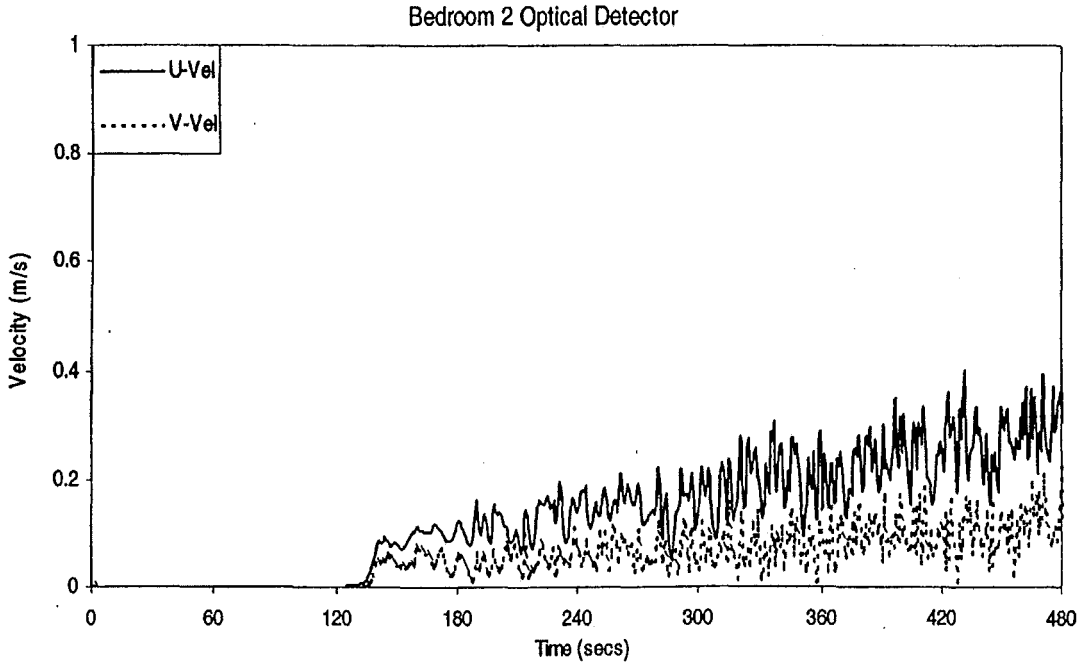

Figure D19. Bedroom 2 Optical Detector Velocity – Test CDT20

Appendix E FAMILIES OF CURVES FOR 75mm GRID SIMULATION

During this study, an investigation took place to assess what impact the choice of grid size has on the results of the simulations. This investigation was performed by comparing 75mm and 100mm grid size simulations for CDT17. This section presents the results of this investigation.

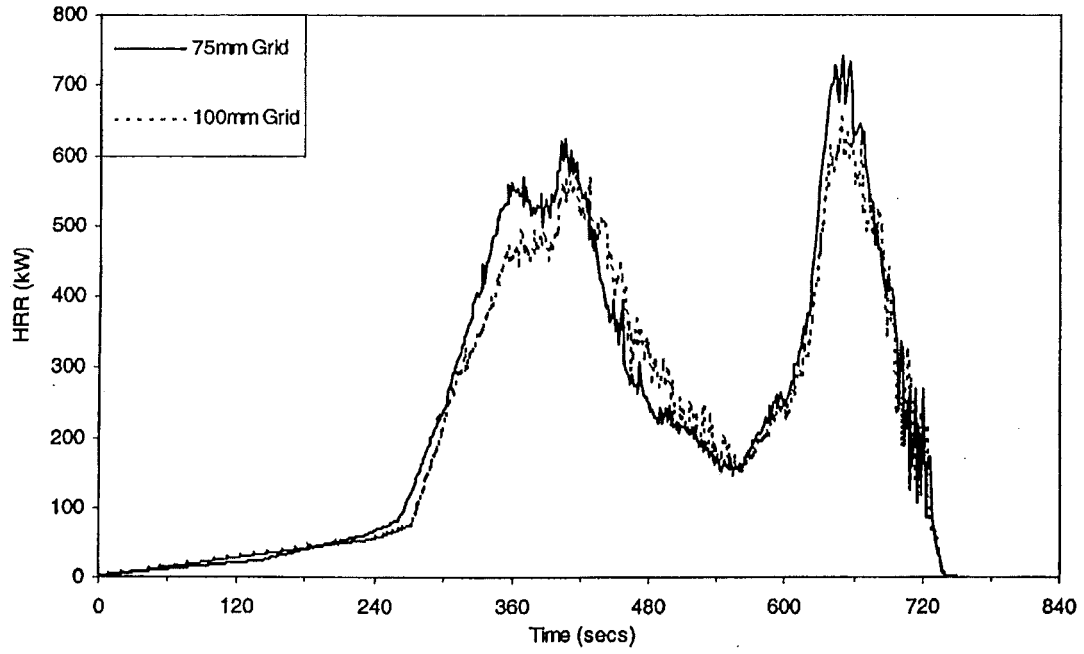

Figure E1. HRR Curve – TestCDT17

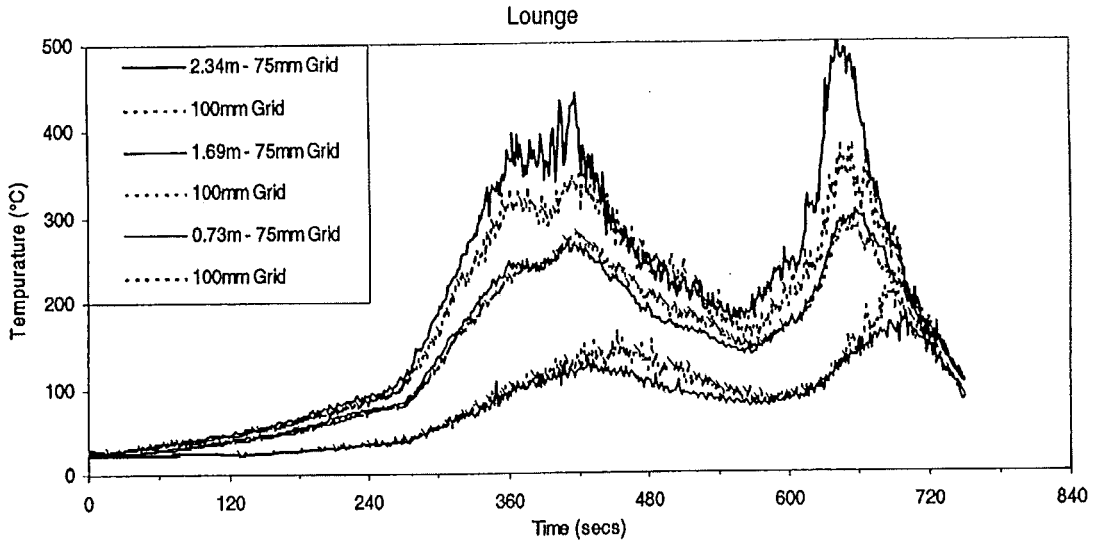

Figure E2. Lounge Temperatures – TestCDT17

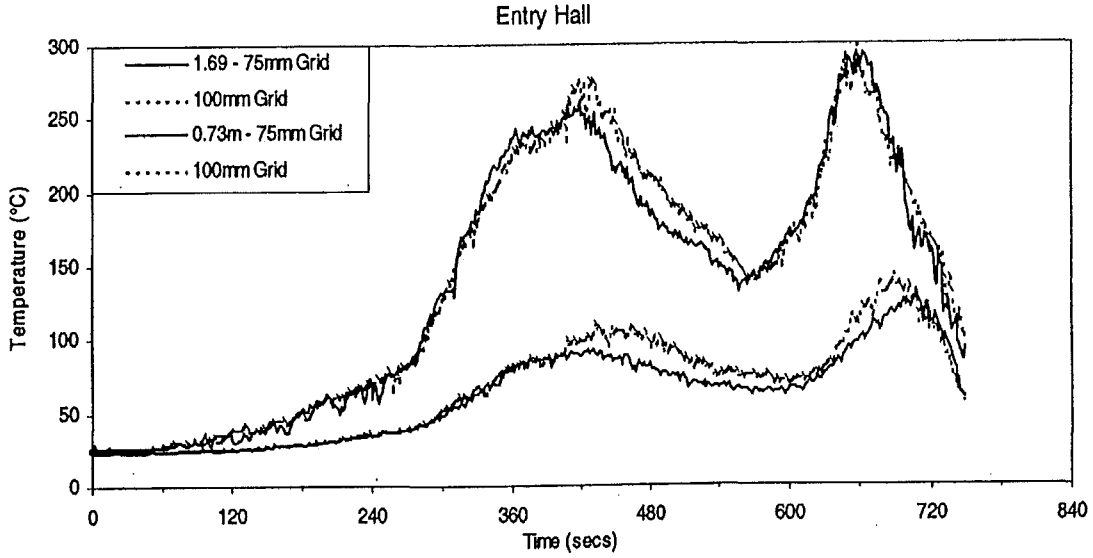

Figure E3. Entry Hall Temperatures – TestCDT17

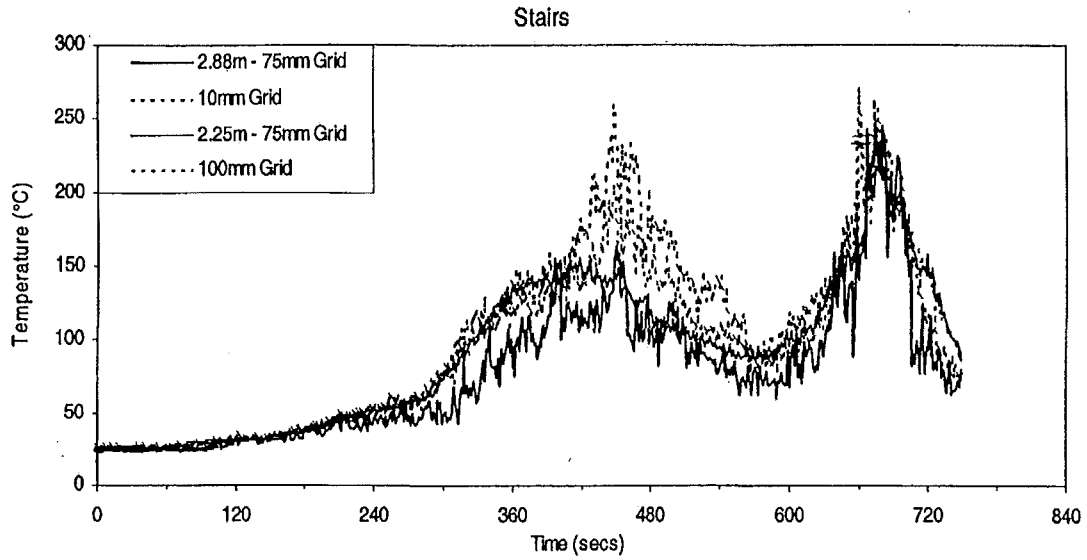

Figure E4. Stairs Temperatures – TestCDT17

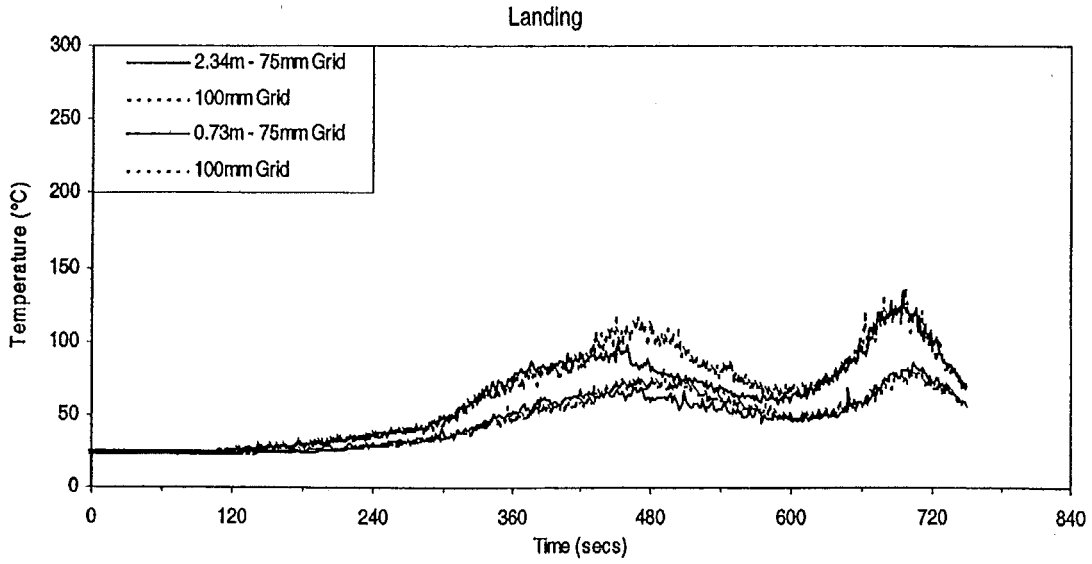

Figure E5. Landing Temperatures – TestCDT17

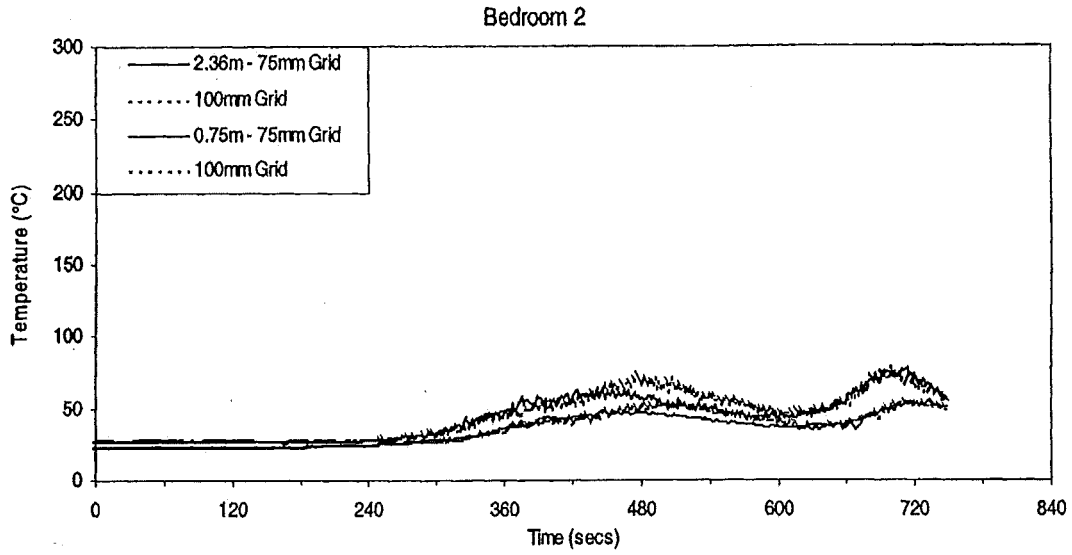

Figure E6. Bedroom 2 Temperatures – TestCDT17

FIRE ENGINEERING RESEARCH REPORTS

95/1	Full Residential Scale Backdraft	I B Bolliger
95/2	A Study of Full Scale Room Fire Experiments	P A Enright
95/3	Design of Load-bearing Light Steel Frame Walls for Fire Resistance	J T Gerlich
95/4	Full Scale Limited Ventilation Fire Experiments	D J Millar
95/5	An Analysis of Domestic Sprinkler Systems for Use in New Zealand	F Rahmanian
96/1	The Influence of Non-Uniform Electric Fields on Combustion Processes	M A Belsham
96/2	Mixing in Fire Induced Doorway Flows	J M Clements
96/3	Fire Design of Single Storey Industrial Buildings	B W Cosgrove
96/4	Modelling Smoke Flow Using Computational Fluid Dynamics	T N Kardos
96/5	Under-Ventilated Compartment Fires - A Precursor to Smoke Explosions	A R Parkes
96/6	An Investigation of the Effects of Sprinklers on Compartment Fires	M W Radford
97/1	Sprinkler Trade Off Clauses in the Approved Documents	G J Barnes
97/2	Risk Ranking of Buildings for Life Safety	J W Boyes
97/3	Improving the Waking Effectiveness of Fire Alarms in Residential Areas	T Grace
97/4	Study of Evacuation Movement through Different Building Components	P Holmberg
97/5	Domestic Fire Hazard in New Zealand	KDJ Irwin
97/6	An Appraisal of Existing Room-Corner Fire Models	D C Robertson
97/7	Fire Resistance of Light Timber Framed Walls and Floors	G C Thomas
97/8	Uncertainty Analysis of Zone Fire Models	A M Walker
97/9	New Zealand Building Regulations Five Years Later	T M Pastore
98/1	The Impact of Post-Earthquake Fire on the Built Urban Environment	R Botting
98/2	Full Scale Testing of Fire Suppression Agents on Unshielded Fires	M J Dunn
98/3	Full Scale Testing of Fire Suppression Agents on Shielded Fires	N Gravestock
98/4	Predicting Ignition Time Under Transient Heat Flux Using Results from Constant Flux Experiments	A Henderson
98/5	Comparison Studies of Zone and CFD Fire Simulations	A Lovatt
98/6	Bench Scale Testing of Light Timber Frame Walls	P Olsson
98/7	Exploratory Salt Water Experiments of Balcony Spill Plume Using Laser Induced Fluorescence Technique	E Y Yii
99/1	Fire Safety and Security in Schools	R A Carter

99/2	A Review of the Building Separation Requirements of the New Zealand Building Code Acceptable Solutions	J M Clarke
99/3	Effect of Safety Factors in Timed Human Egress Simulations	K M Crawford
99/4	Fire Response of HVAC Systems in Multistorey Buildings: An Examination of the NZBC Acceptable Solutions	M Dixon
99/5	The Effectiveness of the Domestic Smoke Alarm Signal	C Duncan
99/6	Post-flashover Design Fires	R Feasey
99/7	An Analysis of Furniture Heat Release Rates by the Nordtest	J Firestone
99/8	Design for Escape from Fire	I J Garrett
99/9	Class A Foam Water Sprinkler Systems	D B Hipkins
99/10	Review of the New Zealand Standard for Concrete Structures (NZS 3101) for High Strength and Lightweight Concrete Exposed to Fire	M J Inwood
99/12	An Analytical Model for Vertical Flame Spread on Solids: An Initial Investigation	G A North
99/13	Should Bedroom Doors be Open or Closed While People are Sleeping? - A Probabilistic Risk Assessment	D L Palmer
99/14	Peoples Awareness of Fire	S J Rusbridge
99/15	Smoke Explosions	B J Sutherland
99/16	Reliability of Structural Fire Design	JKS Wong
99/17	Heat Release from New Zealand Upholstered Furniture	T Enright
00/1	Fire Spread on Exterior Walls	FNP Bong
00/2	Fire Resistance of Lightweight Framed Construction	PCR Collier
00/3	Fire Fighting Water: A Review of Fire Fighting Water Requirements (A New Zealand Perspective)	S Davis
00/4	The Combustion Behaviour of Upholstered Furniture Materials in New Zealand	H Denize
00/5	Full-Scale Compartment Fire Experiments on Upholstered Furniture	N Girgis
00/6	Fire Rated Seismic Joints	M James
00/7	Fire Design of Steel Members	K R Lewis
00/8	Stability of Precast Concrete Tilt Panels in Fire	L Lim
00/9	Heat Transfer Program for the Design of Structures Exposed to Fire	J Mason
00/10	An Analysis of Pre-Flashover Fire Experiments with Field Modelling Comparisons	C Nielsen
00/11	Fire Engineering Design Problems at Building Consent Stage	P Teo
00/12	A Comparison of Data Reduction Techniques for Zone Model Validation	S Weaver
00/13	Effect of Surface Area and Thickness on Fire Loads	H W Yii
00/14	Home Fire Safety Strategies	P Byrne
00/15	Accounting for Sprinkler Effectiveness in Performance Based Design of Steel Buildings in Fire	M Feeney

00/16	A Guideline for the Fire Design of Shopping Centres	J M McMillan
01/1	Flammability of Upholstered Furniture Using the Cone Calorimeter	A Coles
01/2	Radiant Ignition of New Zealand Upholstered Furniture Composites	F Chen
01/3	Statistical Analysis of Hospitality Industry Fire Experience	T Y A Chen
01/4	Performance of Gypsum Plasterboard Assemblies Exposed to Real Building Fires	B H Jones
01/5	Ignition Properties of New Zealand Timber	C K Ngu
01/6	Effect of Support Conditions on Steel Beams Exposed of Fire	J Seputro
01/7	Validation of an Evacuation Model Currently Under Development	A Teo
01/8	2-D Analysis of Composite Steel - Concrete Beams in Fire	R Welsh
01/9	Contribution of Upholstered Furniture to Residential Fire Fatalities in New Zealand	C R Wong
01/10	The Fire Safety Design of Apartment Buildings	S Wu
01/11	Smoke Alarm Ownership in Relation to Socio-Economic Factors in Christchurch	N Buchanan
01/12	Accounting for Sprinkler Effectiveness in Performance Based Design of Steel Buildings for Fire	M Feeney
01/13	Equivalent Fire Resistance Ratings of Construction Elements Exposed to Realistic Fires	J Nyman
02/1	Performance of Expanded Polystyrene Insulated Panel Exposed to Radiant Heat	G Baker
02/2	A Comparison Between Predicted and Actual Behaviour of Domestic Smoke Detectors in a Realistic House Fire	D Brammer
02/3	Development of Bench-Scale Testing of Sprinkler and Smoke Detector Activation/Response Time	K S Chin
02/4	The Effect of Door Angle on Fire Induced Flow Through a Doorway	L R Clark
02/5	Implementation of a Glass Fracture Module for the BRANZ Fire Compartment Fire Zone Modelling Software	R Parry
02/6	Assessing the Feasibility of Reducing the Grid Resolution in FDS Field Modelling	N Patterson
02/7	Fire Safety Design of Ferrymead Heritage Park	M Rangi
02/8	Experimental Results for Pre-Flashover Fire Experiments in Two Adjacent ISO Compartments	L Rutherford
02/9	Measurement of Magnitude and Direction of Hot Gas Flow in a Fire Compartment with a Five-hole Probe	J Schulz
02/10	Assessment of the Current False Alarm Situation from Fire Detection Systems in New Zealand and the Development of an Expert System for Their Identifications	Y F Tu
02/11	Performance of Unprotected Steel and Composite Steel Frames Exposed to Fire	C Wastney

School of Engineering
University of Canterbury
Private Bag 4800, Christchurch, New Zealand

Phone 643 364-2250
Fax 643 364-2758